All Optical Signal Processing Devices and Clock Recovery by Fabry-Perot Filters Based on Fiber Bragg Gratings.

Thesis submitted to

Cochin University of Science and Technology

In partial fulfillment of the requirements

for the award of the degree of

Doctor of Philosophy

Submitted by

Gopakumar V T.

Reg No. 4517

Department of Instrumentation

Cochin University of Science and Technology

Cochin – 682 022, Kerala, India

May 2017

All Optical Signal Processing Devices and Clock Recovery by Fabry-Perot Filters Based on Fiber Bragg Gratings.

Author

Gopakumar V T.

Department of Instrumentation,
Cochin University of Science and Technology,
Cochin- 682 022, Kerala, India
E-mail :vtgopakumar111@gmail.com

Supervising Guide

Dr.K N Madhusoodanan,

Associate Professor & Head,
Department of Instrumentation,
Cochin University of Science and Technology,
Cochin- 682 022, Kerala, India.

May 2017

Dr.KN Madhusoodanan,

Associate Professor & Head,

Department of Instrumentation,

Cochin University of Science and Technology,

Cochin- 682 022, Kerala, India.

Certificate

Certified that the thesis **"All Optical Signal Processing Devices and Clock Recovery by Fabry-Perot Filters Based on Fiber Bragg Gratings"** submitted by **Mr. Gopakumar V T(Reg. No. 4517)**is an authentic record of research work carried out by him under my supervision at the Department of Instrumentation in partial fulfillment of the requirement for the award of degree of Doctor of Philosophy of Cochin University of Science and Technology and the work embodied in this thesis has not been included in any other thesis submitted previously for the award of any other degree.

Cochin-682 022,

Date:

Dr.KN. Madhusoodanan,

Supervising Guide

e-mail: madhu@cusat.ac.in Mob: +91- 9349406334,+91-0484 2575008

Declaration

I hereby declare that the thesis entitled **"All Optical Signal Processing Devices and Clock Recovery by Fabry-Perot Filters Based on Fiber Bragg Gratings"** submitted for the award of degree of Doctor of Philosophy of Cochin University of Science and Technology is based on the original work done by me under the guidance of **Dr. K N Madhusoodanan**, Associate Professor and Head of Department of Instrumentation, Cochin University of Science and Technology, Cochin-682022 and this work has not been included in any other thesis submitted previously for the award of any other degree.

Cochin-682022, **Gopakumar V T.**

Date:

"Thanks to the Almighty God"

Dedicated to All My Teachers ,My Family Members and My Students

Contents

Page No.

Acknowledgement

I would sincerely acknowledge my adviser and research guide Dr. K N Madhusoodanan for his whole hearted support and guidance throughout the work. I also express my sincere thanks to my guide and mentor since 2002, Dr. Balaji Srinivasan of Electrical Engineering Department of IIT Madras for his kind guidance and support for the entire research work, which includes the fabrication and characterization of FBGs and Fabry-Perot filters in the Grating facility lab. I am also thankful to Prof Asokan of IISc Bangalore for his timely advices. My acknowledgement also goes to Prof. DeepaVenkidesh of IIT Madras for her kind helps and technical advices during the clock recovery experiments. I also express my sincere gratitude to my co- authors of different conference publications, Dr. Hari V S, Dr. Kalaga Venu Madhav and Mr. Manas Srivasthava. I express my sincere gratitude to my M-Tech classmates, Mr. FijoTherattil, Dr.Rajeev Shenoy and Mr.Tony James for their moral supports throughout the work. I also acknowledge my thanks to Ms.Renju Aziz, Mr.Joe Mathew, Prof. Manilal and family, Mr. Tittu, Dr. Subin and research scholars in the department of instrumentation, CUSAT, Mr.Vishnukumar and Mr.Sreesankar. I sincerely express my thanks to my family members for their encouraging moral support throughout the work. My sincere thanks also go to my M-Tech students Mrs.Nandu, Mrs.Aswathy, Mrs.Pournamy, and Mrs.Gayathri. Finally it is the fact that without God's help and His wishes nothing would be possible, thanks to the Almighty God for completing this thesis work.

Preface

All optical networks and circuits are the first and most important candidate constituting the main backbone of high speed and high bandwidth hungry applications. The global data and voice traffic, whose volume has been growing at a fast rate, around 40% per year, are not expected to slow down in the near future. The all optical networks are designed to overcome the electronics speed bottleneck that is, the maximum electronics speed will be of a few gigabits per seconds. But the high bandwidth requirement applications like real-time video transmission, telemedicine, distance learning and video on demand require an ultra-high bandwidth with acceptable quality of service, which can only be provided by the high speed all optical networks and circuits.

While considering the all optical networks, there must be equivalent circuits in optical domain, which could process the signal and data similar to electronics signal processing, such as pulse shaping, optical memory, bit counting, switching interfaces and data clock recovery at the regenerative repeater centers and receiver.

This research work reports simulation and fabrication of fiber Bragg gratings (FBGs) and Fabry-Perot filters using FBGs (FP-FBGs) and a simple, passive and cost effective simulation and experimental validation of all optical data clock recovery at 10Gbps from an optically modulated signal. The research work also explains novel design and simulation methods for the basic optical signal processing circuits, the integrators and differentiators. The simulated optical integrator and differentiators are tested with standard input signals like Gaussian, double Gaussian and pi-phase shifted Gaussian. The fundamental component used for the research work is Fabry-Perot filters using Fiber Bragg gratings.

Different chapters of the thesis are organized as follows:

Chapter 1, is mainly an introduction to the necessity of All Optical Networks (AON), all optical '3R' (Re Amplify, Re-shape and Re-Time) current status, brief note on this research objectives and an overview of Optical Signal Processing. **In chapter 2** we give the basic working, simulation and fabrication of Fiber Bragg gratings (FBGs) and Fabry-Perot cavities based on FBGs (FP-FBGs). FBGs are widely used for wavelength division multiplexing (WDM) network filters and as sensors. The Fabry Perot-FBGs are two FBGs separated by finite distance. More details of FBGs and FP-FBGs such as the simulation, fabrication and characterization of FBGs and FP-FBGs are included in this chapter. **Chapter 3** explains the design and simulation of optical integration circuits using FBGs and FP-FBGs. It has been noted that there are some advantages like extra high processing speed, high signal to noise ratio (SNR) and high energy efficiency of FP based integrators over the FBG based integrators. The simulations are carried out with standard Gaussian, double Gaussian and π-phase shifted Gaussian pulses with variance in the order of a few tenths of picoseconds. **Chapter 4,** gives the details of another important signal processing device, the optical differentiators, which is the signal processing counterpart of the integrators. Here the author is proposing a novel, low cost method for fabricating the first order differentiators by FP-FBGs. The fabricated FP-FBGs for high speed differentiator is shown in this chapter. Here also the simulations are done with the Gaussian, double Gaussian and π-phase shifted Gaussian pulses and the results are compared with theoretical simulation results. **Chapter 5** explains the all optical data clock recovery by FP-FBG narrow band filters. The simulation and the experimental validation of data clock recovery at 10Gbps are included in this chapter. The performance analysis of data clock recovery by FP-FBGs are also discussed here. **Chapter 6** gives the concluding remarks and future scope of the research work.

The speed limitation of electronics devices and circuits can be overcome by optical communication devices and circuits. In the last couple of decades there is a tremendous progress in the area of optical communication technologies especially fiber optic communication, over its wired and wireless communication counter parts.

In optical communication, the information is carried in the form of light. The most widely used wavelengths are around 1550nm (C band). Wavelength of 1550 nm the corresponding to a carrier frequency of 193THz. The other wavelengths of interests are 850nm, 1310nm, 1490nm and 1610nm. The main advantage of optical communication is its wide bandwidth. As a rule of thumb, the band width requirement for reliable and error free communication system is one tenth of carrier frequency. So at 193THz carrier frequency, the bandwidth availability is approximately 20THz. In addition to the availability of wide bandwidth, the fiber optical communication system gives more resistance to electromagnetic interference and data security.

While considering a generalized communication system, the main components are the transmitter, the channel and the receiver. When it comes to optical communication system the transmitter is mostly a Laser with modulation circuits. The channel is an optical fiber and the receiver is a photo detector circuit. The input electrical data modulates the Laser light (emitting at any of the wavelengths mentioned) and it is coupled to the fiber optic cable for transmission to the destination and at the receiver end it is detected and demodulated by a photo receiver.

The fiber optic communication has to address the attenuation (losses) and dispersion (pulse spreading and pulse overlapping) as the signal is propagating through the fiber. So in order to overcome the power loss and dispersion of the

transmitted signal there is a need of power booster. It is also necessary to and re-time the data signal periodically around 80 to 100KM. At 1550nm the attenuation is nearly 0.2dB/Km. The network centers which compensates the power loss and dispersion within the communication link are called regenerative repeaters. The regenerative repeaters mainly do the '3R'operation, which is 'Re-Amplify', 'Re-shape' and 'Re-time'. For the above '3R' operation the optical data stream is first converted to electrical signal called optical to electrical conversion (O/E). It is followed by the 3R operation and conversion back to the optical stream (E/O) before re-transmission to the receiver destination. This optical to electrical (O/E) and electrical to optical (E/O) conversion at the regenerative repeater center are severely limiting the speed of optical data communication. This is because the speeds at which the data which can process electronically is up to 40Gpbs. But currently the data rate requirement for long haul long distance communication networks are much above 100Gbps. More over the Optical-Electrical-Optical (O/E/O) operation are involving high equipment cost, additional overhead and delays. Here comes the need for all optical signal processing circuits, avoiding O/E and E/O operation at the regenerative receiver, making everything optical so as to transmit all data optically from transmitter to the final destination.

This research work reports, simulation of all optical signal processing components like integrator and differentiators. In addition to that there is simulation and experimental validation of a low cost passive optical data clock recovery at 10Gbps data rate. Above three all optical based circuits are working with a new innovative optical component called the Fabry-Perot narrow band filters based on FBGs (FP-FBGs).

This research work also gives the details of the simulation and fabrication of Fiber Bragg Grating and FBG based Fabry-Perot filters. The FBG is a matured technology for fiber optical communication system and as fiber sensors. Here the

FP-FBGs are explained as an ideal candidate for all optical signal processing component for optical integrator, differentiators and for all optical data clock recovery. The FBGs are working in reflection mode, but the FP-FBGs are working in transmission mode. The basic theory behind the working of FBG is contra directional mode coupling. The coupled mode theory has been used for the simulation of FBGs and FP-FBGs. The phase mask technology has been used to fabricate the FPGs and FP-FBGs, where the Excimer laser is operating at 248nm with energy 6mJ and pulse repletion rate of 200Hz. After the fabrication, the FBGs and FP-FBGs are properly pigtailed and characterized with light wave measurement (LWM) system with 1pm resolution.

An optical integrator is widely used as a basic building block of all optical signal processing circuits and devices. An optical integrator is a recent concept proposed as a basic building block of the ultrafast all-optical signal processing system.It performs the time integral of the intensity or the complex envelope of an arbitrary optical input signal. It finds concrete applications in pulse shaping, photonic bit counting, optical memory units and analogue computing of differential equations.Usually FBGs are used as optical narrowband filters and sensors. FBGs are designed to give a decreasing exponential impulse response in reflection which is similar to an ideal integrator impulse response. The impulse response of FP-FBGs is also decreasing exponential in nature but has far better energy efficiency and noise immunity than that of a FBG integrator. The Matlab simulation of integrator (using both FBGs and FP-FBGs) is tested with Gaussian, double Gaussian and pi-phase shifted Gaussian pulses with FWHM in the order of a few tenths of picoseconds.

Similar to optical integrator, another important optical signal processing component is the optical differentiator. Integrator and differentiator form the basic building blocks of signal processing. The differentiator is the signal processing

counter part of an integrator. An all-optical temporal differentiator is a fundamental function for ultrafast signal processing, which is providing the derivative of the time-domain complex envelope of an arbitrary input optical signal.There are the two key features of the filter's transmission, when it is used as a differentiator, are that it should depend linearly on the base band frequency and should be zero at the signal central frequency ω_0. These two features imply an exact π phase shift across the central frequency ω_0. Here the FP-FBG based optical differentiator is explained by taking its advantages over FBGs in terms of speed, cost and noise immunity. The response of Matlab simulation of the optical differentiators based on FP-FBGs with Gaussian, double Gaussian and π- phase shifted Gaussian pulses are also been included in this chapter. The variances of all pulse shapes are a few tenths of picoseconds (typically 20ps).

Another important optical signal processing application explains here is the simulation and experimental validation of optical clock recovery using FP-FBG filters at 10Gbps. All-optical clock recovery is a key circuit of all-optical signal processing such as 3R regeneration for network synchronization. Optical clock recovery (OCR) methods may be divided into two main categories as active pulsating and passive filtering techniques. The active techniques typically produce a high-quality clock signal, but usually at the price of higher device complexity and manufacturing costs. The passive filtering techniques simply remove a part or all of the information from the received signal and preserve only the base-frequency B_S associated with the symbol rate of the data signal. These techniques typically have simple construction and low manufacturing cost. Among the passive methods, the optical clock recovery through direct filtering of the frequency components of the clock signal with Fabry-Perot (FP) filter is very simple and very fast. The clock can be recovered within few bits, and here the wavelength is transparent with respect to the data signal**.** Moreover, the environmental sensitivity is relatively low since the FP filter is an optical passive

tank circuit. A Fabry- Perot filter with a free spectral range (FSR) matched to the data rate and a relatively large finesse will work effectively for this application.

The FBGs can be used for the simulating and fabricating the optical integrator and differentiators. But the author has designed the above optical signal processing components using FP-FBGs, as it is found to have the ability to handle much higher speed, low noise and high energy efficiency. The optical integrator and differentiators are simulated and tested with standard Gaussian pulses with FWHMs of order of a few tenths of pico seconds, which correspond to a data speed of few tens of GHz. For example 10ps FWHM Gaussian pulse gives out a speed of 100GHz. The speed at which the optical integrators or differentiators can process the signal depends on the total round trip propagation time within the FP cavity. The speed can go up to a few hundreds of GHz processing bandwidth by adjusting the FP-FBG physical parameters, like grating length of FBGs and FP-FBG center to center separation. For a 10μm cavity, the round trip time is as fast as 0.3ps, corresponding to processing speed up to ≈650GHz.

The FBGs in FP-FBGs are of moderate reflectivity and in the simulation, the FBG reflectivity >90%, corresponds to an index change (Δn) in the order of 10^{-4} or more. The FBG length is only 1mm, which gives out maximum energy efficiency. The cavity length is 1mm which is formed by 1mm narrow opaque slit in the UV beam path just before the phase mask (length L=3mm). The optical integrator and differentiator proposed here based on FP-FBGs are cost effective and easy to fabricate using phase mask technology. While considering the optical clock recovery (OCR) using FP-FBG filters, the active techniques typically produce a high-quality clock signal, but usually at the price of higher device complexity and manufacturing costs. The passive filtering techniques simply remove a part or all of the information from the received signal and preserve only the base-frequency B_S associated with the symbol rate of the data signal. These

techniques typically have simple construction and low manufacturing cost. Among the passive methods, the optical clock recovery through direct filtering out of the frequency components of the clock signal with Fabry-Perot (FP) filter is very simple and very fast. The clock can be recovered within a few bits and the wavelength is transparent with respect to the data signal. Moreover, the environmental sensitivity is relatively low for FP cavity filters. The OCR does not necessarily require a self-pulsating arrangement and do not require any nonlinear components (such as an SOA). The operation speed of the method is virtually unlimited (depending on resonator length).

As data rate speed requirements are increasing in an exponential rate, the all optical networks and circuits are progressing and achieving new heights day by day. The research and technology are moving such a pace that the researches are going on in the area of optical signal processing with overall speed much higher than 100Gbps. Though here the design and simulations are done for first order integrator and differentiator, it may be extended to the fabrication and testing of first and higher order of the above optical signal processing components. In the clock recovery experimental validation, we need to fabricate the FP- FBGs with high power extinction in the order of >50dB and more accurate free spectral range (equally spaced FSR) for cost effective and data clock recovery from higher data rate optical signals.

List of Publications

Journal Publications:

1. ***VT Gopakumar***, KN Madhusoodanan and BalajiSrinivasan*"Simulation and Experimental Validation of Optical Clock Recovery Using Fiber Fabry-Perot Filters"***Journal of Optics ,Springer***,** No 44, Volume2, pp.178-181, (2015).
2. ***VT Gopakumar*** and K N Madhusoodanan, *"Design of All Optical Integrators and Differentiators Based on Fabry-Perot Filters Based on FBGs".***Journal of Photonic Network Communications,Springer**, Volume 33, Issue 3, pp 377–388, (June,2017)

International Conference Publications

3. Nandu VS, ***VT Gopakumar***, V P MahadevanPillai, Madhusoodanan andBalajiSrinivasan*"Optical Clock Recovery with Fabry-Perot-Fiber Bragg Gratings's"* (Paper WPo.45 Proceedings of International Conference on Fiber Optics and Photonics, Chennai) ***Publisher- IEEE***, (2012).
4. Aswathy M S, Pournamy S S, ***V T Gopakumar***, V P MahadevanPillai, Madhusoodanan and BalajiSrinivasan*"All Optical integrators based on FBG &Fabry-Perot-Fiber Bragg Gratings"* (Paper WPo.46 Proceedings of International Conference on Fiber Optics and Photonics, Chennai) ***Publisher- IEEE,***(2012).
5. ManasSrivasthava, **VT Gopakumar**, DeepaVenkidesh and BalajiSrinivasan, *"Performance analysis of All-Optical Clock recovery using Fary-Perot Fiber Bragg Gratings"* (Paper Tu2A-4- The 13thInternational Conference on Fiber Optics and Photonics (Photonics2016,IIT Kanpur) **Publisher - OSA Technical Digest(online),** (2016).

Chapter 1

INTRODUCTION

1.1 All Optical Networks

New technological developments for data processing in the all-optical domain are fast growing and promising field of study [1]. It helps for numerous applications in diverse areas such as ultrahigh-speed optical communications, metrology, optical sensing, image processing (which includes the medical image processing also) cloud computing, high speed high definition (HD) internet video streaming and sharing, and for computing [2]. Advantages of processing the information in the all-optical domain include the tremendous available bandwidth and the ultrahigh processing speeds [3]. It has to be noted that high bandwidth hungry applications like cloud computing, where more and more data is stored remotely. A good example for cloud computing is Google cloud storage. For the above cloud computing we require a very high speed communication network and system for data storage and retrieval. Consumer data traffic has seen a substantial

increase in part due to new services like internet video. Smart phone manufacturers have also predicted future growth for internet video and IP traffic [4]. It has been estimated that the smart phones will carry 30% of total internet traffic in year 2020, compared to the 8% in year 2015 [4]. Internet video to TV will continue to grow at a rapid pace, increasing 3.6 times by the year 2020. It has been estimated that the internet video-to-TV traffic will be 26 percent of consumer internet video traffic by the year 2020, up from 24 percent in 2015 [4, 5]. Control of the optical pulse shape is also finding applications in new photonic technologies [6]. The possibility of changing the pulse waveform from the well-known Gaussian and hyperbolic secant shapes to more exotic parabolic or triangular pulses can be used for various applications in optical signal processing and manipulation [7].

It is clear that the bandwidth requirements for communication networks are increasing day by day. The best possible solution to provide high bandwidth requirements is to transmit and receive the data optically. The most promising channel solution to transmit data is optical fibers. The carrier frequency used widely in fiber optical communication is around 193THz (1550nm). So the bandwidth availability from the above carrier frequency is in the order of 20THz [8]. Optical data communications through free space also getting momentum now a days [9]. The fiber optic data communication is mainly taking place in the wavelength around 1550nm, which is in the 'C' (Commercial) band (1530nm-1575nm). 1550nm provides the lowest attenuation in third window (~0.2dB/Km). The availability of fiber amplifier, Erbium Doped Fiber Amplifier (EDFA) at this band is an added advantage [10]. The optical data rate carrying capacity of an optical fiber is very high (160Gbps/channel and after multiplexing it can go up to a few terabits per seconds) [11]. The attenuation in the fiber and fiber impairments caused by chromatic and polarization dispersion, amplifier noise, and fiber nonlinearities are limiting the transmission rate in optical fiber communication

systems [10, 11]. In electrical communication system, there are periodic regenerators at regular intervals (around 25Km) to re-amplify, re-shape and re-time (3R) the transmitted signal [12]. The 3R makes low bit error rate (BER) and high signal to noise ratio (SNR) for the signal being transmitted. Similarly, in optical communication system also there are regenerators of around 100Km spacing. This is much higher than the regenerator spacing in electrical communication system. In the optical communication networks the regenerator system convert the optical signal in to electrical domain and process the signal (3R) and converts back to optical (O/E/O) before retransmitting to the next regenerator or to the final receiving end [13]. In electronics the very large scale integration (VLSI) with latest digital signal processors (DSP) make the signal processing very effective. But all signals processing starts with analog signals, so there must be analog to digital converter (ADC) which is of low speed, power consuming and costly. While considering the electronic technology we must take in to account the size, weight and power (SWaP). For ADC technology the SwaP is comparatively higher. In addition, aperture jitter, transistor gain bandwidth and thermal noise limit the performance of ADC technology [14].

The usage and market out-reach for optical communication technology, which include the optical signal processing technology and components used for the same predict that compared to Europe and North America, the Asia Pacific region will emerge as major users of optical data communication applications in year 2020. A comparison with reference to the 2013 is shown in figure (1.1) [15]. In fact, in 2013, Asia as a whole accounted for 70 percent of global photonics production. Asian countries like China and Japan together make 42 percent of that. These two countries together account for more than €75 billion of the world's photonics production markets. According to Mark Boroush [16] a senior analyst with US National Center for Science and Engineering Statistics (NCSES),

China averaged a 19.5 percent annual growth rate between 2003 and 2015. It is reported that the total global R&D performance expanded from $836 billion in 2003 to $1.673 trillion in 2013with Chinais alone accounted for 34 percent of this increase and the US 20 percent [16].

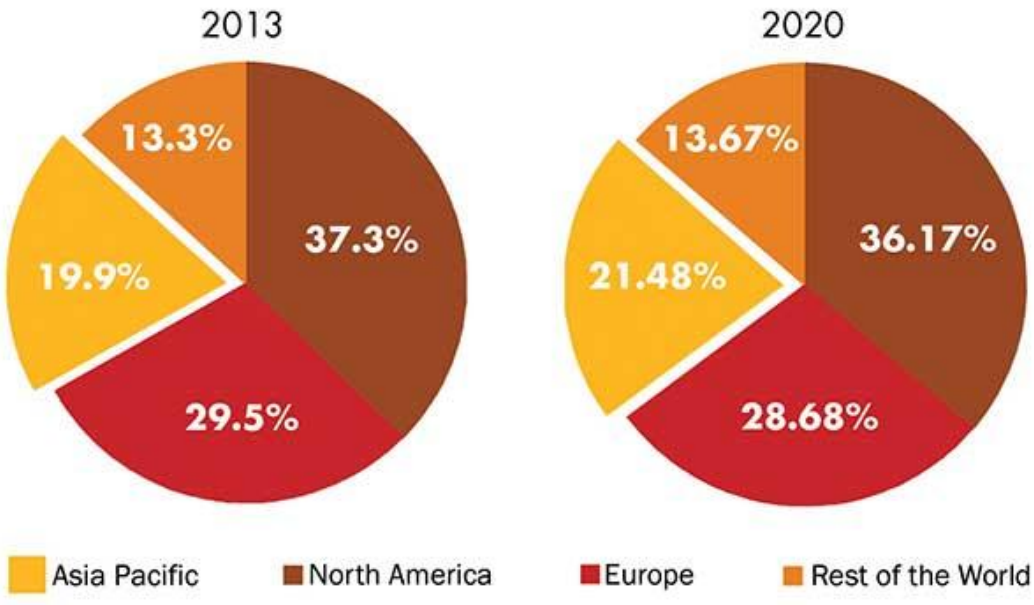

Fig. (1.1) *Global usage prediction of optical technology [15]*

The other two key players in photonic research and production markets are Taiwan and Korea. Their shares are more than €40 billion (about $45 billion) [17]. In order to support the above facts, the data traffic demands worldwide and the different multiplexing techniques to compensate the data demand going almost 200% per year [18]. It is very well understood that the optical multiplexing technique only can satisfy the growing demand for the high volume data traffic [18].

While considering our country, India has the objective of achieving 175 million broadband connections by the year 2017 and 600 million by the year 2020 at a minimum of 2 Mbps download speed. Higher speeds of at least 100 Mbps on demand is dependent on the success of the National Optical Fibre Network

(NOFN) [19]. The original project report on NOFN was prepared by Telecommunications Consultants India Limited (TCIL) in year 2011. It has estimated a uniform broadband speed of 100 Mbps across all Gram Panchayats in the country [19]. However, the growing demand for data and the proliferation of video – for both, utility and entertainment purposes and also the booming digital economy point to the need for higher broadband capacities in the country.

The Very Large Scale Integration (VLSI) technology with Digital Signal Processors (DSPs) makes the electrical/optical signal processing very efficient and effective. But all signals, which is to be processed starts with analog. So there must be Analog to Digital Converter (ADC). There are different types of ADCs [20]. But there are some limitations of using ADCsas mentioned in the section (1.1).

The following table shows (Table 1.1) in year 2017 the total cost per meter for fiber including hardware is USD 4.83 for 204 million KM of fiber, which is of very marginal increase against the same in year 2011 where the fiber length only 147million KM [21]. The table shows the linear reduction in cost of optical fiber and other fiber hardware components as its usage increases around 15% per year.

Table (1.1) *Year wise the total fiber and hardware cost [19]*

	2011	2012	2013	2014	2015	2016	2017
Optical Fiber (in millions of kilometers)	147	162	159	172	182	190	204
Unit Price (US$)	9.00	8.75	9.00	8.50	8.50	8.50	8.75
Total	1.32	1.42	1.43	1.46	1.55	1.62	1.79
Fiber Cable Hardware	2.1	2.4	2.43	2.62	2.79	2.92	3.04
Total Fiber, Cable and Hardware	**3.42**	**3.82**	**3.86**	**4.08**	**4.34**	**4.54**	**4.83**

So, for high bandwidth requirement applications mentioned above, there should be equivalent optical processing circuits (the 3R) to that of electrical domain. The above mentioned applications mentioned lead to the development of all optical networks (AON) [22]. The main components in AON are the optical switches, mathematical and logic circuits equivalent signal shaping and processing circuits like integrators and differentiators, timing extraction circuit like optical data clock recovery and carrier recovery etc. [23].

1.2 The 3R operation (Re-Amplify, Re-Time and Re-Shape)

While considering the AON, it is very important to develop optical 3R regeneration technique to "clean-up" the optical signal, as mentioned. There are several methods for All-optical 3R regeneration [24, 25]. The nonlinear optical processes include self-phase modulation and four-wave mixing. In the nonlinear optical processing, nonlinear fibers of lengths a few kilometers are used for signal regeneration [26]. Recently it is reported that silicon-on-insulator (SOI) and nano-photonic waveguide technologies allow the fabrication and implementation of highly nonlinear devices on integrated platforms for high speed regeneration [26]. The most popular among these are the four-wave mixing in silicon nano-waveguides for signal regeneration [26]. It is mainly because of its power-efficient and broadband characteristics. The above four-wave mixing technique in silicon nano-waveguides gives out simultaneous wavelength conversion, optical signal reshaping, retiming and re-amplification over a wide wavelength range. The signal power can also be improved by the signal regeneration using four-wave mixing. The main disadvantage seen on the above techniques is the complex fabrication procedure [26].

Long distance high data rate optical communication research was started in 1980s because of the improved receiver sensitivity [27]. Those days the Er-doped fiber amplifiers (EDFAs) had not been developed. The wavelength division multiplexing (WDM) was expensive due to the repeater cost and complexity associated with de-multiplexing, optical-electrical conversion, amplification, electrical de-multiplexing to a lower data rate, regeneration, multiplexing back up, electrical-optical conversion, and multiplexing into optical fiber.

In electrical communication system, there are periodic regenerators at regular intervals (around 25Km) to re-amplify, re-shape and re-time (3R) the transmitted signal which limit the data transmission speed as shown in figure (1.2) [12].The solution for the above problem is to process the signal data optically [28, 29].

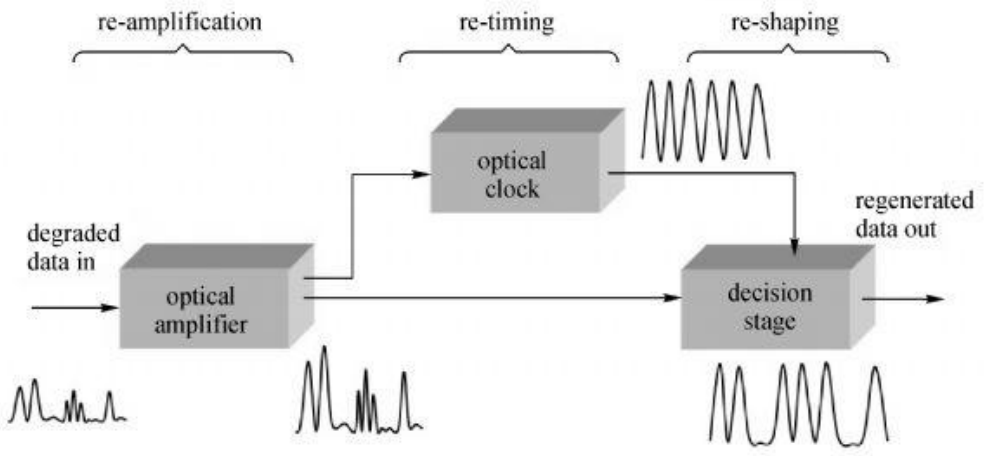

Fig. (1.2) *the 3R operation*

So, in order to overcome the data speed limitations caused by the electrical processing of signals at regenerative centers, there must be optical equivalent of electrical processing devices (3R). If the 3R centers become all optical, the communication system can make use of the total available bandwidth offered by the optical fiber channels. This will eventually results the high speed data communication and signal processing.

As the demand for high data rate increased, researchers come out with different optical multiplexing techniques. The development of in-fiber amplification (EDFA), tunable laser inexpensive, integrated arrayed-waveguide, grating-based multiplexers and de-multiplexers has given the momentum for optical multiplication techniques. The widely used multiplexing techniques are wave length division multiplexing (WDM) and dense wavelength division multiplications (DWDM).

The WDM systems using amplitude modulation techniques (On-OFF Keying (OOK)) and Quadrature Amplitude Modulation (QAM) have so far been able to meet the growth of traffic in optical network communications [30]. But the currently deployed communication systems and fibers are close to the maximum capacity that it can handle. As mentioned before, the data traffic on the optical fiber network is now growing by two orders of magnitude per decade. The aggregate optical network traffic, both historic and predicted, is shown in figure (1.3) [18]. Figure shows some data for fiber capacity on this total demand curve for both research and commercial fiber links. The straight lines indicate trends for commercial systems, which show tremendous growth in bandwidth. WDM adoption in yearly time frame now reached saturation due to the limitation in the number of practical WDM channels, as well as the data rate in each of them.

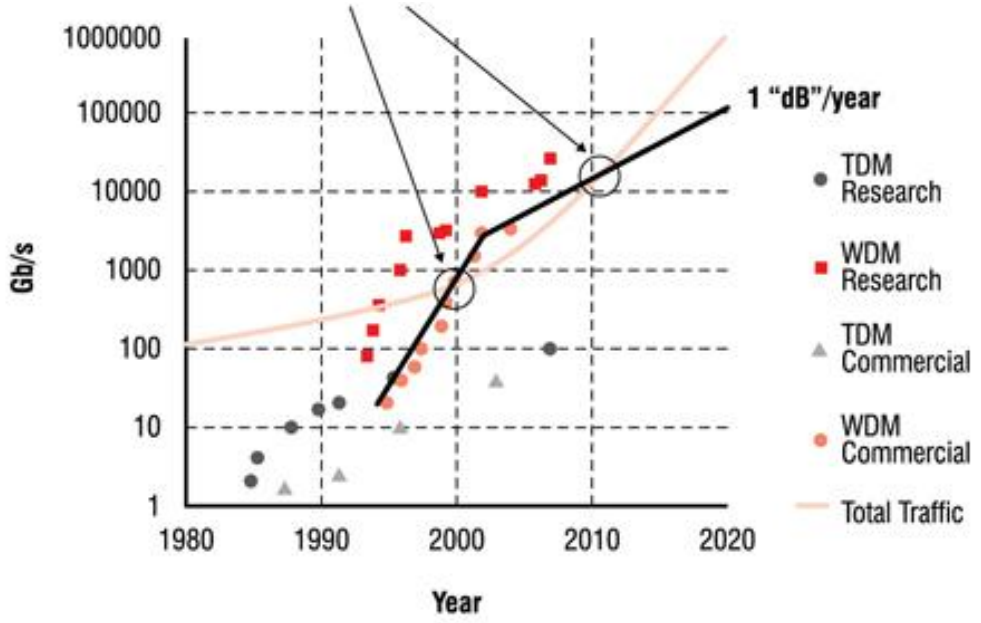

Fig. (1.3) *Different multiplication scheme and yearly data rate progression [22]*

The two arrow marks shown in this figure is the total traffic available to satisfy the trend for commercial needs in year 2000 and 2010.

Multiplexing is a technique in which multiple information channels can be transmitted simultaneously in a single fiber. Normally it is a single mode fiber (SMF). Wavelength Division Multiplexing (WDM) is based on assigning a different wavelength for each communication channel. At the receiver the different wavelength or the 'color channels' are de-multiplexed and then directed to an optical detector/receiver. The first generation of WDM technique incorporates 8 to 16 wavelengths on one fiber (total capacity ranges from 20 to a maximum of 40Gbps [31].

And now the WDM technology has migrated to the Dense Wavelength Division Multiplexing (DWDM) [32]. It is expected that next generation WDM systems will carry 80 channels. Though 80 channels are the standard, but it is not necessary that a given link always uses all the 80 channels. Depending on the service provider, bandwidth requirements the number of channels actually used changes. 100 Gbps data rate is routinely installed per fibre per channel in a WDM system. High data rate communication link can be done by 25 Gbaud combined with polarisation mode multiplexing (PM) is the Quadrature Phase Shift keying (PM-QPSK) modulation scheme [33]. It is possible to move to 10 Tbps (Terra bits per second) in practice with super channel polarization-multiplexed Quadrature amplitude modulation (PM- 16QAM). At present100 Gbps for each 50 GHz spaced DWDM channels. So the spectral efficiency is 2 bits/sec/Hz. By 2018, it is expected to have 400Gbps roll out. This could occupy 75 GHz or more depending on the pulse shaping techniques going to use and will give a spectral efficiency of 5.3 [34]. 40 GHz electronics emerged just after the 10G, but it was made obsolete by the PM-QPSK, which could deliver 100G with 25G electronics [35]. The electronics speed up to 100Gbps has been reported for opto-electronics applications [36]. The WDM and DWDM networks permit the data rate in the order of terabits. So there emerge the requirements for high speed regenerative repeaters. As mentioned before the electronic regenerative repeaters are introducing network delay, more power consumption and making the communication link more costly.

1.3 Energy Efficiency in Optical Signal Processing

It has been noted that the internet traffic is growing all over the world. The annual growth ratio of the traffic is nearly >250 % for the past decade. The above demand is widely believed to continue at least for another decade or more because of the very strong demands to high-definition video contents for future [37]. It

shows that there must be very effective and rapid technological development to overcome such an exponential growth of the internet usage. A well-known statement made by Paraschis and Gerstel [37] may be mentioned here, "Twenty homes in 2010 would generate more traffic than the entire 1995 Internet backbone". The electricity consumption of communication networks has shown a growth rate of 10% per year over the last five years, with its relative contribution to the total worldwide electricity consumption increasing from 1.3% in 2007 to 1.8% in 2012 [38]. It has been estimated in year 2006 that the total electric power consumption of entire IP routers in Japan was approximately 1% of Japan's total electricity consumption [38]. This is calculated without considering the power consumption for air-conditioning the network equipment. It also shows the power consumption by the electronic IP network high-end core-/edge-routers is directly proportional to the internet usage. The figure (1.4) shows the actual picture of the above statements. To offset this growing trend, research efforts have focused on photonic alternatives to provide improved performance with lower material and energy costs. This concept of "green photonics" is driven by several beneficial properties of optics [39]. In this paper the authors report that the green photonics can support single-channel data rates well beyond 100Gb/s in a single element with photonic materials with femto-second response time. Another report shows [40] an energy saving of ~*0*.5 nJ/bit for the elimination of an optical-electrical-optical (O/E/O) conversion process by optical signal processing methods. It has been estimated that, the use of optics instead of electronics could reduce the power consumption of access points by a factor 3 to 8, another reduction of 20% to 50% optical network terminal compared to electronics system can be achieved by the improved design of optical system [41]. More details of the same are explained below.

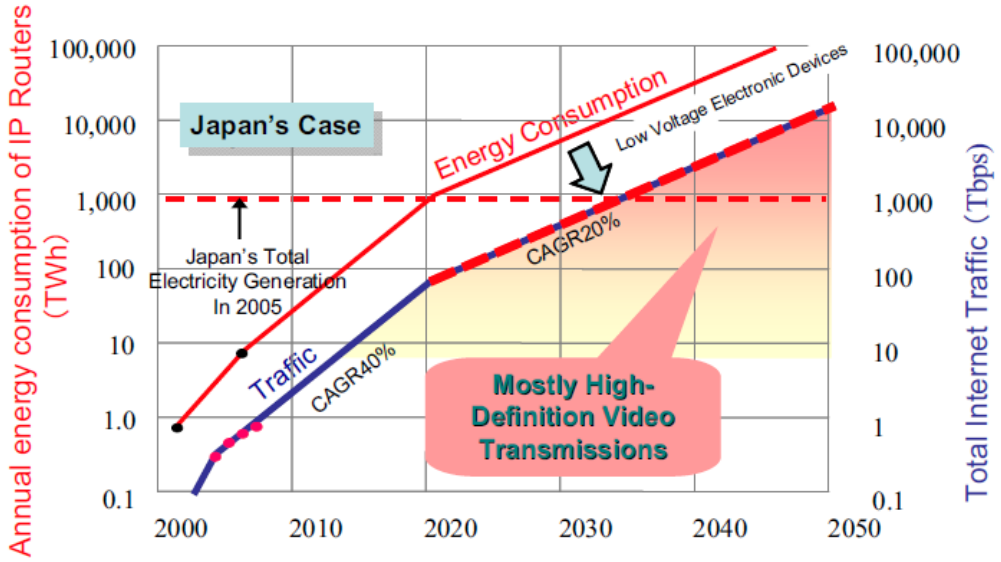

Fig. (1.4) *The annual internet traffic growth versus the energy consumption [38]*

The total energy consumed to execute a signal processing function is calculated by the number of high-power lasers required. The various losses in fiber optic systems incurred are the coupling and filtering losses. The addition of high-power optical amplifiers limited with the pump-laser efficiencies often greatly increase the power consumption, and number of components requirement for the fiber optic communication system. The large possibility of green photonics can be achieved by utilizing nonlinear processes that require a minimum number of high-power pump lasers. In order to make energy efficient the optical signal processing, each optical technique or processing is compared using the total optical energy per bit required to achieve the desired function. By using the above method, wide variation in equipment and experimental setups used can be minimized. An example is, amplified and filtered pump laser can be exchanged with a single standing high-power laser unit eliminating a high-power amplifier and a filter [40, 41].

It has been reported that [39, 42-47] there are wide variety of photonic materials capable of providing green operation through optical signal processing. These include highly nonlinear specialty fibers, periodically poled lithium niobate (PPLN) waveguides, chalcogenide glass chips and silicon waveguides. Silica-based highly nonlinear fiber (HNLF) is the most common choice for energy efficient optical signal processing. There are other fiber structures and materials using commonly are the photonic crystal fiber, bismuth-oxide-doped fiber (Bi-HNLF) and chalcogenide fibers. It is to be noted that fiber based devices have the advantages of easy integration to existing fiber networks and it can be implemented with low cost fiber components. All these fiber structures mentioned are being used for variety of all optical applications such as wavelength conversion, regeneration, and format conversion. As the silicon processing is a very mature technology, the silicon photonics has become one of the driving goals of current green photonics research today. Both silicon (Si) and chalcogenide-based alternatives are widely used for direct chip-level integration. Impressive results are being reported by the potential of waveguide (WG) devices in ultrahigh-speed optical signal processing up to 1.28 Tb/s [48, 49].

Another area of energy efficient all optical signal processing is the integrated photonics, as it allows for more cost-effective production and easier packaging. Its smaller chip size assists in realizing faster electro-optic interaction and less energy-consuming photonic devices [50]. Integrated photonic systems are operating as a very efficient signal processing system by cascading many low power basic functional components on a single chip.

1.4 The Optical Signal Processing

As mentioned, the exponential increase in the demand for internet usage is mainly focusing on high capacity networking in support of a variety of

applications like 3-D multimedia entertainments, telemedicine, medical imaging, high speed video streaming, video conferencing, Internet of Things (IoTs), cloud computing etc. [51]. The Medical Optical Signal Processing (MOSP) is to enhance the capabilities of present and future medical imaging system and technology [52]. The medical imaging systems are developed for military, surveillance, and commercial applications. Now a day the medical community is favoring to the imagery information than the more costly and complicated invasive procedures. In medical imaging system, the optical signal processing (OSP) technology has shown an excellent signal to noise ratio and different pattern recognition rates of over, 2000 comparisons per second [52]. The image processing helps an increase in imagery size and high resolution depth.

All the above mentioned technologies need a physical medium which should support the high bandwidth operations. The medium must also be able to support secure transmission, reception and storage of the data. The technological possibility for the same is Fiber Optical Communication (FOC), where the Laser or LED is the transmitter and optical fiber is the medium or channel and the Photo Detector (PD) is the receiver. We have already mentioned the advantages of optical fiber. But there are some disadvantages also for the optical fibers. Those are, there must be very precise manufacturing technologies, and fibers are very fragile and need good protection around the cable [53].

The optical signal processing has strong potential for numerous applications like ultrahigh-speed optical communications, metrology, optical sensing, high speed audio/video and image processing and optical computing [54]. Optical pulse shaping is important for a variety of optical communication applications [55]. The pulse shape changes from Gaussian and hyperbolic secant shapes to parabolic or triangular pulses are finding many applications in optical signal processing and optical signal manipulation [55].

As discussed in the broadband data communication networks the information is usually transmitted by means of optical fibers. At the transmitter, electrical signal data is converted to the optical domain and at the receiver the reverse operation takes place. More number of fibers can be accommodated to meet increasing demand for high bandwidth capacity. The different multiplexing and modulation techniques to meet the demand have already been mentioned.

Even though the fiber optics communication support the high bandwidth operations, there are two main problems faced by the signal transmitted through the optical fibers. Those are the signal attenuation and dispersion. Signal attenuation means the power loss (0.2dB/KM @1550nm), and dispersion means the pulse spreading. Both the attenuation and dispersion limit the quality (Optical Signal to Noise Ratio, OSNR) of the signal received at the receiver [56]. In order to overcome this power loss and dispersion, the signal transmitted should be corrected periodically. The periodic signal power boosting and dispersion compensation centers along the transmission path are called regenerative repeaters. The regenerative repeaters will first convert the optical signal to electrical (O/E conversion), then do the 3R (Re-Amplify, Re-Shape and Re-Time). After the 3R, again the electrical signal converted back to optical (E/O) and re transmitted to the next regenerative center or to the final receiver [57]. The above process, Optical-Electrical-Optical (O/E/O) process is making the communication system costly; introduces time delay and more power consumption [57]. Moreover the electrical signal processing makes the 3R regeneration process difficult with speeds exceeding 100Gbps [58].

Here comes the need for all optical signal processing circuits, which do not require O/E and reverse operation at the regenerative receiver, making everything optical so as to transmit all data optically from transmitter to the final

destination. So in order to make the 3R regenerative repeater to work all optical, there must be optical amplifier [59] (Re-Amplify), optical pulse shaping circuits (Re-Shape) and optical data clock recovery circuits (Re-Time) [60].

All-optical regenerators reset to their original shape the signals that have accumulated noise and distortion due to propagation in fibre communication lines. We have mentioned that the optical regenerators that enable signal re-amplification combined with re-shaping (2R), and even re-timing (3R) are used to limit signal degradation by noise sources in optical communication systems. In both cases, it requires a reshaping optical device having a suitable transfer function (TF) so that the dependence of the output optical power P_{out} versus input power P_{in} is as close as possible to a step function [58]. All-optical regeneration is a very valuable and necessary functionality that can potentially extend the distance of digital-signal transmission for a larger network, by overcoming the various fiber losses. All-optical regenerators must have the capability of signal processing at ultra-high speeds and potentially lower power consumption. The 3R regenerators perform the retiming function and reducing timing jitter. An SPM based 3R regenerators can be built by adding a modulator to the 2R regeneration scheme [61]. Another work seen is Combination of a dispersion-compensating fiber and a fiber grating is found to be effective in suppressing timing jitter [62].

Earlier the regenerators providing an output power depending only on the instantaneous input power and they do not improve the bit error ratio (BER) of a signal processing by it [63]. That is, a noisy signal that enters such an optical regenerator exits with a BER that is $\leq$ input BER. But it has been demonstrated that [64, 65] bit error ratio improvement of a noisy signal from $3x10^{-6}$ without regenerator to $2x10^{-10}$ with regenerator. A 3R regeneration of DPSK signal is reported [66] by using a Mach-Zehnder interferometer with 1-bit delay is added before an SPM-based 2R regenerator. It converts DPSK signal into an OOK

signal. The output is fed into a second fiber together with an optical clock. The XPM transfers data to clock pulses, regenerating DPSK signal. The reported highest data rate achieved for single channel all-optical regeneration is 640-Gbit/s in a periodically poled lithium niobate waveguide (PPLN) [67]. Another demonstration reported is the simultaneous all-optical regeneration for four 160-Gbit/s WDM and PDM channels, using FWM in a HNLF [68]. These regeneration performances are confirmed by BER measurements showing improvements of 1.5-1.9 dB for the four data channels.

The most commonly used optical amplifier is Erbium Doped Fiber Amplifier (EDFA) in 'C' band. The optical pulse shaping circuit can be implemented by fiber Bragg gratings (FBGs) based technologies, which will be discussed in the following chapters. And finally the re- timing can be done by many methods, like optical PLL or optical tank circuit [69, 70]. The optical data clock recovery using the optical tank based on FBGs circuit will be discussed in the following chapters.

As explained, the increasing demand for higher data transfer rates and larger bandwidths results the development of optical networking technologies and the implementation of optical networks. The optical switching is one of the most important technologies for establishing the all optical networks [71]. The optical switching includes, optical circuit switching (OCS), optical burst switching (OBS) and optical packet switching (OPS) [72]. The monolithic integration of the optical switch fabric, keeping the high-speed data in the optical domain allows lower power consumption and smaller real estate, eventually reducing the cost [73]. The major equipment that can be used for the optical switching are Optical Add-Drop Multiplexing (OADM) and optical cross connect (OXC). Due to the increasing requirements for the network flexibility, reconfigurable Optical Add-Drop Multiplexing (ROADM) attracts a lot of attention [72, 73].

1.5 FBG in Optical signal processing

Fiber Bragg grating (FBG) structures have found wide applications in optical communications and sensing. Fiber gratings are periodic or quasi-periodic structures that are usually generated in optical fiber core/cladding of photo sensitive fiber with laser inscription techniques. Due to their natural in-fiber characteristics, fiber gratings can serve as a perfect platform for all-optical signal processing in optical communication systems. They can directly process optical signals in optical fiber without the need for coupling/re-coupling alignments required by bulk-optics or chip based devices. These advantages are making fiber grating a low-loss, stable, cost-effective and ultra-fast solution for optical signal processing. The FBG can also be used a very good signal processing component as it offers design flexibility for arbitrary spectral characteristics. Here we propose the FBG based FPs designed and fabricated for various signal processing tasks like optical differentiation, Optical integration, optical pulse shaping, optical clock recovery and so on.

A pulse shaping application by using FBGs are shown recently [6, 55, and 74]. The pulse shaping offers an important solution to generate a desired pulse profile from a different one. A FBG working in transmission is designed and fabricated for saw-tooth pulse generation from usual Gaussian-shape pulse. In this application the grating has uniform coupling coefficient but with complex period variation. The authors reported that various waveforms such as flat-top, bright parabolic and dark parabolic pulses can be generated using this approach, illustrating the capability of these phase-modulated FBGs to obtain sophisticated spectral responses.

Another application of FBG in signal processing is the data format conversion. All-optical networks may include a variety of modulation and data formats. Data format conversion enables an important interface technology at the nodes of different optical networks technologies such as wavelength division multiplexing (WDM) and optical time division multiplexing (OTDM) networks. The format conversion can be done through either time-domain waveform processing or frequency domain spectrum tailoring. As mentioned, the FBGs are very flexible to design and realize almost arbitrary spectral response and therefore are very promising candidates to serve as spectrum tailing based converters. One example is given in [74], shows FBG designed and fabricated for carrier-suppressed return-to-zero (CSRZ) to non-return-to-zero (NRZ) conversion. Another example [74] shows FBG designed and fabricated for multi-channel RZ to NRZ format conversion. Here the spectral response of this FBG is designed according to the algebraic difference of the optical spectra of isolated NRZ and RZ pulses. It has also been reported that [75] designing a single grating to realize multi-channel CSRZ-NRZ conversion. Numerical investigations and simulations show that optimally-designed FBG is capable of converting the input RZ-OOK/DPSK/DQPSK signals with different duty cycles to NRZ-OOK/DPSK/DQPSK signals with high Q-factor [76]. While we consider the optical signal processing components, the use of a suitable FBG with linear chirp in the grating period has proved successful to increase the operation bandwidth of transmission FBG filters while keeping realistic coupling-strength specifications [77]. High-order optical differentiators have been designed and fabricated using the above strategy [78].

Design of FBG-based optical signal processors offering operation bandwidths well into the THz regime (corresponding to sub-picosecond time features) have been reported recently [79, 80]. These high speed FBG structures

are based on especially-apodized chirped (C)-FBGs working in transmission. The proposed FBG is with quadratic spectral phase response with linear or quasi linear chirp along the grating length. The FBG Reflectivity is set to 99.9999%, corresponding to a transmission notch of 60dB and $\Delta n = 0.72*10^{-3}$. The linearly chirped FBG structure designed and simulated is used for 1ps flat-top (rectangular-like) optical pulse shaper from a 150fs-FWHM Gaussian input. Optical signal processing techniques using long-period gratings (LPGs) in terahertz (THz) - bandwidth working in transmission are also demonstrated recently [81]. But comparing with FBG devices, LPGs suffer from serious limitations, particularly instabilities and high sensitivity to environmental fluctuations, and a significantly larger footprint for implementation in integrated circuits.

1.6 Current status and the present research objectives.

A temporal integrator is a device that is capable of performing the time integral of an arbitrary input waveform and is characterized by its ability to store energy in one form or another (e.g. optical, electrical). As mentioned, the biggest advantage of optical communication technology is the availability of huge bandwidth. Optical systems and components have the capability to perform a large number of complex mathematical operations per unit time. Optical signal processing is capable of doing large number of parallel computations simultaneously. The speed of data processing optically is several orders of magnitude higher than that achievable by the electronics components and systems. So the all-optical circuits for complex mathematical operations, signal processing, and data networking can overcome the speed limitations of electronic-based systems. In order to process the signal in all optical domains, there must be equivalent basic building block as that of electronic processing of signals [75, 82]. Integrators and differentiators are good examples for basic signal processing components. Thus, the design and implementation of these fundamental optical

devices is the first step towards the realization of all-optical signal processing circuits.

There are many proposals and implementation of optical integrators in various literatures. One literature shows [83] the functionality of an ideal integrator over a finite time window using a linear optical passive FBG filters. In this FBG integrator a weak-coupling uniform FBG working in reflection will give a constant impulse response. The simulation results are based on a FBG of length 1cm with reflectivity~13%. The main drawback seen in this approach is the energetic efficiency (ratio of the output signal energy to the input signal energy of the proposed optical integrator) is very less, nearly $2.3*10^{-3}$ %. The energetic efficiency depends on the spectral bandwidth of the optical signal to be processed; a lower energetic efficiency is obtained when processing a waveform with a broader bandwidth since in this case, a larger portion of the input signal spectrum is transmitted than reflected. The energetic efficiency increases to 0.3% when the FBG length becomes 10cm. It is to be noted that, in the weak coupling regime, where the reflectivity is very low (R<15%), the grating length L is of the order of $6\tau c/2n_{eff}$, where the exponential function is limited to a duration of 6τ, c is the speed of light in a vacuum, and n_{eff} *is* the average refractive index of the grating and τ is the time constant. Thus, from $\tau \geq \Delta t$, we can deduce that $L \geq 6\tau\Delta t\, c/2n_{eff}$must be satisfied for accurate operation in the weak coupling regime [83], where Δt is the time period of the input signal that is to be processed.

Another proposal [84] is not restricted to a weak or strong coupling regime and performs a close to ideal integration of few-picosecond and sub-picosecond pulses. The main drawback seen in this approach is that long FBGs are required for accurate integration of long pulses (100ps or longer). Energetic efficiency of eight FBG integrators with lengths of 24, 12, 6, 3, 1.5, 0.75, 0.375, and 0.1875 cm are simulated and all of them with the same maximum reflectivity of 80% when applied over the first derivative of a 10ps Gaussian pulse. It has

been noted that the energetic efficiency is very low for long length FBGs. Fabrication of long length FBGs is another major task of the above proposal.

Another design [85] is based on a phase-shifted fiber Bragg grating (FBG), in which two FBGs form a resonant cavity. In the resonant cavity the light resonates between two FBG reflectors that have relative π-phase shift. The phase shift ensures that the constructive resonance condition occurs at the center of the FBG reflection bandwidth. But here the FBGs should provide a minimum reflectivity of 99.99%, which leads to high fabrication challenges in practice.

Finally a temporal integrator is fabricated by incorporating an active medium into a resonant cavity configuration [86]. Here two superimposed chirped FBGs were photo-inscribed into a specialty high-gain (~40 dB/m) fiber co-doped with Er and Yb with photosensitive inner cladding (ErYb-302, INO, Canada) loaded with Deuterium. The Grating writing was done by scanning a chirped phase mask (period chirp of 0.5nm/cm) with a laser beam from a frequency-doubled Argon ion CW laser (244 nm and power of 50 mW). The above scheme has high cost and high fabrication complexity.

In this thesis we are proposing two FBG-made FP mirrors, with cavity length (δL) limits the minimum achievable FP cavity length and thus also the cavity round-trip time *T* that determines the integrator processing speed. To get an integration time window of $T<10$ ps with corresponding processing bandwidth of tens of GHz, we need a mirror spacing of 1 mm or less when considering a cavity with refractive index of 1.45. Such short FBGs are fabricated by us without using a gain medium. We have easily fabricated two FBGs of length 1 mm each with a cavity length of 1mm using a novel shadow mask short FP-FBGs cost effectively [87]. Moreover, our proposal of optical integrator using FP-FBG filters, whose

cavity length can be adjusted very easily by changing the separation between the two FBG writing for processing signals of different spectral width.

A first-order optical temporal differentiator is a device that provides the first-order derivative of the complex envelope of an arbitrary input optical signal. This evaluates the real time derivative of the input optical signal intensity. Many works and implementations have been seen in different literatures for optical differentiators using long period gratings (LPGs) and FBGs. A FBG-based differentiator, however, has a comparatively higher tolerance to the environmental changes [88] although the LPG approach has been proved to have a good performance in a regime of huge bandwidths (up to 19 nm) [89]. But the transmission spectrum of an LPG is more difficult to be tailored as compared to that of an FBG. However the FBG based optical differentiator needs very complex fabrication techniques as it need very high reflectivity of 99.9999%, corresponding transmission dip of 60dB with very high coupling coefficient ~6600/m for an FBG length of 10cm [90]. Another technique seen in literature is phase shifted FBG differentiators [91, 92] but of complex fabrication procedure. Another drawback seen in the above method is the spectrum of the signal to be differentiated must lie within the FBG reflection resonance dip which limits the differentiation bandwidth to 20 GHz. There has been another simulation of all-fiber approach for optical time differentiation based on specially apodized linearly chirped FBGs (LC-FBGs) working in transmission [93]. They have overcome the bandwidth limitations FBG-based solutions for all-optical time differentiation but the authors stating about very complex fabrication procedure of the same. Finally a 25 THz first order optical differentiator has been demonstrated [94] using a wavelength selective fiber asymmetric directional coupler with high cost and high complex fabrication procedure.

We are proposing Fabry-Perot filters based on FBGs (FP-FBGs) for all optical differentiators. The most important advantage of FP-FBG based filters are its ultra-high bandwidth. The narrow bandwidth (FWHM) seen from the fabricated spectrum of FBGs and FP-FBGs are discussed in chapter 4. This ultra-narrow bandwidth of FP-FBG filters can be made use for high speed and high bandwidth applications. Moreover the narrow bandwidth response of filter can increase the energy efficiency of the processing. Here the FP-FBG based differentiators are working in transmission to avoid the use of optical circulator which will add the coupling loss and cost of the system. In addition to that the FBGs in reflection are more sensitiveto the presence of noise in the grating amplitude and phase profiles than in transmission.

All-optical clock recovery is a key ingredient of all-optical signal processing such as 3R generation and network synchronization in the present and next generation high speed optical networks [95, 96]. A clock recovery unit is an important block for a high speed optical communication link as it provides synchronization for all receiver functions. It is highly desirable that the clock recovery is performed in the optical domain itself as it reduces the relatively high latency of electronic circuits [97]. The recovered clock signal is used for much functionality that requires synchronous operations, such as reshaping and retiming, OTDM de-multiplexing, modulation format conversion, and signal processing. The high-speed synchronization is a serious challenge for the current and development of future Optical Networks, whether it is addressed to point-to-point optical links or Optical Packet Switching (OPS) environment [98]. These optical burst/packet switching is expected to improve the utilization of the network resources through statistical multiplexing and reduce latency in future optical networks. Development of a reliable clock recovery unit, efficient to extract the clock signal from short asynchronous bursts at high data rates, is essential for processing and routing the packets. All-optical clock recovery (CR)

circuits are supposed to play a critical role in current and future high-speed all-optical networks as a stable and low-jitter synchronization signals will be required in several network sub-systems like receivers, regenerators etc.

Several optical timing extraction techniques suitable for high speed operation have been demonstrated [100]. Electrical data clock timing extraction circuits usually use a phase-lock loop (PLL) configuration, where a microwave mixer acts as a phase detector. The speed of operation of such PLL circuits is limited by the phase detector to about 40 GHz (very high timing resolution is required as the bit-time slot is very short) [101]. Another problem faced with PLL based clock recovery is that the locking time works inversely with the timing jitter. The advantage of using a PLL is low relative phase error as the phase of the incoming signal is constantly compared with the phase of the local oscillator. There is report of a self-clocking method that allows for fast synchronization, low timing jitter and highly stable clock performance for time-de-multiplexing functions. The method consists of inserting a 10 GHz clock pilot signal at the transmitter, and extracting this pilot signal at the receiver [102]. The above method is simple and scalable but has the disadvantages of manufacturing complexity and cost. The injection locking utilizes multi-electrode laser diodes (LDs) or optical inverters which switch between TE and TM modes. Here the output repetition frequency is locked to that of an injected optical pulse train. Using this technique, 5-GHz and 10-GHz clocks were generated all-optically [103]. The optical clock recovery by PLL and injection locking are intriguing since the clock is generated all-optically. But the disadvantages faced with these are rms jitter and relative phase error, which limits the operation speed up to 50Gbps [104]. Other methods reported are all-optical clock recovery schemes based on mode-locked Erbium fiber laser [105] and nonlinear optical fiber loop mirror (NOLM) regenerator [106]. But it has insufficient performances for 3R

operations though it finds applications for very long 1R repeated transmission systems. In another simulation work seen in literature two FBGs are used in between an EDFA and transmitted 10Gbps; 25Gbps and 40Gbps signal transmitted around 8km with BER improvement. No experimental validation is shown here [107]. Another clock recovery method seen [108] is a wavelength-converted signal is sent into a FP filter which is made of a solid glass slit with high reflective film coated on both sides. In this study, the authors demonstrated 100 GHz CR with an improved version of FP and SOA scheme. The wavelength conversion is employed before clock recovery to locally perform the precise wavelength matching of the FP transmission peaks. A programmable wavelength selective switch (WSS) filter is used to reshape the wavelength-converted signal. The spectral peaks of the wavelength converted signal are tuned to match the transmission peaks of the FP filter. In the SOA, the data signal is wavelength converted to the CW wavelength of λc by the combined effects of cross gain modulation (XGM) and cross phase modulation (XPM). The above method seems to be complicated and it has been tested only at laboratory set up. Another demonstration seen in literature is [109] passive all-optical clock recovery technique based on spectral Phase-only (all-pass) optical filtering for RZ-OOK data signals at 640Gbps OTDM. The phase filtering can be practically implemented using a variety of technologies such as line-by-line optical pulse shapers, fiber Bragg gratings (FBG), thin film filters, photonic ring resonators, and photonic crystals [109]. They reported that a line by-line optical pulse shaper has been used to retrieve the phase of the individual spectral lines. Recovering the clock signal requires a phase-coherent RZ-OTDM signal a wavelength conversion of the original incoherent OTDM signal. Therefore, the multiplexed 640Gbps OTDM signal has undergone a wavelength conversion by a polarization-rotating Kerr switch to obtain the phase-coherent OTDM signal. The converted RZ signal is then amplified by an EDFA before being input to the phase-only filter, then line

by line phase shaper. Even though there is a marginal improvement in the quality of the recovered clock, the CR system becomes complex and very costlier. Another FBG based Clock recovery demonstrated the CR with 40 Gbps RZ-DPSK by custom made periodic FBG filters [110]. They made FBG filters in the entire C band with 100GHz channel separation. Even though there is a slight OSNR improvement reported, how FBG could recover the clock at 40Gbps is not shown explicitly. As they reported the custom made FBG array in the entire C band makes the CR system costlier and fabrication challenges.

Here we are proposing a passive all optical clock recovery circuit based on FP-FBGs. The optical clock recovery through direct filtering out of the frequency components of the clock signal with Fabry-Perot (FP) filter is very simple and very fast. The clock can be recovered within few bits, and the wavelength is transparent with respect to the data signal. Moreover, the environmental sensitivity is relatively low since the FP filter is an optical passive tank circuit. Clock recovery does not necessarily require a self-pulsating arrangement. While the scheme is fully passive and uses no nonlinear components (such as an SOA), the operation speed of the method is virtually unlimited (depending on resonator length). Fabry-Perot filters based on fiber Bragg gratings are strong candidates for optical clock recovery, even in WDM passive optical networks. Here we report all optical clock recovery at 10Gbps, using a Fabry-Perot filter consisting of two Bragg grating reflectors. Unlike bulk optical filters, the FBG-based FP filters possess high mechanical stability and ease of tuning.

1.4 *References*

1. E. Alan, Willner, Salman Khaleghi, Mohammad Reza Chitgarha, and Omer FarukYilmaz,"*All-Optical Signal Processing*", Journal of Lightwave Technology ,Vol. 32, pp 660-680, (2014).

2. Ivan Glesk "*Approaches to Ultrafast All-Optical Signal Processing Asia Communications and Photonics Conference and Exhibition Technical Digest (CD)*" Optical Society of America, paper FR2.(2009)

3. K. Sergei, Turitsyn and Sonia Boscolo ,*"All-Optical Nonlinear Fibre Signal Processing"*, Photonics Research Group, School of Engineering and Applied Science, Aston University Birmingham B4 7ET, UK, (2009).

4. *"Cisco Visual Networking Index: Forecast and Methodology 2015–2020"* -White Paper (2016).

5. *"Measuring the Information Society Report"* International Telecommunication Union (ITU), (2014).

6. M. Andrew Weiner*"Ultrafast optical pulse shaping: A tutorial review"* Optical Communication, Elsevier, Volume 284, Issue 15, pp 3669–3692, (2011).

7. David Richardson *"Pulse Shaping in High Power Fiber Laser Systems"*, High-Power Fiber Lasers and Amplifiers (OWU) Optical Fiber Communication Conference, (2008).

8. R.K. Shevgaonkar *,"Analysis of Signal Distortion in Optical Fiber"* , Department of Electrical Engineering IIT, Bombay, NPTEL Lecture 8.

9. W.Vincent, S. Chan, "*Free-space optical communication"*, Journal of Light Wave Technology Volume: 24, Issue: 12, pp 4750 – 4762, (2006).

10. DjafarK.Mynbaev, Lowell L.Scheiner, *"Fiber Optic Communication Technology"*Prentice Hall, USA (2000).

11. Biswanath Mukherjee, "*Optical WDM Networks"*Springer, USA (2006).

12. L. Roger Freeman,"*Fundamentals of Telecommunications"*IEEE Society Press, John Wiley & Sons, USA (2005).

13. B.Sartorius,*"3R regeneration for all-optical networks"*, Proceedings of 3rd International Conference on Transparent Optical Networks, (2001).

14. T. K. Woodward, T. C. Banwell, *"Signal processing in analog optical links."*, A. Agarwal Avionics, Fiber-Optics and Phototonics Technology Conference, AVFOP '09. IEEE,(2009).

15. Primary Interviews, Transparency Market Research "*Global photonics market by geography, size and forecast, 2013 vs. 2020 (Value %)" Courtesy of Transparency Market Research, (2015).*

16. *"Photonics industry report: current situation 2015*" AG Market Research Photonics, A a report compiled by the German industrial associations Spectaris, VDMA, ZVEI, as well as market analyst group Optech Consulting, and BMBF, the German Federal Ministry for Education and Research,(2015).

17. Developed by the U.S. National Science Foundation's National Center for Science and Engineering Statistics (NCSES), (2015).

18. L. Milan,Mašanović A. Coldren*"Photonic Device Technology for Coherent Optical Communications"* Freedom Photonics LLC and University of California, Santa BarbaraLarry, University of California, Santa Barbara, (2012).

19. *"Beyond NOFN to Digital India: A case for BharatNet*" Report of committee on National Optical Fibre Network, (2015).

20. Walt Kester*"Which ADC Architecture Is Right for Your Application?"* Analog Dialogue 39-06, (2005).

21. C. David Chaffee *"The Coming Market for Optical Fiber and Cable"* Photonics Spectra Vol 46 pp 61-64, (2012).

22. A.M Adel Saleh, Jane M Simmons "*All-Optical Networking—Evolution, Benefits, Challenges, and Future Vision"*Proceedings of the IEEE, Volume: 100, pp1105 – 1117, (2012).

23. M.S. Borella, J.P. Jue, D. Banerjee, B. Ramamurthy, B. Mukherjee, *"Optical Components for WDM Lightwave Networks,"* Proceedings of the IEEE, vol. 85, no. 8, pp 1274-1307, (1997).

24. Shigeki, Watanabe Reinhold, Ludwig Fumio,Futami Colja,Schubert Sebastian, Ferber Christ,Boerner Carsten, Schmidt-LangHorst, Joern Berger and Hans-Georg Weber, *"Ultrafast all-optical 3R-Regeneration IEICE TRANSACTIONS"* ,Electronics Vol. E87-C No. 7 pp 1114-1118, (2004).

25. E.S. Awad,P.S. Cho, C. Richardson, N. Moulton,J. Goldhar,*"Optical 3R regeneration using a single EAM for all-optical timing extraction with simultaneous reshaping and wavelength conversion"* ,IEEE Photonics Technology Letters Volume: 14, Issue: 9, pp1378 – 1380, (2002).

26. Reza Salem, Mark A. Foster, Amy C. Turner, David F. Geraghty, Michal Lipson & Alexander L. Gaeta*"Signal regeneration using low-power four-wave mixing on silicon chip"*. Nature photonics 2, pp 35 – 38, (2008).

27. Nakazawa, Masataka, Kikuchi, Kazuro, Miyazaki, Tetsuya *"High Spectral Density Optical Communication Technologies"*, Springer, Chapter 2, pp 42-48, (2010).

28. Yong Liu, Shangjian Zhang, and YongzhiLiuf. Gomez-Agis, E. Tangdiongga, "*High-Speed Optical Signal Processing for Telecom Applications*" and "*Wireless and Optical Communication Conference (WOCC)*" H. J. S. Dorren, (2010)

29. Masatoshi Saruwatari "*All-Optical Signal Processing for Terabit/Second Optical Transmission*", Senior Member, IEEE, IEEE journal on selected topics in quantum electronics, vol. 6, no.6, pp 1363-1374,(2000).

30. Jianjun Yu, Ming-Fang Huang, Dayou Qain, Lin Chen, Gee-Kung Chang, *"Centralized Lightwave WDM-PON Employing 16-QAM Intensity Modulated OFDM Downstream and OOK Modulated Upstream Signals*", IEEE Photonics Technology Letters, Volume: 20,pp1545 – 1547, (2008).

31. Krishna, M.Sivalingam**,** Suresh Subramaniam, "*Optical WDM Networks, Principles and Practice"*, Kluwer Academic Publishers, New York, Boston, London, Moscow, (2002).

32. Stamatios, V. Kartalopoulos *"Introduction to DWDM Technology: Data in a Rainbow"* Wiley-Interscience,(2000).

33. John Zyskind, AtulSrivastava, *"Optically Amplified WDM Networks Academic Press 2010"Coherent WDM Technologies"* Infinera Whitepaper (WP-CT-04-2016), (2016)

34. Jacklyn D. Reis, Vishnu Shukla, David R. Stauffer, Karl Gass *"Technology Options for 400G Implementation"* Optical internetworking forum,(2015).

35. Steven Gringeri, E.BertBasch,TiejunJ.Xia ,*"Technical considerations for supporting data rates beyond 100Gbps"*,IEEE Communication Magazine vol 2, pp 21-23, (2012).

36. J. H. Sinsky, A. Adamiecki, G. Raybon, P. Winzer, O. Wohlgemuth, M. Duelk, C. R. Doerr, A. Umbach, H. G. Bach and D. Schmidt, *"107Gb/s optoelectronic receiver with hybrid integrated photodetector and demultiplexer,"* in Proceedings of Optical Fiber Communication Conference (OFC) 2007, Anaheim, California, USA, PDP30, (2007).

37. *"Broadband Access in the 21st Century: Applications, Services, and Technologies"* Cisco white paper, (2011).

38. S. Namiki1, T. Hasama1, H. Ishikawal, *"Energy bottlenecks in future networks and optical signal processing"*, International Conference on Photonics in Switching, (2009).

39. Alan E. Willner, Omer FarukYilmaz, Jian Wang, *"Optically efficient nonlinear signal processing"* IEEE Journal of selected topics in quantum electronics, VOL. 17, NO. 2, MARCH/APRIL (2011)

40. R. S. Tucker, *"Switching and energy,"* presented at the Int. Conf. on Photonics in Switching, Pisa, Italy, Sept. (2009)

41. Esther Le Rouzic et.al, "*TREND towards more energy-efficient optical networks",* 17th conference on Optical Network Design & Modeling (ONDM) Brest, France, (2013).

42. F. Parmigiani, S. Asimakis, N. Sugimoto, F. Koizumi, P. Petropoulos, and D. J. Richardson, *"2R regenerator based on a 2-m-long highly nonlinear bismuth oxide fiber," Opt. Exp.*, vol. 14, no. 12, pp. 5038–5044, Jun.2006.

43. K. K. Chow, K. Kikuchi, T. Nagashima, T. Hasegawa, S. Ohara, and N. Sugimoto, *"Four-wave mixing based widely tunable wavelength conversion using 1-m dispersion-shifted bismuth-oxide photonic crystal fiber," Opt. Exp.*, vol. 15, no. 23, pp. 15418–15423, Nov. 2007.

44. W. Astar, C.-C.Wei, Y.-J. Chen, J. Chen, and G. M. Carter, *"Polarization insensitive, 40 Gbit/s wavelength and RZ-OOK-to-RZ-BPSK modulation format conversion by XPM in a highly nonlinear PCF," Opt. Exp.*, vol. 16, no. 16, pp. 12039–12049, Aug. 2008.

45. M. D. Pelusi, F. Luan, E. Magi,M. R. Lamont, D. J.Moss, B. J. Eggleton,J. S. Sanghera, L. B. Shaw, and I. D. Aggarwal, *"High bit rate all-optical signal processing in a fiber photonic wire,"Opt. Exp.*, vol. 16, no. 15, pp. 11506–11512, Jul. (2008).

46. J. Fatome, C. Fortier, T. N. Nguyen, T. Chartier, F. Smektala, K. Messaad, B. Kibler, S. Pitois, G. Gadret, C. Finot, J. Troles, F. Desevedavy, P. Houizot, G. Renversez, L. Brilland, and N. Traynor, *"Linear and nonlinear characterizations of chalcogenide photonic crystal fibers,"J. lightw. Technol.*, vol. 27, no. 11, pp. 1707–1715, Jun. (2009).

47. J. Hu, C. R. Menyuk, L. B. Shaw, J. S. Sanghera, and I. D. Aggarwal*,"Maximizing the bandwidth of supercontinuum generation in As2Se3 chalcogenide fibers," Opt. Exp.*, vol. 18, pp. 6722–6739, Mar.(2010).

48. T. D. Vo, H. Hu, M. Galili, E. Palushani, J. Xu, L. K. Oxenløwe, S. J. Madden, D.-Y. Choi, D. A. P. Bulla, M. D. Pelusi, J. Schroder,B. Luther-Davies, and B. J. Eggleton, "*Photonic chip based 1.28 Tbaud transmitter optimization and receiver OTDM demultiplexing"* presented at the OFC, San Diego, CA, paper PDPC5 (2010).

49. H. Ji, H Hu, M. Galili, L. K. Oxenløwe,M. Pu, K. Yvind, J. M. Hvam, and P. Jeppesen, *"Optical waveform sampling and error-free demultiplexing of 1.28 Tbit/s serial data in a silicon nanowire,"* presented at the OFC 2010, San Diego, CA, paper PDPC7, (2010).

50. L. Zhang and A. E. Willner, *"Micro-resonators for communication and signal processing applications,"* in *Photonic Microresonator Research and Applications* (Springer Series in Optical Sciences). NewYork: Springer-Verlag, Apr. (2010)

51. *"5G Systems",* Ericsson White Paper, (2015).

52. R. Barry Dydyk, Thomas M. Burke, David T. Carrott,*"Medical Optical Signal Processing, Enhancing the Quality of Care for the 21st Century"* PACMEDTEK '98 Proceedings of the Symposium on Pacific Medical Technology. pp 376-377, (1998).

53. *Dan Hewak, "Fabrication of optical fiber",* Academic Press, Elsevier Inc, Oxford, UK (2004)

54. Hoss in Abdeldayem, Donald O. Frazier *"Optical computing: need and challenge" Communications of the ACM",* Vol. 50 No. 9, pp 60-62, (2007).

55. Nicolas Forget*"Ultra short optical pulses: Shaping up"*Nature Photonics 4, pp 154 - 155 (2010).

56. G. P. Agarwal, *"Fiber-Optic Communication Systems",* 3rd Edition, JohnWiley & Sons Inc, New York, (2002).

57. Lianshan Yan, Alan E. Willner, Xiaoxia Wu, Anlin Yi, AntonellaBogoni, Z.Y. Chen, and H.Y. Jiang*"All-Optical Signal Processing for UltraHigh Speed Optical Systems and Networks"* Journal of Lightwave Technology Vol. 30,pp 3760-3770, (2012).

58. Masatoshi Kagawa, Hitoshi Murai *"Multi-format all-optical-3R-regeneration technology"* Technical Review Issue 219 Vol. 79 (2012).

59. S. Shimada, Hideki Ishio *"Optical amplifiers and their applications"* John Wiley &Sons, England, New York (1994).

60. T. Von Lerber a, S. Honkanen, A. Tervonen, H. Ludvigsen a, F. Küppers *"Optical clock recovery methods: Review (Invited)"* Optical Fiber Technology, Elsevier Vol. 15, Issue 4, pp363–372, (2009).

61. M. Matsumoto "*Performance analysis and comparison of optical 3R regenerators utilizing self-phase modulation in fibers"* IEEE JLT 22, 1472 (2004)

62. Lu Li,Pallavi G. Patki, Young B. Kwon, Veronika Stelmakh Brandon D. Campbell, Muthiah Annamalai , Taras I. Lakoba2 & Michael Vasilyev "*All-optical regenerator of multi-channel signals"* NATURE COMMUNICATIONS, DOI: 10.1038/s41467-017-00874-0

63. 9. M. Rochette, J. N. Kutz, J. L. Blows, D. Moss, J. T. Mok, and B. J. Eggleton, *"Bit error ratio improvement with 2R optical regenerators,"* IEEE Photon. Technol. Lett. **17**, 908-910 (2005).

64. P. V. Mamyshev, *"All-optical data regeneration based on self-phase modulation effect,"* in Proc. *of 24thEuropean Conference on Optical Communication, 1998* (IEE, UK, 1998), pp. 475-476.

65. Martin Rochette, Justin L. Blows, and Benjamin J. Eggleton *"3R optical regeneration: An all-optical solution with BER improvement "* OPTICS EXPRESS / Vol. 14, No. 14 /10 July (2006).

66. M. Matsumoto, *A Fiber-Based All-Optical 3R Regenerator for DPSK Signals* IEEE PTL 19, 273 (2007).

67. Antonella Bogoni, Xiaoxia Wu, Scott R. Nuccio, andAlan E. Willner, *"640 Gb/s All-Optical Regenerator Based on a Periodically Poled Lithium Niobate Waveguide"* JOURNAL OF LIGHTWAVE TECHNOLOGY, VOL. 30, NO. 12, (2012).

68. Wang, Ju; Ji, Hua; Hu, Hao; Yu, Jinlong; Mulvad, Hans Christian Hansen; Galili, Michael; Jeppesen, Palle; Oxenløwe, Leif Katsuo "*4 × 160-Gbit/s multi-channel regeneration in a single fiber"* Vol. 22, No. 10 Optics Express (2014).

69. Xiang Zhou, Chao Lu, Ping Shum, Hossam, H. M. Shalaby, T. H Cheng,Peida Ye *"A Performance Analysis of an All-Optical Clock Extraction Circuit Based on Fabry–Perot Filter"* Journal of Lightwave Technology, Vol. 19, No. 5, pp 603-613, (2001).

70. C. Porzi,P Ghelfi, FPonzini, ABogoni, LPoti*"Ultra-fast clock recovery by all-optical PLL"*Lasers and Electro-Optics Society (LEOS) The 16th Annual Meeting of the IEEE (2003).

71. R.Ramaswami and K. Sivarajan, "*Optical networks: A practical perspective"*, 3rdEdition, Morgan Kaufmann Publishers, Elsevier Inc, USA, (2009).

72. S. J. B. Yoo, "*Optical packet and burst switching technologies for the future photonic internet,"* IEEE/OSA Journal of Lightwave Technology, vol. 24, pp 4468– 4492, (2006).

73. A. Saleh and J. Simmons, *"Evolution toward the next generation core optical network,"* IEEE/OSA Journal of Light wave Technology, vol. 24, pp 3303–3321, (2006).

74. Miguel A. Preciado, XuewenShu, and Kate Sugden, *"Proposal and design of phase-modulated fiber gratings in transmission for pulse shaping,"* Opt. Lett. Vol 38, 70-72 (2013).

75. XuewenShu*"Advanced FBG Structures Designed and Fabricated for Optical Signal Processing"* AM3C.1 OSA Asia Communications and Photonics Conference, (2015).

76. Hui Cao, XuewenShu, JavidAtai, AdenowoGbadebo, BangyunXiong, Ting Fan, HaiShu Tang, Weili Yang, and Yu Yu, *"Optimally-designed single fiber Bragg grating filter scheme for RZ-OOK/DPSK/DQPSK to NRZ-OOK/DPSK/DQPSK format conversion,"* Opt. Express 22, (2014)

77. J. Azaña and L. R. Chen, *"Synthesis of temporal optical waveforms by fiber Bragg gratings: A new approach based on space-to-frequency-to time mapping," J. Opt. Soc. Amer. B*, vol. 19, no. 11, pp. 2758–2769, (2002).

78. L. M. Rivas, K. Singh, A. Carballar, and J. Azaña, "*Arbitrary-order ultrabroadband all-optical differentiators based on fiber Bragg gratings,"IEEE Photon. Technol. Lett.*, vol. 19, no. 16, pp. 1209–1211, Aug. (2007).

79. María R. Fernández-Ruiz, *Student Member, IEEE,* Alejandro Carballar, *Member, IEEE,* and José Azaña*, Member, IEEE "Design of Ultrafast All-Optical Signal Processing Devices Based on Fiber Bragg Gratings in Transmission"* Journal of Lightwave Technology, vol. 31, no. 10, (2013).

80. María R. Fernández-Ruiz,1,* Ming Li,1 Mansour Dastmalchi,2 Alejandro Carballar,3 Sophie LaRochelle,2 and José Azaña1 *"Picosecond optical signal processing based on transmissive fiber Bragg gratings"* vol. 38, no. 8 / Optics Letters (2013).

81. Y. Park, M. Kulishov, R. Slavík, and J. Azaña, "*Nonlinear pulse compression of picosecond parabolic-like pulses synthesized with a long period fiber grating filter"* Opt. Express 14, 12670 (2006).

82. J. Azaña, *"Ultrafast analog all-optical signal processors based on fiber-grating devices,"* IEEE Photon Journal, Vol2, pp 359–386, (2010).

83. José Azaña **"***Proposal of a uniform fiber Bragg grating as an ultrafast all-optical integrator"* Optics Letters / Vol. 33, No. 1 / January 1, (2008).

84. Miguel A. Preciado, and Miguel A. Muriel *"Ultrafast all-optical integrator based on a fiber Bragg grating: proposal and design"* Optics Letters / Vol. 33, No. 12 / June 15, (2008).

85. N. Q. Ngo, *"Design of an optical temporal integrator based on a phase-shifted fiber Bragg grating in transmission,"* Opt. Lett. 32, 3020-3022 (2007).

86. RadanSalivic, Yongwoo Park, Nicolas Ayotte, LaRochelle, Serge Doucet, Tae-Jung Ahn, Sophie, and José Azaña2 *"Photonic temporal integrator for all-optical Computing*" / Vol. 16, No. 22 / Optics Express 27 (2008).

87. V.S Hari, K.V Madhav, V.T Gopakumar, B.Srinivasan, S. Asokan,"*Novel Technique for Fabricating Fabry-Perot Filters Based on Fiber Bragg gratings"* Paper OFD23.In: International Conference on Fiber Optics and Photonics, Hyderabad (2006).

88. M Kulishov, J.Azaña, *"Long-period fiber gratings as ultrafast optical differentiators"*. Opt. Lett. 30,pp 2700–2702, (2005),

89. C.K Madsen, J.H. Zhao, "*Filter Design and Analysis: a Signal Processing Approach"* Wiley, New York (1999).

90. M.A Preceiadio, M.A. Muriel, *"Design of an ultrafast all-optical differentiator based on a fiber Bragg grating in transmission"* Optics Letters. 33(21), pp 2458–2460, (2008).

91. N. K. Berger, B. Levit, B. Fischer, M. Kulishov, D. V. Plant, and J. Azaña, "*Temporal differentiation of optical signals using a phase-shifted fiber Bragg grating*," *Opt. Express*, vol. 15, pp. 371–381, (2007).

92. M. Kulishov and J. Azaña, "*Design of high-order all-optical temporal differentiators based on multiple-phase-shifted fiber Bragg gratings*" *Opt. Express*, vol. 15, pp. 6152–6166 (2007).

93. Luis M. Rivas, Kanwarpal Singh, Alejandro Carballar, and José Azaña , *"Arbitrary-Order Ultrabroad band All-Optical Differentiators Based on Fiber Bragg Gratings"* IEEE Photonics Technology Letters, vol. 19, no. 16, (2007).

94. Ming Li, Hoe-SeokJeong, José Azaña, and Tae-Jung Ahn, *"25-terahertz-bandwidth all-optical temporal Differentiator"* Optics Express ,Vol. 20, No. 27, (2012)

95. Bernd Sartorius "*All-Optical Clock -Recovery for 3R Optical Regeneration*" MG7, Optical Fiber Communication Conference and Exhibit, OFC (2001).

96. Weiming Mao, Yuhua Li, Mohammed Al-Mumin, and Guifang Li "*All-Optical Clock Recovery for Both RZ and NRZ Data"* IEEE PHOTONICS TECHNOLOGY LETTERS, VOL. 14, NO. 6, (2002).

97. A. D. Ellis, K. Smith and D. M. Patrick "*All optical clock recovery at bit rates up to 40Gbitps. Electronics letters" , Vol. 29 No. 15 (1993***).**

98. Michael J. O'Mahony, Christina Politi, DimitriosKlonidis, Reza Nejabati, and Dimitra Simeonidou "*Future Optical Networks"* Journal of Lightwave Technology,Vol. 24,Issue 12,pp. 4684-4696,(2006).

99. Tuomo von Lerber, SeijaHonkanen,A.Tervonen,FrankoKueppers*"Optical clock recovery methods: review,* Elsevier, optical fiber technology*"*, vol. 15, pp 363–372, (2009).

100. Masatoshi Saruwatari, Senior Member, *IEEE"All-Optical Signal Processing for Terabit/Second Optical Transmission"* IEEE Journal on selected topics in Quantum Electronics, vol. 6, pp 1363-1374, (2000).

101. Yong Liu, Shangjian Zhang, and Yongzhi Liu, F. Gomez-Agis, E. Tangdiongga, and H. J. S. Dorren *"High-Speed Optical Signal Processing for Telecom Applications"* Wireless and Optical Communications Conference (WOCC), 19th Annual, (2010).

102. Austo Gomez-Agis, Nicola Calabretta, Aaron Albores-Mejia, and Harm J. S. Dorren *Clock-distribution with instantaneous synchronization for 160 Gbit/s optical time-domain multiplexed systems packet transmission, Optics* Letters, Vol. 35, Issue 19, pp. 3255-3257, (2010).

103. M.Jinno and T.Matsumoto*"All optical timing extraction using a 1.5um self-pulsating multi-electrode DFB LD"* Electron letters Vol 24, pp 1426-27,(1988).

104. Masatoshi Saruwatari, Senior Member, *IEEE "All-Optical Signal Processing for Terabit/Second Optical Transmission"* IEEE Journal on selected topics in Quantum Electronics, vol. 6, pp 1363-1374, (2000).

105. K.Smith and J.K Lucek *"All optical clock recovery using a mode locked Laser"* Electron letters Vol 28, pp 1814-16, (1992).

106. M.Jinno and M,Abe "*All optical regenerator based on nonlinear fibre Sagnac interferometer"* Electron letters, vol 28, pp 1350-1352,(1992).

107. Christos Kouloumentas, Anna Tzanakaki, and IoannisTomkos *"All-Optical Clock Recovery at 160 Gbit/s and beyond,Based on a Fabry-Pérot Filter and Self-Phase Modulation Effect"* ICTON 2006, Th.B1.8 (2006).

108. Zhixi Zhao, Li Huo, Xin Chen, Caiyun Lou *"Short Pulsewidth Clock Recovery at 100 GHz Using Fabry- Perot Cavity and Semiconductor Optical Amplifiers"*W2A.27, OFC (2016).

109. Reza Maram, Deming Kong, Michael Galili, Leif Katsuo Oxenløwe, and José Azaña *"Ultrafast all-optical clock recovery based on phase-only linear optical filtering"* Optics Letters, Vol. 39, No. 9 (2014).

110. G. Contestabile, R. Proietti, N. Calabretta, A. D'Errico, M. Presi and E. Ciaramella*"40 Gb/s WDM NRZ-DPSK all-optical clock recovery and data demodulation based on a periodic Bragg filter"* OMN2, OFC/NFOEC (2008).

.....ꕥ❋ꕥ.....

Chapter 2

FIBER BRAGG GRATING (FBGs) AND FABRY-PEROT NARROW BAND FILTERS BASED ON FBGs (FP-FBGs)

2.1 Introduction

Fiber Bragg gratings (FBGs) is a matured technology. It is widely used as an optical filter for optical communication applications like multiplexing and de-multiplexing [1]. FBGs are also finding applications in sensing like temperature and strain sensors [2, 3]. In this Chapter, we will discuss the implementation of Fabry-Perot filters based on FBGs (FP-FBGs). The FP-FBGs are two FBGs in a same photosensitive fiber, separated by a finite distance. The FP-FBGs are showing far better performance compared to FBGs in all optical signal processing applications [4]. This chapter gives an overall idea of FBGs, FP-FBGs and their simulation, fabrication and characterization results. The simulations are done with Matlab programming based on couple mode theory [5]. The fabrications of FBGs and FP-FBGs are done at the grating fabrication center at the Electrical Engineering Department of IIT Madras, Chennai. The phase mask technology had been used for the fabrication of FBGs.

The fiber Bragg grating can perform reflection and filtering in a highly efficient and low loss manner. Fiber Bragg gratings are widely used in the modern telecommunication system. FBG filtering properties are widely used in Wavelength Division Multiplexing and Dense Wavelength Division Multiplexing (WDM & DWDM) system, Optical Add/Drop Multiplexing (OADM) and laser single mode operation [6]. The chirped grating, where the period of the grating is changed along the fiber, is widely used as dispersion compensators [7]. Apart from the telecom applications, the FBGs are widely used as a temperature and strain/pressure sensors [8]. The Bragg wavelength changes with the applied temperature ($12pm/^0C$) and applied strain (1.3pm/microstrain). The FBG temperature sensor finds applications in industries where temperature control is crucial [8]. The strain/pressure sensor application are using for structural health monitoring of buildings and bridges. [9, 10].

2.2 FBG Theory

A FBG is a periodic refractive index change along the core of a photo sensitive fiber. A Silica fiber become photo-sensitive while it is doped with Germanium (10mol %) [11]. Photosensitivity in optical fiber refers to a permanent change in the index of refraction of fiber core when exposed to light with characteristic wavelength and intensity that depends on the core material. The photosensitivity arises when normal silica structure is getting changed. Initially photosensitivity was thought to be a phenomenon only associated with optical fibers having a large concentration of germanium in the core when it is photo excited with 240-250nm UV light [12]. There are numerous examples in the literature of photosensitivity in a wide range of fibers, many of which do not contain Germanium as a dopant. Such fibers use Europium or Cerium or Erbium as dopants [13]. Germanium show varying degrees of sensitivity in a silica host optical fiber, but none of the other dopants are as sensitive as Germanium.

Germanium doped optical fibers remains one of the most important materials for the fabrication of devices utilizing photosensitivity [14].

Several models have been proposed to explain the photosensitivity effect, but no single model can fully explain the effect in all cases.

The densification model interprets the photosensitivity mechanism with UV-induced glass density change [15, 16]. The bond breaking caused by laser irradiation alters the glass structural network, and leads to the densification as the result of the glass collapse. The increase in the glass density contributes to a positive refractive index change [16, 17].

The color center model is proposed based on the observation of bleaching the absorption band of GODC and forming a new absorption band when the Ge-doped silica fiber is irradiated with a 248 nm laser [21]. The new absorption band

is assigned to the formation of a color center, which is a photo-excited electron or hole trapped by a nearby defect center. The light-induced refractive index change is associated to the absorption change through the Kramers-Kronig relationship [22]. Both these models are explaining below.

Defects are important to optical fibers because their absorption band cause signal losses in transmission. These defects are also called color centers. Color centers are also responsible for nonlinear optical transmission, where the transmission changes in time with the light intensity. During the high-temperature gas phase oxidation process of the modified chemical vapor deposition (MCVP) technique, GeO_2 dissociates to the GeO molecule (in other words Ge^{2+} center) due to its higher stability at elevated temperature [15]. When incorporated into glass, this molecule can manifest itself in the form of oxygen vacancy in Ge-Si and Ge-Ge wrong bonds [16]. Regardless of which particular defect causes an oxygen deficient matrix in glass, it is linked to the 240-250-nm absorption band and its centers are known as Germanium Oxygen deficient centers (GODC) [13].

Light at 240-248nm excites GODC from its ground singlet state (S0) to excited state (S1). From there it can ionize spontaneously or by absorbing another 248nm photon. Such ionization is thought to be necessary for index change. However, a GODC excited to S1 can also relax to the long lived (Peaks of PL bands (eV)/decay constant 3-3.2eV/10.2ms) Triplet state T1 [17].

From the triplet state, the defect undergoes a metamorphosis and changes its structure to a drawing induced defect state (DID) [18]. It is proposed that Structural rearrangement of GODC to DID is the principal cause of light induced refractive index change. The above process is shown in figure (2.1) [19, 20]. Corresponding energy levels and life times are also shown in the same figure.

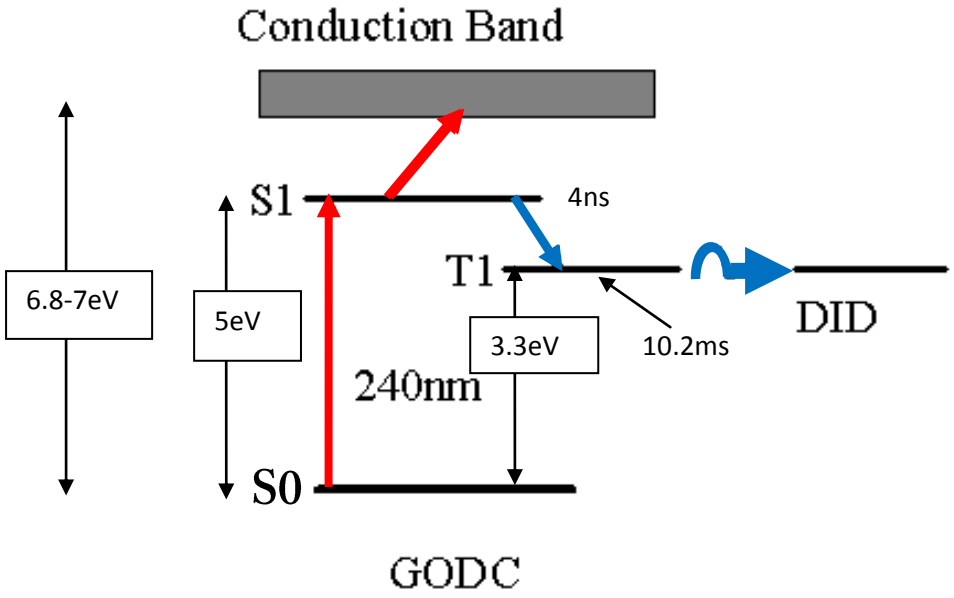

Fig. (2.1) *Energy level diagram of germanium oxygen-deficient defect, showing proposed pathway excited with pulsed mid UV light*

As mentioned the refractive index variations are also explained by the color center model [21]. Here any change in the refractive index resulting in the grating formation is associated with the photo induced change in absorption, which can be obtain through Kramers-Kronig relation expressed as [21]

$$\Delta n_{eff} = \frac{1}{2\pi^2} P \int_0^{\infty} \frac{\Delta\alpha_{eff}(\tau)}{1-(\frac{\tau}{\tau'})^2} (d\tau) \qquad (1)$$

Where P is the principle part of the integral, λ is the wavelength $\Delta\alpha_{eff}$ is the effective change in absorption coefficient of the defect, given by

$$\Delta\alpha_{eff} = \frac{1}{L}\int_0^L \Delta\alpha(\tau, z)dz \qquad (2)$$

'P' denotes the Cauchy principal value. So the real and imaginary parts of such a function are not independent, and the full function can be reconstructed given just

one of its parts. The complex permittivity is usually a complicated function of frequency ω, since it is a superimposed description of dispersion phenomena occurring at multiple frequencies. The dielectric function ε(ω) must have poles only for frequencies with positive imaginary parts, and therefore satisfies the Kramers–Kronig relations. The primary quantity that characterizes the electronic structure of any crystalline material is the probability of photon absorption, which is directly related to the imaginary part of the optical dielectric function ε(ω).

Here 'L' is the sample thickness. This takes into account the fact that bleaching beam is strongly attenuated as it passes through the sample, and thus bleaching does not occur uniformly with increasing depth. Kramers-Kronig relation may be used to calculate the index change that is induced by bleaching of the absorption bands (figure 2.2). The figure represents only the absorption band changes before and after UV irradiation, not the measured value. It is shown in the absorption spectra between 200 and 300nm of a fiber core before and after inscribing a Bragg grating with 81% ($2*10^{-4}$) reflectivity [22]. Using Kramers-Kronig relation, the changes in absorption spectrum indicates that only 16% change index. The substantial part (65%) of index change is coming from the strong absorption in the 190 to 200nm region. It is assumed that the absorption in the 190 to 200nm band is associated with GeE' center. The Ge-Si wrong bonds are transformed in to GeE' centers by two photon absorption. To date, the color centre model is the most widely accepted model for the formation mechanism of fiber gratings.

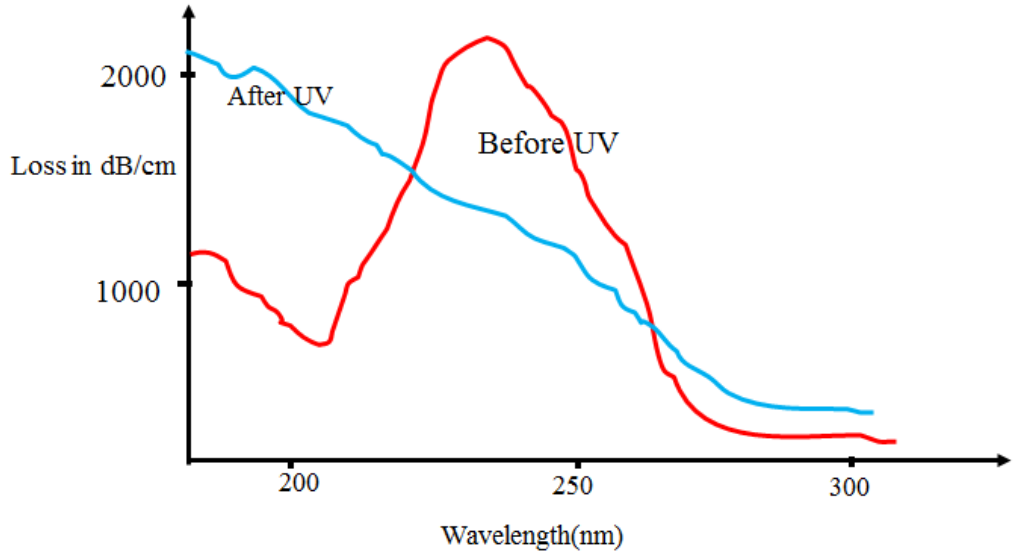

Fig. (2.2) *UV absorption spectra before (red) and after (cyan) of Germano-Silicate fiber [22]*

In this model photo-induced changes in the material properties of glass introduce new localized electronic excitations and transitions associated with the defects. These color-center defects, mainly the GeE', because of their strong optical absorption, are proposed to give rise to photosensitivity and change in refractive index [23].

The refractive index variation under UV light illumination is made use to form the grating, which is the basic periodic structure of FBG. The operation of Bragg grating can be understood by reference to the figure (2.3), which shows a periodic variation in refractive index. The incident wave (with wavelength λ) is reflected from each period (ʌ) of the grating. These reflections are added in phase when the path length difference (corresponding to a period 'ʌ') in wavelength λ at each period of grating is equal to half the incident wavelength λ. This is equivalent to

$$n_{eff} * \Lambda = \lambda / 2 \qquad (3)$$

This is the Bragg condition [19]. Here n_{eff} is the effective refractive index of the fiber.

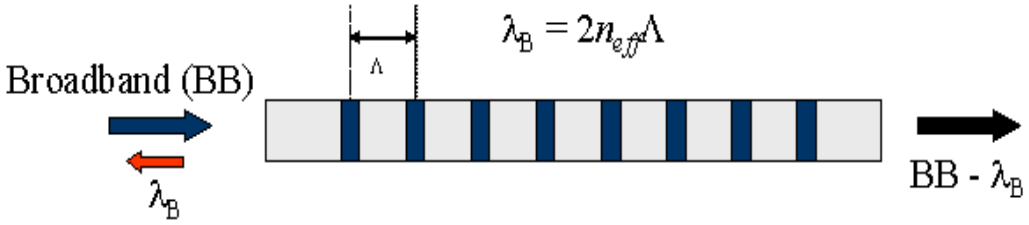

Fig. (2.3) *The operation of a fiber Bragg grating.*

From the above figure, let us consider a light wave with propagation constant β_0 propagating from left to right; the energy from the wave is coupled in to a scattered wave traveling the opposite direction at the same wavelength provided [24,25]. The Bragg grating condition required the energy and momentum conservation.

The energy conservation requires that the frequency of incident and reflected radiation are same ($\hbar\omega_i=\hbar\omega_r$)

The momentum conservation requires the incident wave vector k_i plus the grating wave vector K equal to the wave vector of the scattered or reflected radiation $k_r(k_i+K=k_r)$.

Since the incident and reflected light counter propagate inside the fiber, k_i and k_f should be the propagating constants of fiber modes for forward and backward fields, which have the same magnitude of $2\pi n_{eff}/\lambda_B$ but in opposite directions. For a first-order Bragg grating, the grating wave vector K has a magnitude of $2\pi/\Lambda$ and a direction normal to the grating planes.

$$2 * (\frac{2\pi n_{eff}}{\lambda_B}) = \frac{2\pi}{\Lambda} \quad (4)$$

The above equation leads to the Bragg condition shown equation (7).

The grating condition can be derived from the figure 2.4. It can be seen that at each grating interface there is a forward propagating wave with propagation constant β_0 and a reflected wave at the same propagation constant β_0 if the path length difference is equal to the period of the grating. In other words, in Bragg grating, the energy from the forward propagating mode at right wavelength is coupled in to backward propagating mode at the same wavelength. This type of coupling is called contra directional coupling shown in figure 2.4.

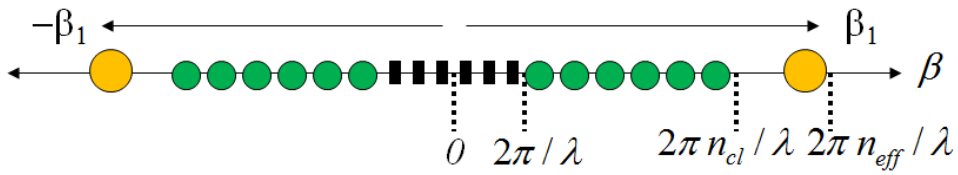

Fig. (2.4) *Contra directional coupling in FBGs.*

The yellow circles represent bound core modes ($n_{cl}<n_{eff}<n_{co}$), the green circles represent the cladding modes ($1 <n_{eff}<n_{cl}$), and the black hatched region represents continuum of radiation modes.

$$|\beta_O - (-\beta_O)| = \frac{2\pi}{\Lambda} \quad (5)$$

Where '**Λ**' is the period of the grating and

$$\beta_O = (\frac{2\pi}{\lambda}) \times n_{eff} \quad (6)$$

Where n_{eff} is the effective refractive index of the fiber; and the wavelength associated with the back reflected wave is given by

$$\lambda_{B=} 2 \times n_{eff} \times \Lambda \quad (7)$$

Where 'λ_B' is called the Bragg wavelength.

In Bragg grating the energy from the forward propagating mode at right wavelength is coupled in to backward propagating mode at the same wavelength. This type of coupling is called contra directional coupling.

2.3 FBG Fabrication

There are two methods of fabricating the FBGs. They are interferometric and phase mask methods [13]. In this work the phase mask method has been used to fabricate the FBGs [26, 27].

The phase mask is a diffractive optical component. This is used to modulate the UV beam spatially. Phase-mask is produced as a one-dimensional surface-relief pattern with a period Λ_{pm} etched in to a fused silica. So the diffractive grating on the phase-mask split the incident UV laser beam into several orders to create required pattern on the photo sensitive fiber [28]. The zero order-diffraction is suppressed to less than 3% of the total diffracted power. But the ±1 orders of diffraction are associated with more than 40% of the diffracted power. A near field fringe pattern is produced by the interference of ±1 diffracted beams. The period of the phase mask fringes (Λ) is one half of the mask ($\Lambda=\Lambda_{pm}/2$) [29]. The interference pattern photo-imprints a refractive index modulation in the core of a photosensitive optical fiber. A cylindrical lens is used to focus the fringe pattern on the fiber.

The phase mask greatly reduces the complexity of the fiber Bragg grating fabrications. The simplicity of using only one optical element provides a robust and inherently stable method for writing the fiber Bragg grating [28, 29]. Since the fiber is usually placed directly in front of the phase mask. The phase mask method of FBG fabrication (figure 2.5) is more stable compared to the interferometric fabrication [30].

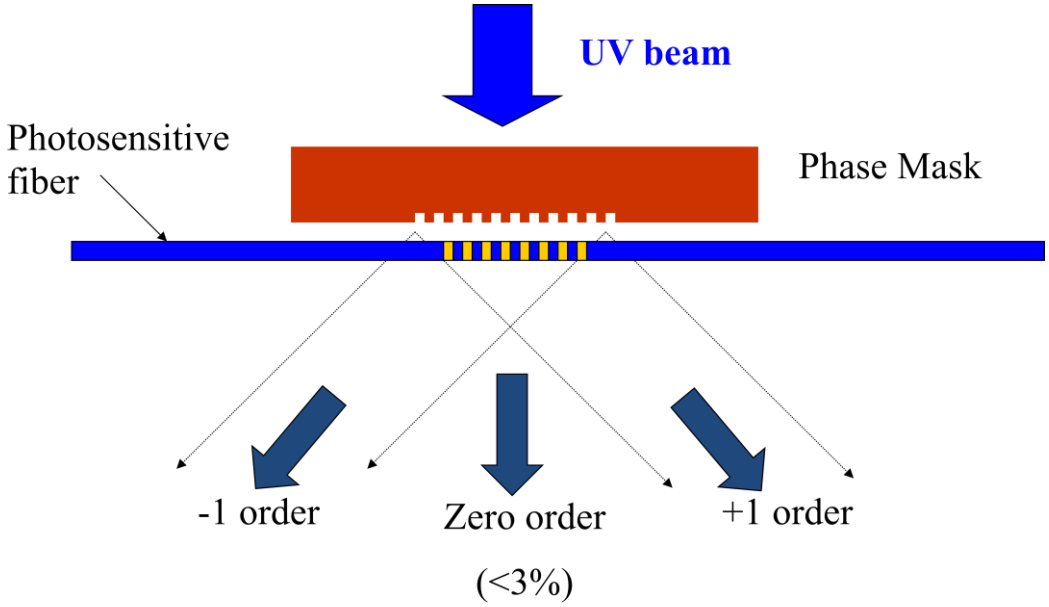

Fig. (2.5) *The schematic of FBG fabrication using phase-mask method*

The experimental setup that has been used to fabricate the FBGs and Fabry-Perot cavities using FBGs are shown in figure (2.6). The Excimer laser that has been used is the Braggstar make. The phase mask used is from Ibsen photonics, the photosensitive fibers used are GF1 fiber from the Thorlabs, and highly Ge doped photosensitive fiber (F-SM1500-4.2/125) from Newport Inc. The FBG fabrication set up also equipped with real time monitoring system for FBG writing, which is running on LabVIEW software.

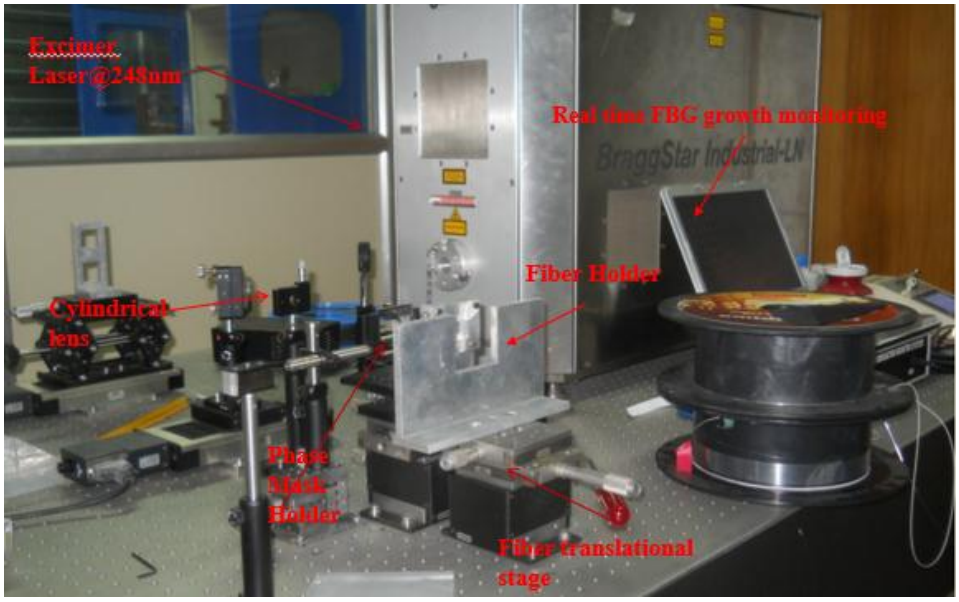

Fig.(2.6) *The fabrication set up used to fabricate FBG at IIT Madras,Chennai*

As mentioned, the phasemask is one of the main components for making the FBGs. We have roughly measured the diffraction efficiency of a phasemask at the grating facility center at IIT Madras, Chennai. The experimental set up is shown in figure (2.7). We have used Ibsen 1071.21nm and 1087.80nm phasemasks for the above experiment. The diffraction efficiency is measured at a distance of 14.6cm using a photo detector. The table (2.1) shows the diffracted power at 3mJ and 5mJ from the two phase masks. The table (2.2, (a) & (b)) is showing the diffraction efficiency at a distance of 14.6cm. It is worth noting that the 0^{th} order power diffracted is less than 3% and maximum diffracted power concentrated on the ±1 orders of diffraction from the phase mask. It has been also noted that the diffracted power get decreases while the orders of diffraction increases.

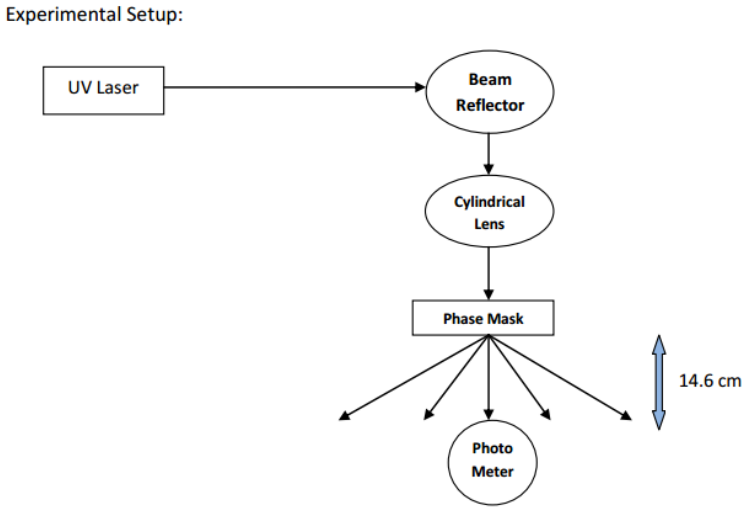

Fig. (2.7) *The schematic of finding the diffraction efficiency calculation of the Phasemask*

Table (2.1) Power diffracted from the phase masks at different input powers (mJ) Efficiency at 14.6 cm (with laser repetition frequency of 5Hz)

Phase MASK	**Frequency**	**Input Power**	**Power at Different Orders**				
			-2	**-1**	**0**	**+1**	**+2**
1071.21nm	5HZ	5mJ	132µJ	1.35mJ	53.4 µJ	1.37mJ	140 µJ
	5HZ	5mJ	82.5 µJ	0.88mJ	35 µJ	0.881mJ	90.2 µJ
1087.80nm	5HZ	5mJ	119.5 µJ	1.34 mJ	54 µJ	1.323 mJ	120 µJ
	5HZ	5mJ	80.1 µJ	0.887mJ	32.5 µJ	0.885mJ	81 µJ

Table (2.2 (a) & (b)) The diffraction efficiency of phase mask with periods 1071.21nm and 1087.80 nm

For 1071.21nm Phasemask

Order	Efficiency at 3mJ	Efficiency at 5mJ
-2	2.64%	2.75
-1	27%	29.3%
0	1.068%	1.167%
1	27.4%	27.4%
2	2.8%	3.06%

For 1087.80nm Phase Mask

Order	Efficiency at 3mJ	Efficiency at 5mJ
-2	2.39%	2.67%
-1	26.8%	29.3%
0	1.08%	1.08%
1	27.4%	27.4%
2	2.4%	2.7%

The total diffraction efficiency calculated from the table is 63.15% and the most of the power is concentrated in the ±1 diffraction orders. Here the measurement is done up to ±2 orders. It may be noted that the measurement is done at a distance of 14.6cm, while fabrication of the FBGs this is much closer than the above distance. More over power carried by higher order diffractions ±3, ±4…is not measured.

2.3.1 FBG Simulation and Fabrication Results

The simulations of the FBGs are carried out by the coupled mode theory, [31] and the simulations are done using Matlab. The grating equation for

perturbation to the effective refractive index n_{eff} of the guided mode is given by [31]

$$\delta n_{eff}(z) = \overline{\delta n}(z)(1+\nu\cos[\frac{2\pi}{\Lambda}z+\phi(z)]) \quad (8)$$

where $\overline{\delta n}(z)$ the "dc" index change is spatially (in the 'z' direction) averaged over a grating period, ν is the fringe visibility of the index change, Λ is the grating period, and $\phi(z)$ is the grating chirp.

$$\text{The reflection coefficient } (\rho^2) = \frac{Sinh^2(\sqrt{\kappa^2-\sigma^2}\,L)}{Cosh^2(\sqrt{\kappa^2-\sigma^2}\,L)-\frac{\sigma^2}{\kappa^2}} \quad (9)$$

where 'κ' is the ac coupling coefficient 'σ' is dc coupling coefficient (period averaged), 'L' is the length of the grating.

$$\text{The power reflectivity } (\rho^2) = \tanh^2(\kappa L) \quad (10)$$

when the dc coupling coefficient (σ) become zero.

The Matlab simulated uniform FBG reflection spectrum based on the above couple mode theory equation is shown in figure (2.8). Here the inputs given are the power reflectivity, the period of the grating, effective refractive index and the length of the grating. The coupling coefficients are calculated using instantaneous changes in the refractive indices.

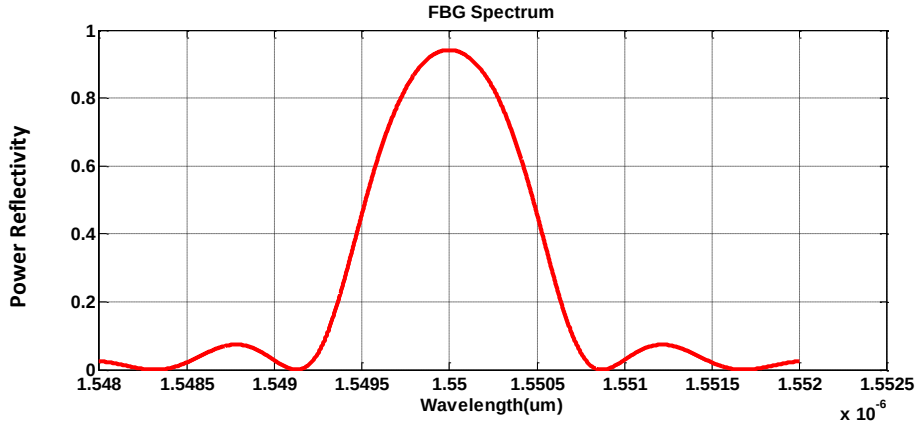

Fig. (2.8) *Reflection Spectrum of simulated Uniform Fiber Bragg Grating*

A uniform fiber Bragg grating in the figure above shows side lobes. While the FBGs used for WDM/DWDM applications the side lobes cause the crosstalk between adjacent channels. The fiber Bragg grating without the side lobes are called apodized grating as shown in figure (2.9). It has very sharp spectral response, with channel spacing down to 50GHz or less [32].

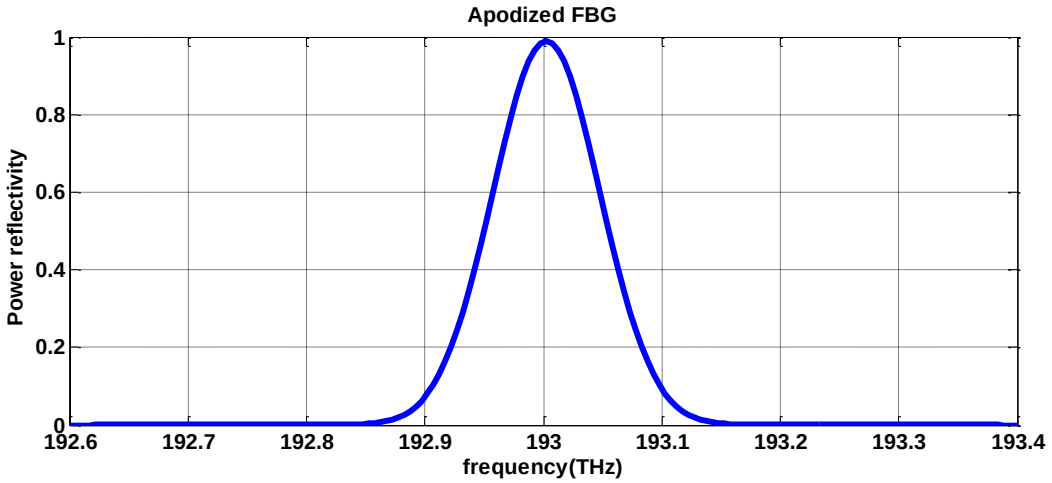

Fig. (2.9) Reflection spectrum of *Apodized fiber Bragg Grating*

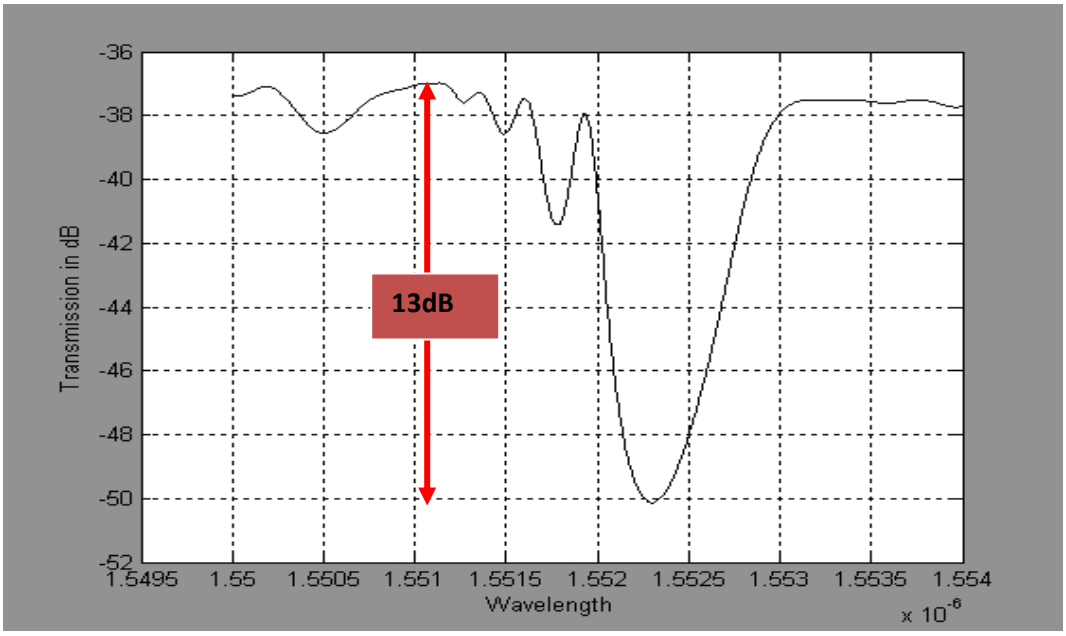

Fig. (2.10) *Fabricated FBG transmission spectrum*

Both figure 2.9 and 2.10 are apodized FBGs, 2.9 is simulated using Matlab and 2.10 is the fabricated. The former is shown in reflection instead of transmission to show that the side lobes in the refection spectrum are removed by apodization. The fabricated FBG transmission spectrum also shows side lobes in the shorter wavelength because of small F-P cavity formation.

After the simulation, using the fabrication set up mentioned above has been used for the fabrication of FBGs. The fabricated FBG is shown in figure (2.8). Here the FBG length is L= 3mm, λ_B=1552.25nm R= ~ 90%, Excimer laser energy =3mJ and 3 minutes of exposure time. From the figure the transmission dip is 13dB, for type 1 grating R+T=1, where R is the reflective power and T is the transmitive power. The reflectivity is calculated by 10*log (1-R) =13, so R=1-$10^{1.3}$, $\Delta n = 3 \times 10^{-4}$, Fiber is GF1 from Thorlab),

The observed dependence of index modulation (as well as Reflectivity) on time is shown in figure (2.11a). It agrees with power law of the form $\Delta n \propto t^{\alpha}$ where the 'α' is the fitting parameter. From the figures the value of α is found to be 0.5051. The evolution of Reflectivity with time is also shown in figure (2.11b) [33].

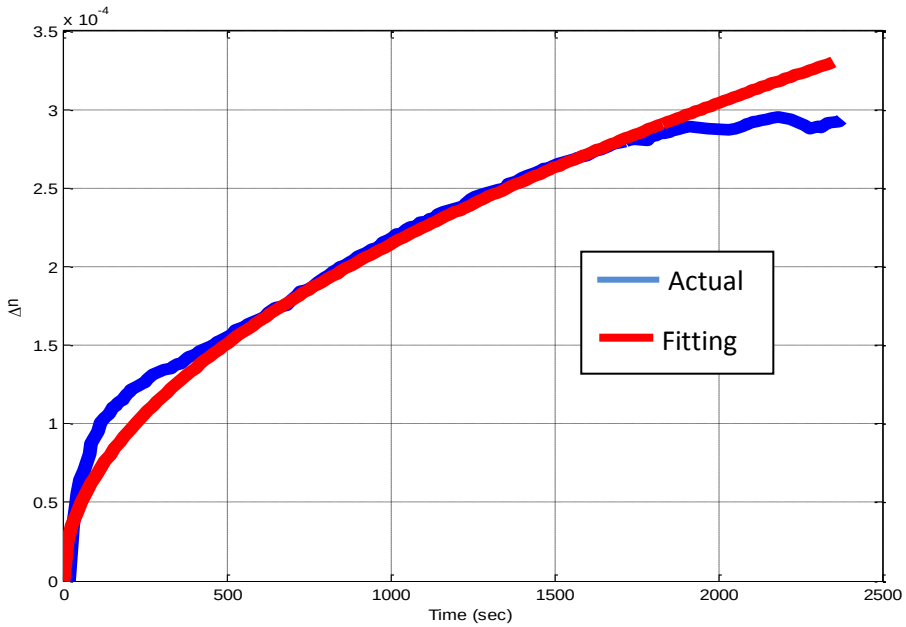

Fig. (2.11a) *The refractive index change (Δn) as a function of time*

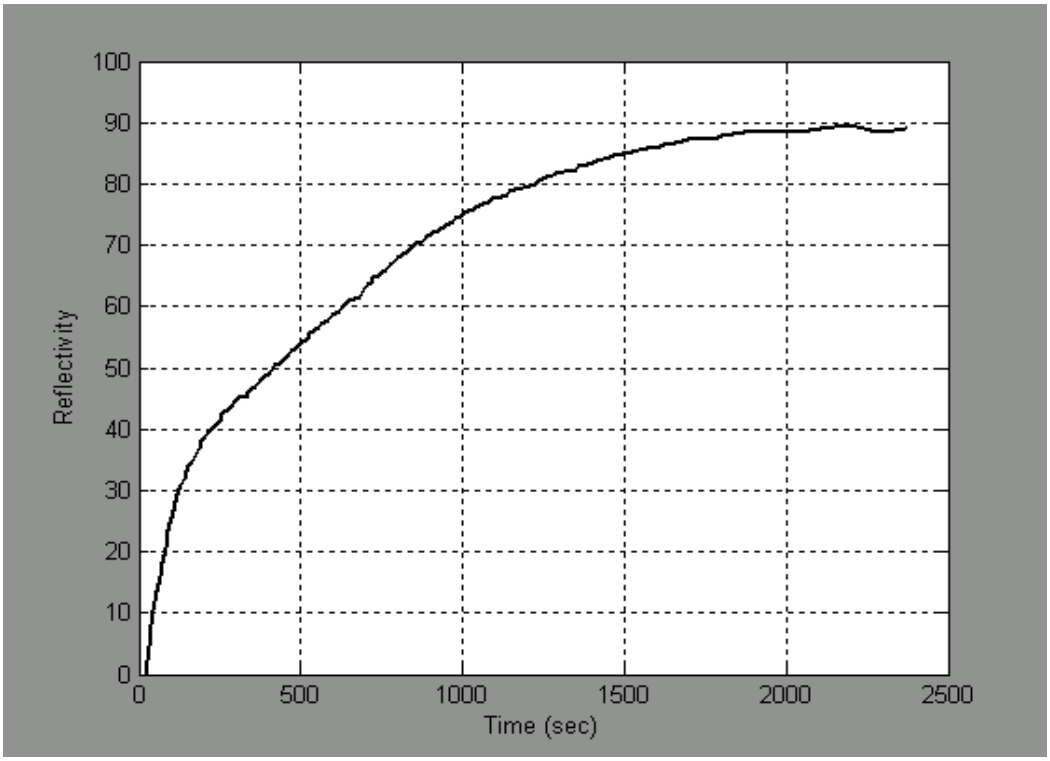

Fig. (2.11b) *The power reflectivity (R) as a function of time*

2.4 Fabry-Perot Filters (Etalon) and its Characteristics.

Fabry-Perot interference filters are formed by two parallel reflective mirrors separated by a finite distance 'δL'. The wavelength selectivity of the filter is associated with the multi-beam constructive interferences. In FPF, when a light beam entering to the cavity a part of the light is transmitted out. The remaining light is reflecting back as shown in figure (2.12). Here a single beam of light, that enters in to the cavity is breaking up in to multiple beams. These multiple beams are interfering each other. Constructive interference of these light beams happens when the path length of the light travelled is an integral multiple of the light's wavelength. More number of reflections in the cavity results in sharper interference maximum.

The figure (2.12) shows two partial reflecting mirrors M1 and M2 arranged in parallel and the separation between them is 'L' [34, 35, and 36]. When the cavity is irradiated with laser source of wavelength λ with an incident angle at one of the mirrors say M1 is θ. As mentioned there will be multiple reflections inside the cavity. A part of the incident light is transmitted through the mirror M2. All the transmitted rays interfere with each other constructively or destructively and correspondingly the output gives maxima or minima respectively. Constructive interference gives the maxima or else the minima, depended on the path length difference between the rays inside the cavity.

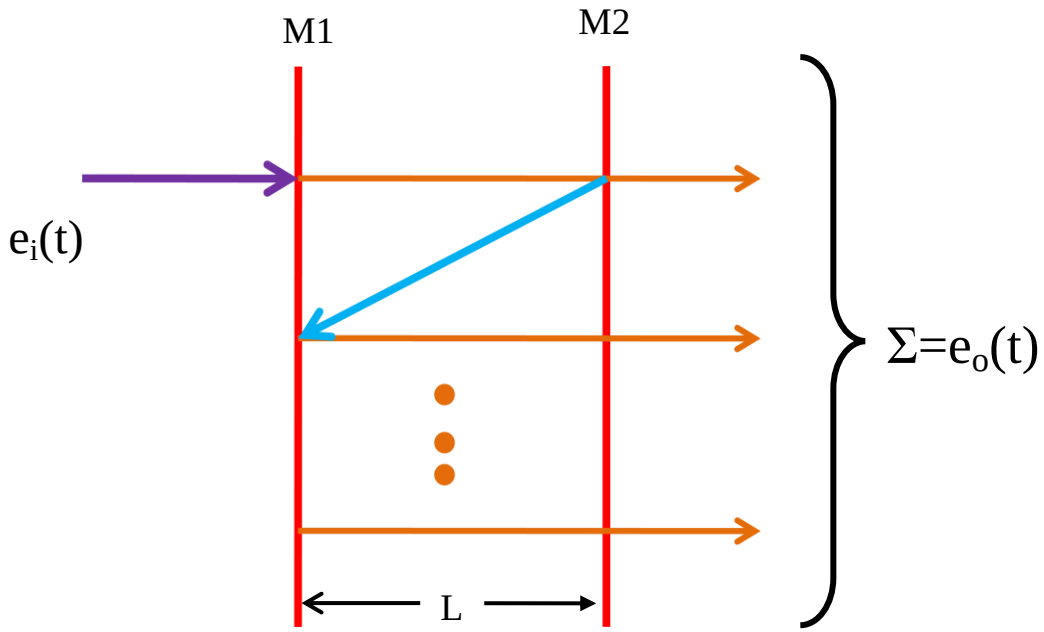

Fig. (2.12) *The Fabry-Perot filter using two parallel mirrors*

The path length difference (ΔL) between two adjacent rays is given as

$\Delta L = 2nLCos\theta$ and the corresponding phase difference is given by

$$\Delta = (2\pi/\lambda) \times \Delta L \quad (11)$$

The resulting transmitted light intensity (I_T) is given by [34, 35]

$$I_T = I_0 \frac{1}{1+\frac{4R}{(1-R)^2}Sin^2\frac{\zeta}{2}} \quad (12)$$

Where I_0 is the intensity of the incident light and R is the mirror reflectivity (Assuming R1=R2=R). From the above equation says I_T is varying with the phase difference ζ. I_T becomes maxima when

$$\Delta = m.\lambda, \text{ where } m=0, 1, 2\ldots. \text{ or } \zeta = 2m\pi \quad (13)$$

and the minima occurs when

$$\Delta = (2m+1).\lambda/2 \text{ where } m=0, 1, 2\ldots \text{ or } \zeta = (2m+1)\pi \quad (14)$$

The measured of the sharpness of transmission peaks is called finesse (F), is given by

$$F=4R / (1-R)^2 \quad (15)$$

The transmission curves of FPF with different finesse is shown in figure (2.13)

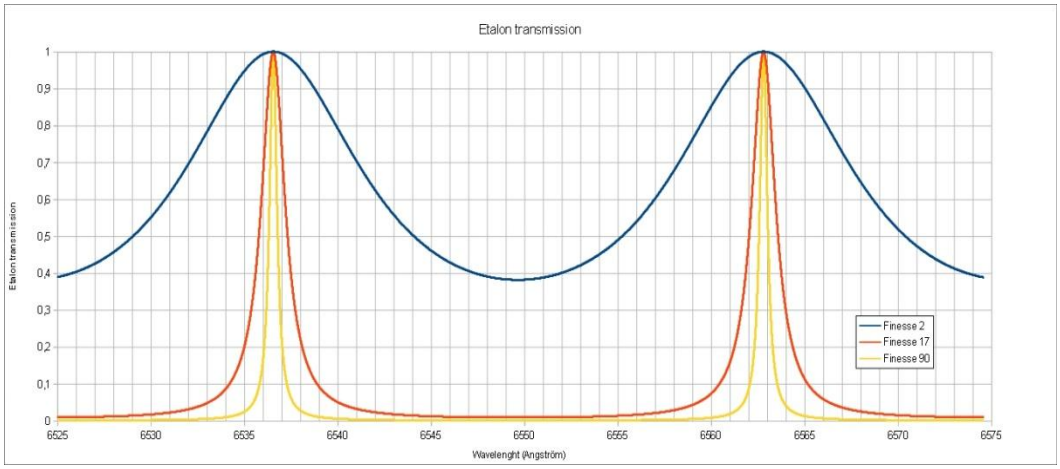

Fig. (2.13) *The transmission curves (modes of FPF) with different values of finesse. [22]*

2.5 Fabry-Perot Filters based on FBGs (FP-FBGs)

While the FBGs are used for the telecommunication and sensing applications it works in reflection. Many applications require the narrowband transmission characteristics of FBGs. An example from optical communication is the multiple channel selection applications in optical add drop multiplexing (OADM) in Wavelength Division Multiplexing (WDM) or Dense Wavelength Division Multiplexing (DWDM). Another example is the carrier and sideband recovery from optically modulated signal. Multiple peaks of transmission spectrum are also used in sensing applications like simultaneous measurement of temperature and strain [37]. As explained in the previous section (2.4) the FP filters using bulk mirrors and there the free spectral range (FSR) values are controlled by adjusting the cavity length mechanically [34] or electronically. The

FBGs can be used to make the Fabry-Perot filters more efficiently. Here the bulk mirrors are replaced by FBGs. The structure of a FP filter using FGBs is shown below (figure 2.14).

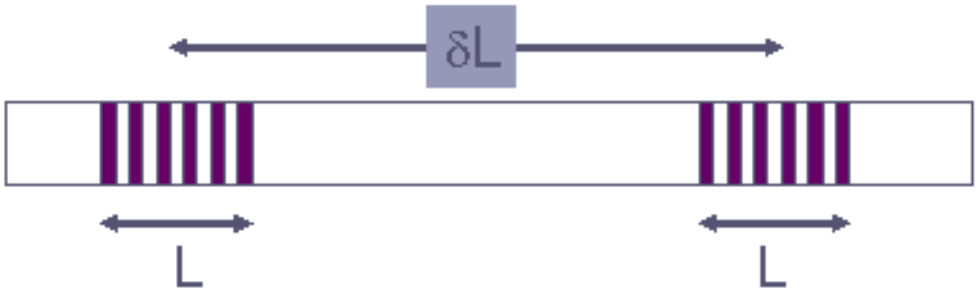

Fig. (2.14) *Fabry-Perot filters using Fiber Bragg Gratings*

The above figure shows the structure of a Fabry-Perot filter based on FBGs. Here two identical FBGs of length 'L' are separated by the distance δL. The center to center separations between the FBGs are called the cavity length. These filters work in the same way as bulk FP interferometers, except that the gratings are narrow-band and are distributed reflectors. The resonant wavelengths (modes) which are within the bandwidth of a FBG appeared as narrow band pass peaks shown in figure (2.15) below. The composite transmission spectrum of this band-pass filter can be a single or a series of high transmission windows separated by bands that are rejected by reflection. The separations between two consecutive transmission peaks are called the free spectral range (FSR). The FSR is a function of the cavity length δL. The FSR is given by c / (2n δL), where 'c' is the velocity of light and 'n' is the index of refraction.

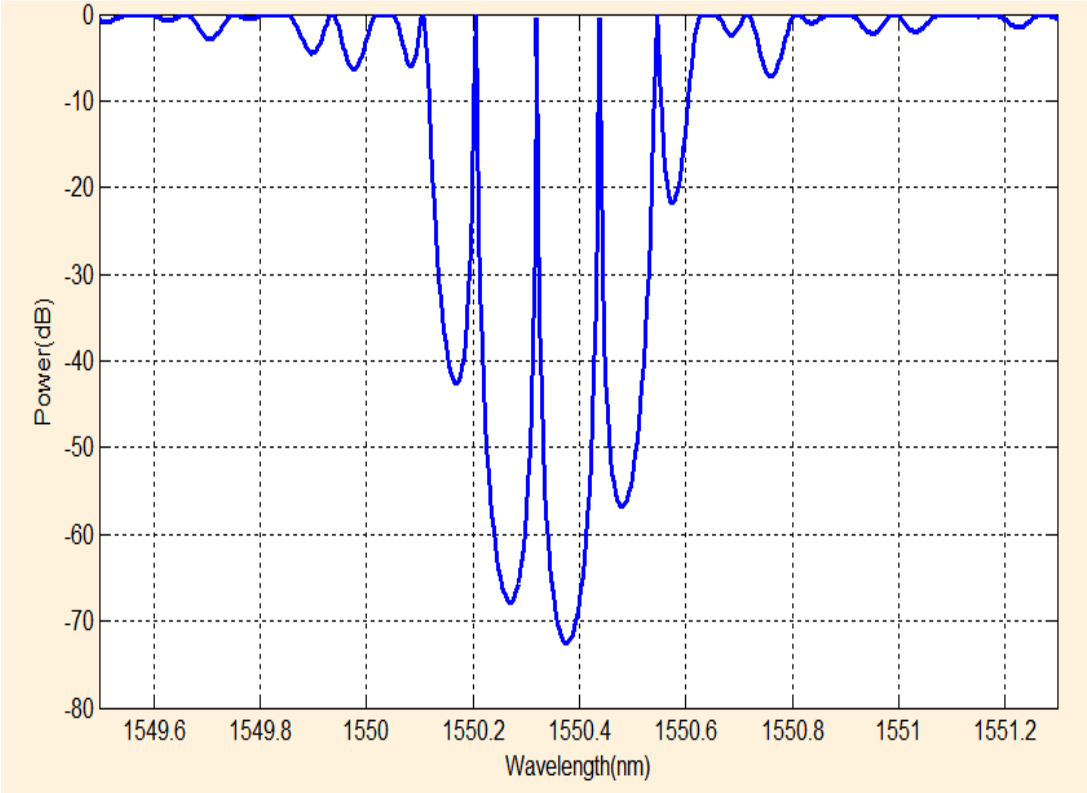

Fig. (2.15) *Matlab simulated transmission Spectrum of FP- FBGs (Cavity length δL=5mm, R1=R2=97% with FSR=12.5GHz)*

2.6 Fabrication and characterization of FP-FBGs.

The Fabry-Perot FBGs are formed by two high reflective FBGs, separated by a finite distance (δL). Unlike in bulk plane mirror FP filters, in FP-FBGs those modes fall within the pass bands of the FBGs are coming out as narrow band peaks with full width half maximum (FWHM) in the order of a few pico-meters as shown in figure (2.13).

For fabrication of FP-FBGs, first we fabricate a single FBG with >95% reflectivity with Phase mask method. The Excimer Laser emits UV at 248nm within an energy range of 5mJ-7mJ with repetition rate of 200Hz and the typical

exposure time is 60-180 seconds. There is a real time monitoring of FBG growth while fabricating using Ibsen interrogation monitor (I-MON) with integrated broad band source, and a receiver. This could help to calculate the required reflectivity and also rectify any problem that arises during the FBG fabrication.

After writing one FBG with required reflectivity, the photosensitive fiber is moved using the translation stage by a distance equal to the separation between the FBGs that is the cavity length (δL). Then write another grating at this position by keeping all other parameters same. After fabrication of FBGs and FP-FBGs it is spliced with proper pigtail connectors. The characterization of these narrow band filters are done using an automated interrogation system (Lightwave Measurement System, LWM) with 1pm resolution and 60dB dynamic range running on LabView. The schematic of the same is shown in figure (2.16), and the corresponding FP-FBG spectrum is shown in figure (2.17) [38]. The base line is not at 0dB because of fiber insertion (coupling and connection) losses.

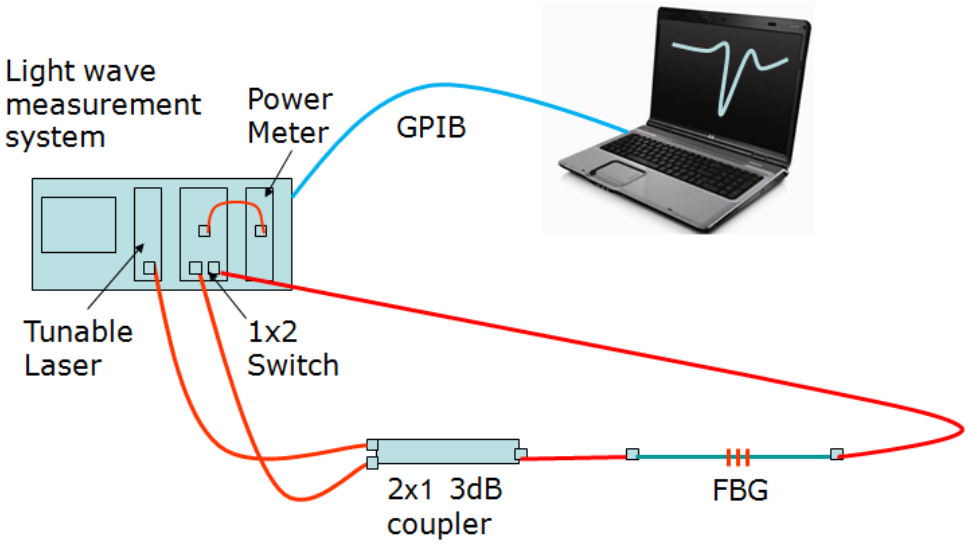

Fig. (2.16) *The characterization set up (LWM) used for FBGs and FP-FBGs at IIT Madras Chennai*

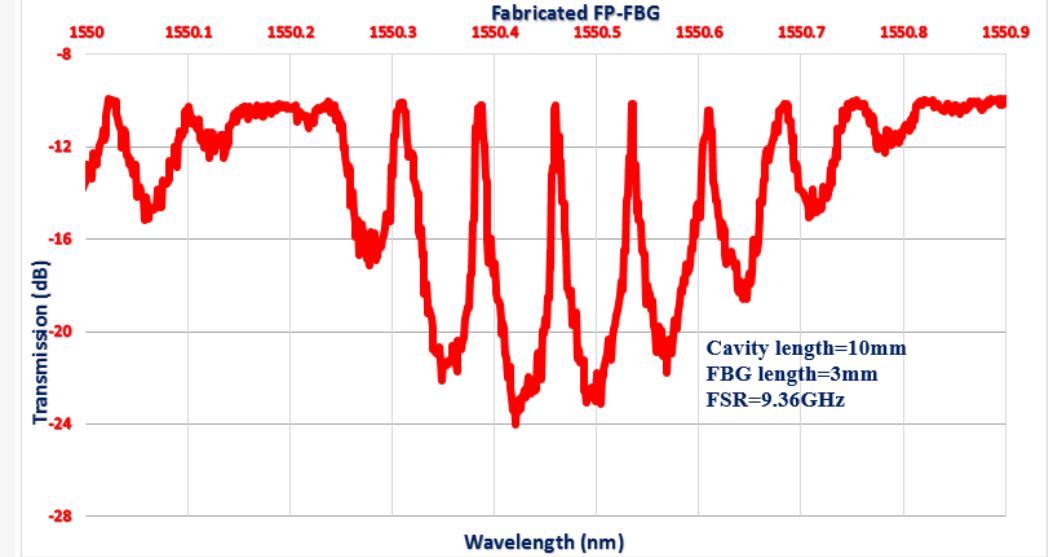

Fig. (2.17) *The Fabricated FP-FBGs after the LWM characterization.*

The spectrum of fabricated FP-FBGs are compared with the Matlab simulated FP-FBGs and is shown in figure (2.18). This figure shows a good agreement with the simulated and fabricated FP-FBGs. The simulation is not matching with the fabrication at short wavelength region because of ripples formation in a practical FBG aprodized grating.

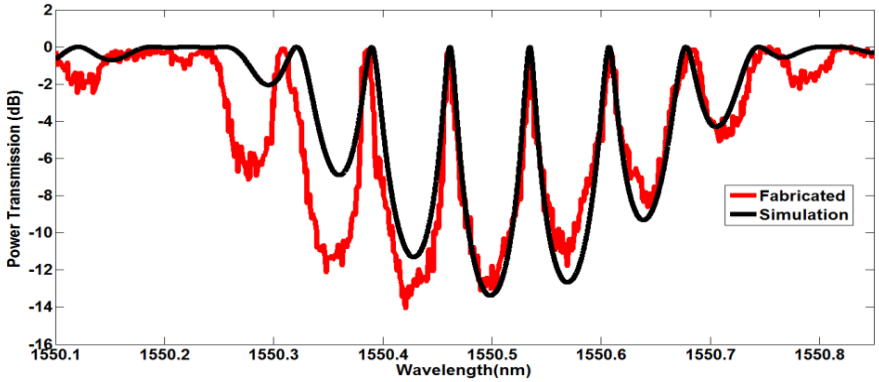

Fig. (2.18) *Simulated and fabricated FP-FBG spectrum with the parameters shown in figure 2.15*

Table 2.2 shows the repeatability study FBG and FP-FBG writing attempts.

Date	Cavity Length	FSR	Extinction	Phase Mask
26-10-12	10mm	11.23/10.58	13dB	Ibsen 1071.21nm
18-02-13	10.2mm	8.8GHz/8.96GHz	3dB	Ibsen 1071.21nm
18-02-13	9.5mm	9.83/16.3/7.12	3.5dB	Ibsen 1071.21nm
18-02-13	9.2mm	11.9471/12.82/11.32	16dB	Ibsen 1071.21nm
18-02-13	9mm	12.07/12.39/	15dB	Ibsen 1071.21nm
19-Feb	11.5mm	9.827/9.8283/9.9537/9.9548	15dB	Ibsen 1071.21nm
06/08/13	FBG	Bragg ƛ=1550.612nm	8dB	Ibsen 1071.21nm
06/0813	FBG	Bragg ƛ=1550. 2nm (Elongated Fiber)	6.5dB	Ibsen 1071.21nm
06/08/13	FBG	Bragg ƛ=1550. 650nm (Elongated Fiber)	9dB	Ibsen 1071.21nm
06/08/13	FBG	Bragg ƛ=1550.143nm (Elongated Fiber	8.3dB	Ibsen 1071.21nm
06/08/13	FBG	Bragg ƛ=1549.644nm (Elongated Fiber)	5.5dB	Ibsen 1071.21nm
06/08/13	11.5 (Burst-mode)	10.1/ 8.7/ 8.4/9.6	7dB	Ibsen 1071.21nm
06/08/13	11.5 (cont - mode)	9.60/9.35/9.2	6dB	Ibsen 1071.21nm
7/08/13	10.6mm	9.73/ 9.73/ 9.6/ 9.73	5dB	Ibsen 1071.21nm

We also carried out the spectral measurement with a FP-FBG purchased from Technica Optical components USA, with following specifications.

FBG length (L)	-3mm
Cavity length (δL)	-10mm (center to center)
FBG Reflectivity	-95%
Fiber type	-SMS 28C-acrylate fiber
Peak extinction (SLSR)	-≥ 15dB

The characterization was done with lightwave measurement system mentioned and we had taken two traces with time duration of 36 minutes each and slight spectral shift observed. The FSR observed is 10.7 GHz and 11.3 GHz in the region (1550nm to 1550.5nm) where maximum power extinction were observed. It is seen from figure (2.19) that power extinction is >15dB and more number of transmission peaks compared to our fabrication results.

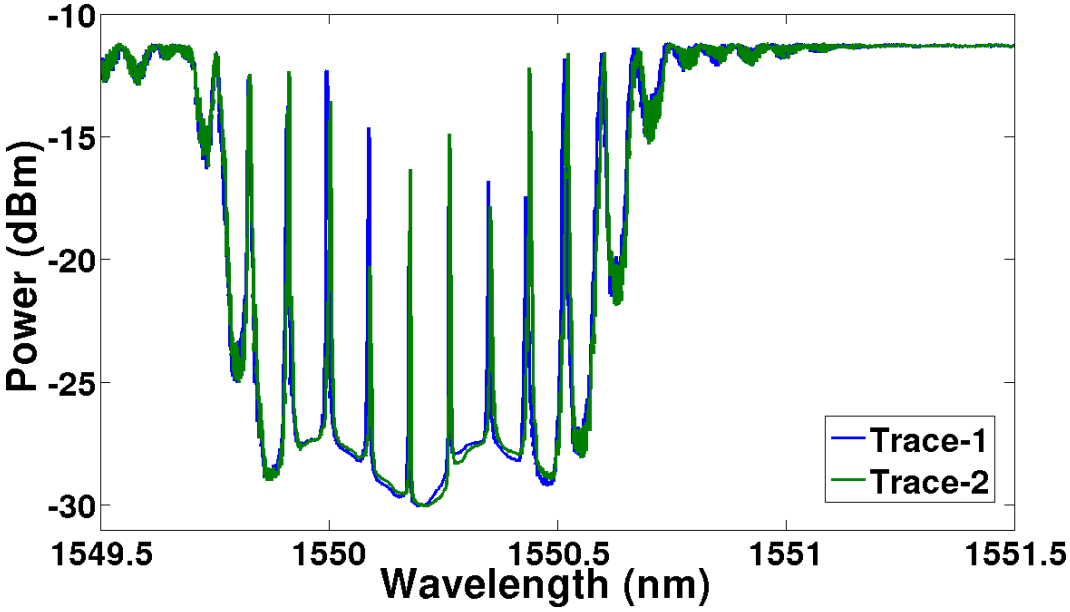

Fig. (2.19) *Transmission spectrum of purchased FP-FBG (*Technica Optical components USA*)*

2.7 Conclusion

In this chapter we describe the simulation and fabrication of Fabry-Perot filters (FPF) based on Fiber Bragg grating (FBGs). It has a lot of merits compared to Fiber Bragg gratings. The full width half maximum (FWHM) of the FBG fabricated FBG filter (shown in figure2.8) is approximately 500pm. But in the case of a FP-FBG (as shown in figure 2.15) the FWHM is approximately 20pm. This very narrowband filter response of FP-FBGs finds applications in all optical signal processing and circuits. The main advantages of narrowband filters are ultra-high speed operations and high energy efficiency in all optical signal processing. The next chapters describe some of the applications of the FP-FBGs in all optical signal processing components and devices. We are focusing on the design and application of FP-FBG as a basic but essential all optical signal processing components like integrator, differentiator and for all optical data clock recovery.

2.8 References

1. Rosa Romero, Orlando Frazão, Filip Floreani, Lin Zhang, Paulo V. S. Marques, Henrique M. Salgado,*"Multiplexers and De multiplexers Based on Fibre Bragg Gratings and Optical Circulators for DWDM Systems"* IEEE International Conference on High Speed Networks and Multimedia Communications. pp 442-451,(2003).

2. M. A. Davis, D. G. Bellemore, and A. D. Kersey, *"Design and performance of a fiber Bragg grating distributed strain sensor system,"* in Proc. SPIE 1995 North American Conf. Smart Structures Materials, San Diego, CA, , vol. 2446, pp 227-29,(1995)

3. V. Reddy M.K, Srimannarayanan, T.V. Apparao, M. Saji Sankar *"Design and development of high-temperature sensor using FBG*" *Proc. SPIE* 9586, Photonic Fiber and Crystal Devices: Advances in Materials and Innovations in Device Applications IX, 95860I, Vol 9586,pp16-17,(2015).

4. RMaría, Fernández - Ruiz, Alejandro Carballar, José Azaña, *"Design of Ultrafast All-Optical Signal Processing Devices Based on Fiber Bragg Gratings in Transmission"* Journal of Light wave Technology, vol. 31, no. 10, pp 1593-1600, (2013).

5. A. W Snyder, *"Coupled-mode theory for optical fibers,"* Journal of Optical society of America, Vol 62, pp 1267-1277, (1972).

6. Sanjeev Dewra, Vikas, Amit Grover *"Fabrication and Applications of Fiber Bragg Grating- A Review"* Journal of Advanced Engineering Technology and Application4, No. 2, pp 15-25,(2015).

7. Zhang, R W Fallon, A. Gloag, I Bennion, F. M. Haran, and P. Foote *"Spatial and wavelength multiplexing architectures for extreme strain monitoring system using identical-chirped-grating-interrogation technique,"* Proceedings of the Optical Fiber Sensors Conference (OFS-12) Williams burg, VA, USA, Paper OThC12, (1997).

8. Y.J. Rao *"Fiber Bragg grating sensors: principles and applications"* Optical Fiber Sensor Technology, Springer Volume 2 ,pp 355-379, (1998).

9. Xu, M.G Reeekie, Y.TChow, J.P.Dakin *"Optical in-fiber grating high pressure sensor"* Electronics Letters Vol 29, pp 398-399,(1993).

10. Sanjeev Dewra, Vikasand Amit Grover *"Fabrication and Applications of Fiber Bragg Grating- A Review"* Adv. Eng. Tec. Appl. 4, No. 2, pp15-25, (2015).

11. H Patrik, S.LGilbert *"Growth of Bragg gratings produced by continuous-wave ultraviolet light in optical fiber"* Optics Letters Vol. 18, pp 1484-1486,(1993).

12. J.Nishii, KoheiFukumi, Hiroshi Yamanaka, Hiroshi Kawazoe *"Photo-chemical reactions in GeO_2-SiO_2 glasses induced by ultraviolet irradiation: Comparison between Hg lamp and Excimer LASER"* Physical Review B, vol 52,pp 1691-95,(1995).

13. Andreas Othonos and Kyriacos Kalli *"Fiber Bragg Gratings, fundamentals and applications in telecommunications and sensing"* Artech House, Boston, London.(1999).

14. J. Stone, *"Photo refractivity in GeO_2 doped silica fibers"*, Applied Physics, 62, pp. 4371-4374, (1987).

15. K. D. Simmons, S. LaRochelle, V. Mizrahi, G. I. Stegeman and D. L. Griscom. *"Correlation of defect centers with a wavelength-dependent photosensitive response in germania-doped silica optical fibers",* Optics Letters, 16, pp. 141-143, (1991).

16. M.J Yuen, *"Ultraviolet absorption studies of germanium silicate glasses"* Applied Optics Vol. 21, pp 136-140, (1982).

17. V. B Neustruev *"Colour centers in germanosilicate glass and optical fibers"* Journal of Physiscs, Condenced matter, Vol 6, pp 6901-36, (1994).

18. E.M Dianov, D.S. Starodubov, and A.A.Frolov, *"UV-Argon laser induced luminescence changes in germanosilicate fiber preforms"* Electronics Letters, Vol 32, pp 247-247,(1996).

19. D.S.Starodubov, V. Grubsky, Jack Feinberg, B. Kobrin, and S. Juma "*Bragg grating fabrication in germanosilicate fibers by use of near UV light; a new pathway for refractive index changes"* Optics Letters, Vol 22, pp 1086-1088,(1997).

20. L.Dong J L Archambault, LReekie, P S Russell, D.N.Payne*" Photo- induced absorption changes in germanosilicate preforms: Evidence for the color-center model of photosensitivity"* , Applied Optics, Vol 34, pp 3436-40, (1995).

21. Philip S. Russell, Duncan P. Hand, Yuk T. Chow, L. J. Poyntz-Wright *"Optically-Induced creation, transformation and organization of defects and colour- centres in optical fibres,"* International Workshop on Photoinduced Self-Organization Effects in Optical Fiber, Quebec City, Quebec May 10-11, Proceedings SPIE,Vol 1516,(1991)

22. R.M Atkins, V.Mizrahi, *"Observations of changes in UV absorption bands of single mode germanosilicate core optical fibres on writing and thermally erasing refractive index gratings"* Electronics Letters Vol 28, pp1743-44,(1992).

23. R.M. Atkins, V. Mizrahi, T. Erdogan, *"248 nm induced vacuum UV spectral changes in optical fiber preform cores: support for a colourcentre model of photosensitivity",* Electronics Letters, 29, pp. 385-387 (1993).

24. D.K.W.Lam,B.K.Garside, *"Characterization of single-mode optical fiber filters"* Applied Optics Vol 20, pp 440-445,(1981).

25. K. O. Hill,G. Meltz*, "Fiber Bragg grating technology - fundamentals and overview,"* Journal of Lightwave Technology, vol. 15, no. 8,pp. 1263–1276, (1997).

26. K.O. Hill, B.Malo, F.Bilodieo, Jalbert *"Bragg gratings fabricated in monomode photosensitive optical fiber by UV exposure through a phase mask,"* Applied Physics Letters Vol 62, pp 1035-36,(1993).

27. D.Z. Anderson, V. Mizrahi, T.Erdogan, AE.White*"Production of in-fiber gratings using a diffractive optical element"* Electronic Letters, vol 29,pp 566-568,(1993).

28. Nahar Singh, Subhash, C.Jain, A.K.Aggarwal and R.P.Bajpai *"Fiber Bragg grating writing with using phase mask technology"* Journal of Scinetific & industrial research vol 64, 2005 pp108-115,(2005).

29. YueQiu, Yunlong Sheng, *"Optimal Phase Mask for Fiber Bragg Grating Fabrication"*Journal of Lightwave Technology, vol. 17, no. 11, pp 2366-2370,(1999).

30. B. A. Tahir, J. Ali, H. S. Phing, R. A. Rahman *"An investigation on the techniques for inscribing Bragg grating structures"* Journal of Opto electronics and Advanced Materials, Vol. 11, No. 8, pp1045 – 1057,(2009).

31. Turan Erdogan "*Fiber Grating Spectra"* Journal of Lightwave Tech- nology, Vol 15, pp 1277-1294, (1997).

32. J.B Albert, Malo,K.O.Hill,L.E.Erickson *"Apodisation of the spectral response of Fiber Bragg grating using a phase mask with variable diffraction efficiency,"* Electronics Letters Vol 31,pp 223-224,(1995).

33. Albert J, B Malo, K.O Hill, DC Johnson, S.Theriault *"Comparison of one-photon and two-photon effects in the photosensitivity of germanium-doped silica optical fibers exposed to intense ArF excimer laser pulses"* Applied Physics letters, Vol67, pp 3529-30,(1995).

34. R. Kashyap, *"Fiber Bragg gratings".* Academic Press, San Diego, (1999).

35. Max Born, Emil Wolf *"Principle of Optics"* Chapter 7,Pergoman Press, Oxford (1970)

36. Luis L Sánchez-Soto, Juan J Monzón, GerdLeuchs *"Many facets of the Fabry-Perot"* European Journal of Physics, Volume 37, Issue 6, PP. 064001-02,(2016).

37. V.S Hari, K.V Madhav, V.T Gopakumar, B.Srinivasan, S.Asokan,,*"Novel Technique for Fabricating Fabry-Perot Filters Based on Fiber Bragg gratings"* Paper OFD23.In: International Conference on Fiber Optics and Photonics, Hyderabad, (2006).

38. V.T. Gopakumar, K.V.Madhav,B. Srinivasan,S. Asokan,*"Fabry-Perot Cavities Based on fiber Bragg gratings"*, Paper OP-FIO-6. In: International Conference on Optoelectroncis and Lasers, Dehradun, (2005).

.....ꕥ.....

Chapter 3

THE OPTICAL INTEGRATOR

3.1 Introduction

As mentioned, the biggest advantage of optical communication technology is the availability of huge bandwidth. Optical systems and components have the capability to perform a large number of complex mathematical operations per unit time. Optical signal processing is capable of doing large number of parallel computations simultaneously. The speed of data processing optically is several orders of magnitude higher than that achievable by the electronics components and systems. So the all-optical circuits for complex mathematical operations, signal processing, and data networking can overcome the speed limitations of electronic-based systems. In order to process the signal in all optical domain, there must be equivalent basic building block as that of electronic processing of signals

[1]. Integrators and differentiators are good examples for basic signal processing components. Thus, the design and implementation of these fundamental optical devices is the first step towards the realization of all-optical signal processing circuits. In this chapter we are designing and simulating the all optical integrators using FBGs and FP-FBGs. There are a lot of works and demonstrations reporting FBG based integrators [2, 3]. Here we propose an integrator based of FP-FBGs. The main advantages of integrators based on FP-FBGs are its higher processing speed and low phase error noise compared to a FBG based integrators [4]. While considering a passive RC integrator, the capacitor C is acting as an electrical energy storing device [5]. That is, a capacitor look like a voltage sources for a short period of time (dt). So in other words, the output from an RC integrator circuit, which is the voltage across the capacitor, is equal to the time integral of the input voltage. A temporal integrator is a device that is capable of performing the time integral of an arbitrary input waveform [3] and is characterized by its ability to store energy in one form or another (e.g. optical, electrical). In electronics, as discussed a simple parallel plate capacitor can store electrons, due to its inherent capability to store electrical charge. But in the case in the optical domain, photons need to be stored and localized in the same fashion as a capacitor accumulates electrical charge [6]. In FBGs the localization of photons are arising from the multiple scattering and interference from each period of the grating [7].

A discrete-time photonic temporal integrator is a linear optical filtering element (e.g. coherent optical resonant cavity) capable of generating a periodic sequence of N amplitude and phase equalized time impulses in response to an input temporal impulse (N = 2, 3, 4 …) with a time resolution of a few picoseconds [8]. This is corresponding to a processing speed in the order of a few hundred GHz. The resonant cavity of a FP-FBG based optical integrator is the cavity formed by two FBGs separated by a finite distance [9]. While considering a photonic integrator, it can process complex data (i.e. both amplitude

and phase), but the electronic integrator can process only the real data [10]. This feature offers new applications for advanced signal processing and various complex computing tasks.

3.2 The FBG Integrators

An optical integrator is widely used as a basic building block of all optical signal processing [2, 11]. A photonic temporal integrator is a device that performs the cumulative time integral of the complex temporal envelope of an input arbitrary optical waveform [12]. It is shown in figure (3.1). The all optical integrator based on FBGs is a passive integrator.

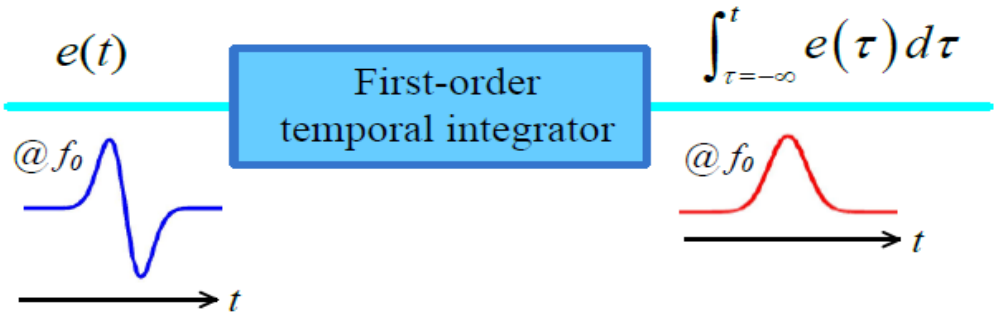

Fig. (3.1) *Schematic representation of optical integration*

FBGs are low-cost, all-fiber, passive optical device. It is widely used as an excellent optical filtering component in optical communication system and for sensing applications. Recently it has been found that the FBGs can also be used as an all optical integrator [2, 11].

The operation of an ideal optical coherent temporal integrator can be expressed as [13].

$$f_{out}(t) = \int_{-\infty}^{t} f_{in}(t)dt \qquad (1)$$

In frequency domain it becomes

$$F_{out}(\omega) = \frac{F_{in}(\omega)}{(j\omega)} \quad (2)$$

The spectral transfer and impulse responses of the ideal integrator are, respectively,

$$H_{out}(\omega) = \frac{F_{out}(\omega)}{F_{in}(\omega)} = 1/(j\omega) \quad (3)$$

This gives out

$$h_{ideal}(t) = u(t) \quad (4)$$

Where the u(t) is the unit step function. From the equation (3.3) gain at ω = 0 is infinite. From the equation (3.2) a finite gain is only possible if F_{in} (ω=0) =0. So the $H_{ideal}(\omega)$ can be accurately approximated with a complex Lorential function [14], which is equivalent to a decreasing exponential impulse response in the temporal domain [15]

$$H_{ideal}(\omega) = \frac{A}{(j\omega + \tau^{-1})}$$

$$h_{approx}(t) = A \exp(\frac{-t}{\tau})u(t)$$

$$\text{Therefore } f_{out}(t) = f_{in}(t) * h_{approx}(t) \quad (5)$$

Where, in the equation (5) '*' represents the convolution operation and τ is the time constant.

In order to find the FBG and FP-FBG impulse responses the following set up (figure 3.2) can be used.

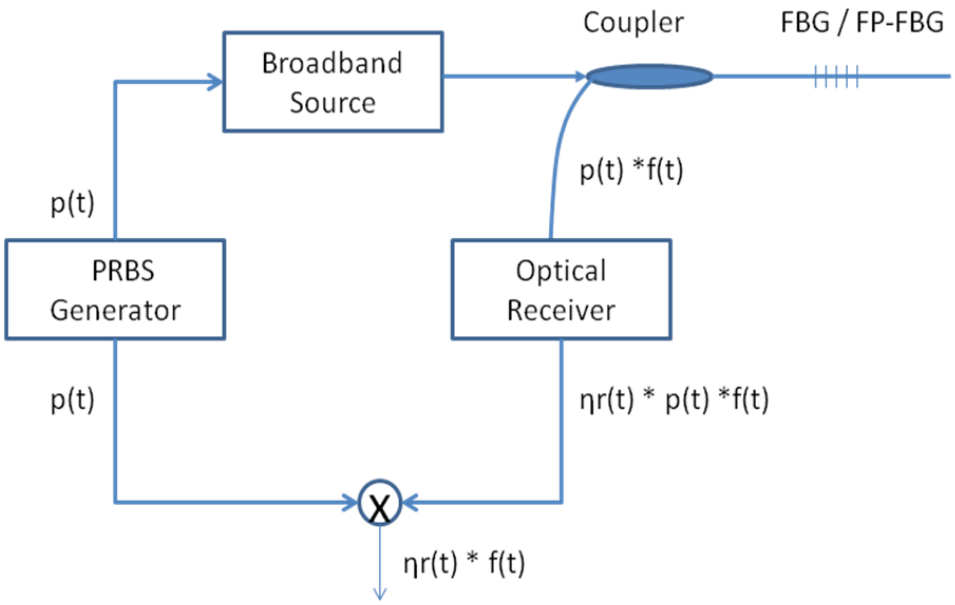

Fig. (3.2) *The experimental set up for finding out the impulse response of a FBG/FP-FBGs*

Similar to an electrical passive Resistor-Capacitor (RC) integrator (figure 3.3), a uniform FBG can also work as an all optical integrator. The impulse response of a uniform FBG shows a decreasing exponential as shown in figure (3.4). Here the impulse response is obtained by convolving the reflection spectrum of FBG with a unit delta signal. In this simulation the FBG length is 10mm and reflectivity is 80%.

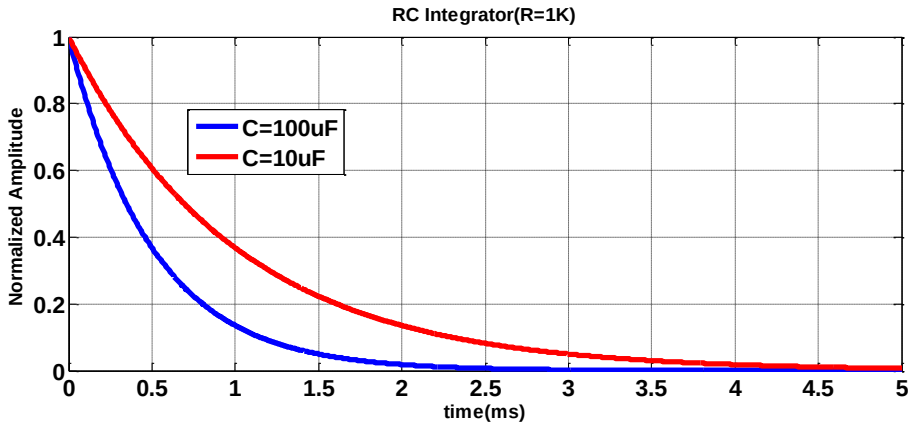

Fig. (3.3) *The electrical RC integrator with different capacitor values*

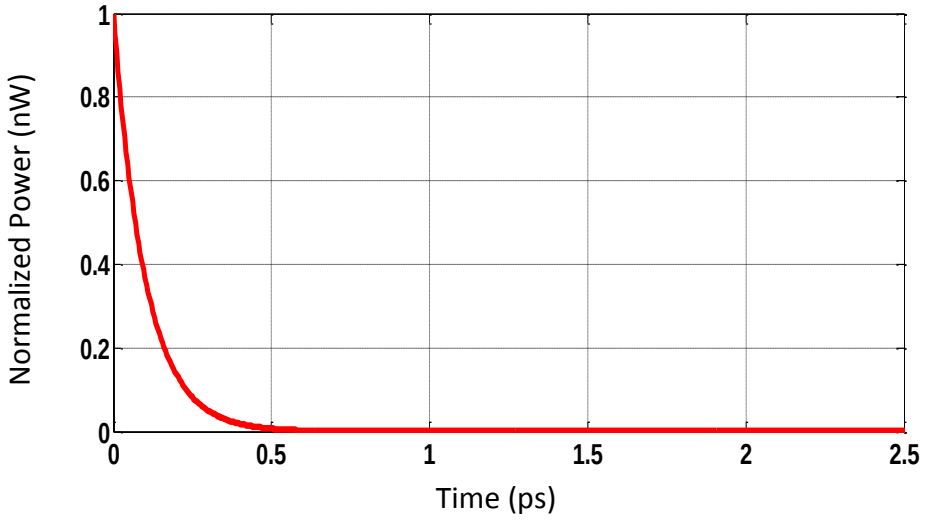

Fig. (3.4) *The FBG impulse response*

So the all optical integration is the convolution of the input signal with FBG impulse response. The FBG impulse response is obtained by convolving the reflectivity of the FBG with a unit impulse pulse, both reflectivity equation and impulse function is (unit delta function) already mentioned. A FBG can act as an integrator in weak coupling regime if the FBG length (grating length) satisfies the condition shown below [16].

$$L \gg 6.\Delta t.c/2.n_{eff} \qquad (6)$$

Where 'Δt' is the time duration of the input waveform and signal, n_{eff} is the effective refractive index of the grating. For strong coupling regime the above grating profile for integration can be obtained by inverse scattering algorithm [15]

The integration can be performed over a limited time window (T_h) which is decided by the round trip propagation time (τ_h) through the FBG length 'L' and is given by the equation (3.7) [17].

$$\tau_h \approx 2.n_{eff}.L/c \qquad (7)$$

3.3 Simulation Results of FBG Integrators

The response of FBG integrator for a normal Gaussian, pi-shifted Gaussian and double Gaussian is shown in figure (3.5) [17]

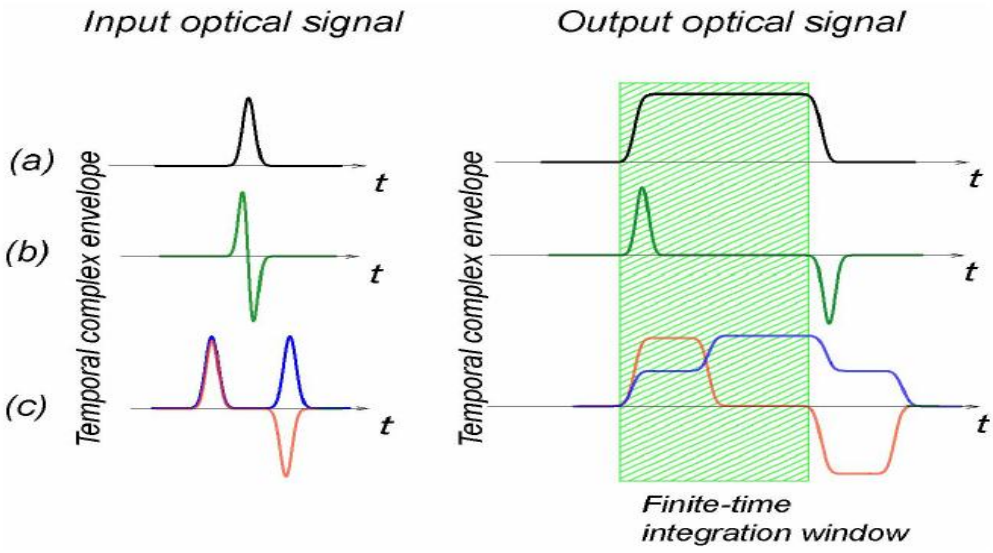

Fig. (3.5) *The FBG integrator response to different pulse shapes [17]*

In a FBG integrator circuit the optical signal at the integrator output signal is need not be zero outside the integration time window. The FBG integration gives an output signal with ending amplitude identical to the starting amplitude as shown the figure (3.5).

The following figure (3.6) shows the response of a FBG integrator to a normalized Gaussian input signal pulse with FWHM of 180ps, and the input pulse energy is taken 1nJ for the simulation. The response is the well-known flat-top pulse. These ultra-short flat top temporal intensity profile pulses are highly desirable for nonlinear optical switching and frequency conversion applications [18].

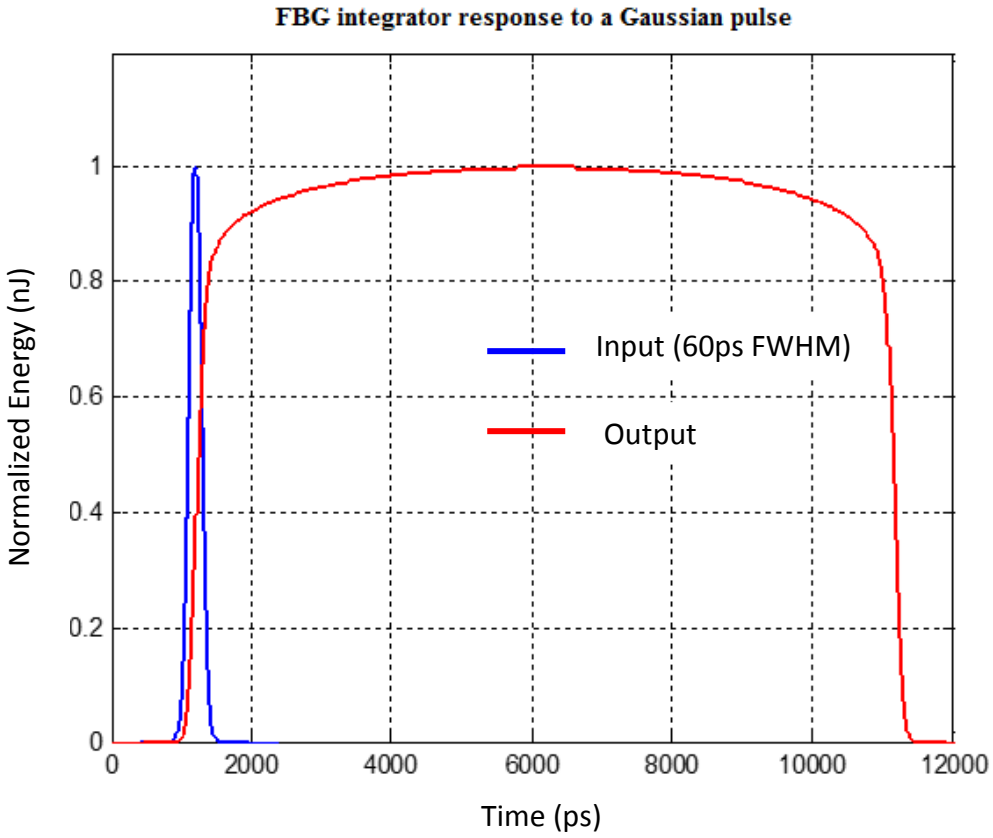

Fig. (3.6) *FBG integrator response to a single Gaussian pulse.*

When the FBG integrator input is in-phase double Gaussian pulses of 200ps FWHM separated by 500ps with total energy of 1nJ, the response consists of consecutive two steps. It can be seen that the double in-phase response simply add the area under the two pulses. This is equivalent to the addition of integration of leading pulse to the trailing pulse as shown in figure (3.7). When the input pulses are pi-shifted, the second Gaussian signal will compensate for the cumulative time integral for first Gaussian pulse and gives out square like (flat-top) pulse waveform as shown in figure (3.8). More explanation on the response of the integrators to different standard input pulses will be explained in the next section, which is the all optical integrator based on FP-FBGs.

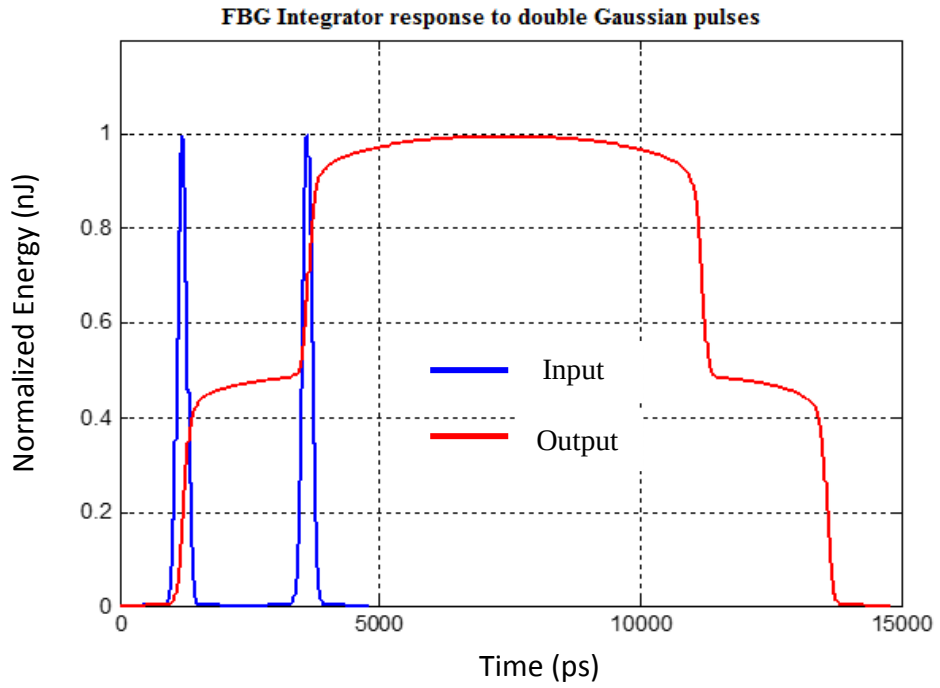

Fig. (3.7) *FBG integration response to the double in-phase Gaussian pulses*

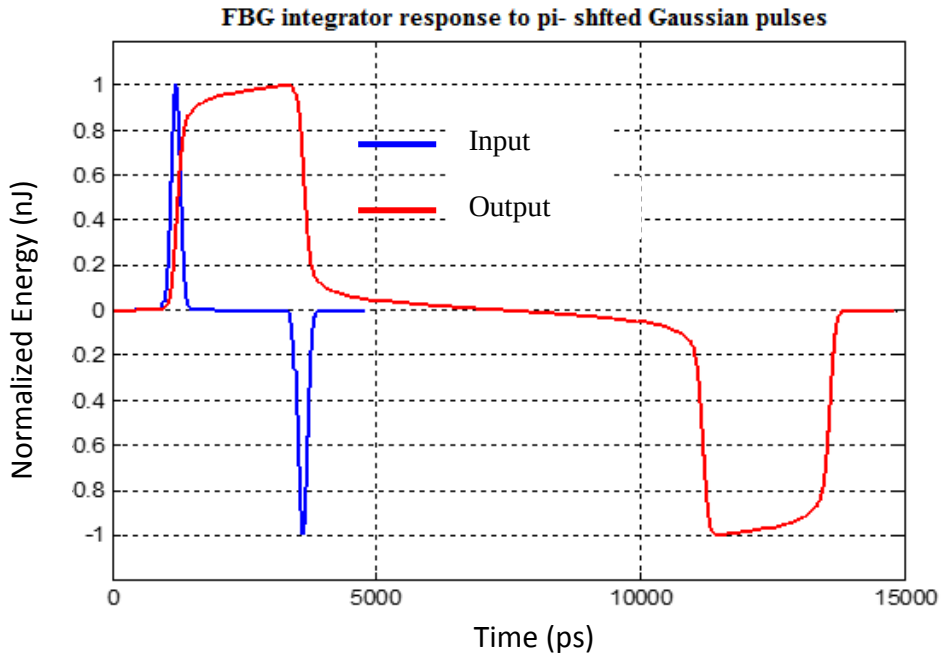

Fig. (3.8) *The FBG integrator response to π-phase shifted pulses*

3.4 Why FP-FBGs is prefer to FBGs for optical signal processing components and devices

Here we exploit some of the advantages of Fabry-Perot filters based on FBGs over FBGs for the design and simulation of optical integrators and differentiators.. The FBG-based optical filters, which usually work in reflection, for time-domain signal processing are severely limiting the time resolution (operation bandwidth). This is due to the fact that the temporal resolution of the filter's impulse response is directly related to the spatial resolution of the grating profile (for short length FBGs), more exactly they are Fourier transform pair (spatial resolution is the minimum spatial distance along which the amplitude of the mode coupling coefficient ($\kappa(z)$) changes significantly). The most important advantage of FP-FBG based filters are its ultra-narrow bandwidth, which is in the order of 10-25ps (FWHM). The narrow bandwidth (FWHM) can be seen from the fabricated spectrum of FBGs and FP-FBGs (figure 2.10 and 2.17 respectively). This ultra-narrow bandwidth of FP-FBG filters can be making use for high speed and high bandwidth applications. Moreover the narrow bandwidth response of filter can increase the energetic efficiency of the processing. FBGs work in reflection which requires the use of additional devices (e.g., optical circulator) to retrieve the reflected outputs, incurring in additional losses and become costlier. Another drawback comes as the reflection FBGs are far more sensitive to the presence of noise in the grating amplitude and phase profiles than in transmission [11, 14]. This is because in the case of FBGs in reflection the signal optical field interacts strongly with the grating length. That is, it must reflect from the grating. This means that any imperfection in the fabrication of the FBG like the noise in the UV writing process and polarization mode dispersion introduced into the signal by the grating can severely degrade system performance. If the grating is operated in transmission as in FP-FBG, the interaction between the optical signal and the grating is much weaker, and hence imperfections in the grating willnot be impressed upon the optical signal field.

3.5 The FP-FBG Integrator

A photonic temporal integrator is a device capable of 'integrating photons'. That is performing the time integral of an arbitrary optical input. Photonic temporal integrator finds application in photonic signal processing and computing applications. It is a fundamental element used as data processing/analysis, photonic bit counting, optical memory units and analogue computing of differential equations. This last application is particularly interesting. In analogy with its electronic counterpart, a photonic integrator is the key element to create ultrafast analogue all-optical circuits aimed at solving the differential equations that model fundamental phenomena and applied processes in virtually any field of science and engineering [2,11].

As expected for an all-optical technology, a photonic integrator can provide processing speed orders of magnitude faster than its electronic counterpart. As mentioned in the introduction of this chapter, the photonic integrator enables the processing of complex information (that is, both amplitude and phase), whereas an electronic integrator is restricted to processing real data. This feature offers an important additional degree of freedom over an electronic integrator, enabling new applications for advanced information processing and various computing tasks [19].

From basic signal processing theory it follows that a temporal integrator can be implemented using a linear filtering device with a temporal impulse response h(t) proportional to a unit step function[2,20]. It has been explained while discussing the theory of FBG based integrator [15].

$$h(t) \propto u(t), where\ u(t) is\ the\ unit\ step\ function \qquad (9)$$

Physically, this requires the use of a structure capable of storing an incoming time-varying waveform (e.g. electric field intensity) with an output

being a continuous signal proportional to the sum of the total stored field at each instant of time.

In the spectral domain, the transfer function H(ω) of an ideal photonic integrator is inversely-proportional to the base-band frequency (ω-ω_0).

$$H(\omega) \propto \frac{1}{j(\omega-\omega_0)} + \pi \times \delta(\omega - \omega_0) \qquad (10)$$

Where δ is the Dirac delta-function, ω is the optical frequency and ω_0 is the carrier frequency of the signal to be processed. This implies that the transmission should be > 1 in the proximity of ω_0 and, ideally, it should become infinite at ω_0.

Let us assume a general FP cavity composed of two identical mirrors, each characterized by a field reflectivity r. where 'r' is defined as the ratio of the reflected and incident field amplitudes. Here we consider the $|r| \leq 1$, and the mirror separation is L. The net gain γ in the cavity medium, defined as the round-trip field amplitude gain that excludes loss due to the mirrors with $\gamma < 1$ for loss and $\gamma > 1$ for gain. Here we use a passive FP filter based on FBG and there is no gain medium, so the value of γ is irrelevant in this work. It can be easily proved that for such FP cavity, the temporal impulse response h(t) is given within a certain fraction of the FP free spectral range.

$$h(t) \propto e^{-kt} \times u(t) \qquad (11)$$

Where $k = \frac{1}{T} \times \ln(r^2\gamma)$

And T is the round-trip propagation time in the FP cavity with 'n' being the cavity refractive index and 'c' the speed of light in vacuum. The equation (11) says that the signal energy stored in a FP cavity is leaking out following an exponential time variation. While we compare the impulse response of the FP cavity with that of an ideal integrator (figure 3.9), the field of an incoming ultra-

short impulse will be stored and subsequently delivered from the FP cavity with a constant flow exactly as required for optical temporal integration. It should be noted that there is a fundamental limitation in terms of the fastest temporal feature of the input waveform that can be processed with a resonant cavity-based optical integrator. This limitation is given by the spectral range over which FP cavity provides the temporal impulse response [21].

For pulses shorter than the round-trip propagation time in the cavity, T, the signal would be released in the form of discrete impulses, temporally spaced by T. In practice, only temporal features longer than ≈5T will be integrated with low processing error. The FP integrator's processing bandwidth is limited to ≈1/5 of the integrator free spectral range.

The Fabry-Perot FBG-based integrator is based on time-domain design method. The functionality of an ideal integrator is emulated over a finite time window using a passive linear optical filter [20, 22].

The temporal impulse response of an ideal integrator (response of the device to an input ultra-short temporal impulse launched at the time t = 0) is proportional to the unit step function u(t) [19]. As mentioned above, the required impulse response can be practically achieved from a Fabry-Perot FBG. In this scheme, the optical signals to be processed must be spectrally centered at the Bragg frequency of the FBG. The accurate temporal integration of complex-field optical signals with time-features as fast as ~6 ps is only limited by the processing bandwidth of the FP-FBG integrator. The integration time window of ~200 ps by the FP-FBG integrators is a 4-fold improvement over the operation speed of (~50ps) optical signal to be processed with a FBG integrator [9]. Another advantage of FP-FBG based integrator is related to linear filtering process, the energetic efficiency (ratio of the output signal energy to the input signal energy)

of an optical integrator depends on the spectral bandwidth of the optical signal to be processed; a lower energetic efficiency is obtained when processing a waveform with a broader bandwidth since in this case, a larger portion of the input signal spectrum is filtered out by the FBG spectrum. The spectral bandwidth of FP-FBG is much narrower than a FBG spectrum. The spectral width (FWHM) of FBG fabricated is around 1nm and that of a FP-FBG is in the order of 0.01nm (figure 2.10 and 2.17).

The principle of optical integration by FP-FBG can be better illustrated by evaluating the frequency response of a general optical resonant cavity. The spectral transfer function of a standard optical resonator, such as the FP, is a periodic frequency comb with a period fixed by the FSR which is already explained the section 2.5. The shape of the spectral response around any given resonance is well approximated by a Lorentzian function. Figure (3.9) illustrates the matching between the amplitude spectral transfer functions of an ideal integrator (black curve, defined by equation (11) and an optical resonator (red curves) around a specific resonance ω_0 [17]. The regions inside the dashed boxes represent the frequency range over which the resonator response resembles very nearly that of an ideal integrator. From this representation, it can be easily understood how a larger FSR (that is, a shorter round-trip propagation time achieved through a reduction of the physical device dimensions) translates into high energetic efficiency and broader integration bandwidth, that is, a higher processing speed [16, 17].

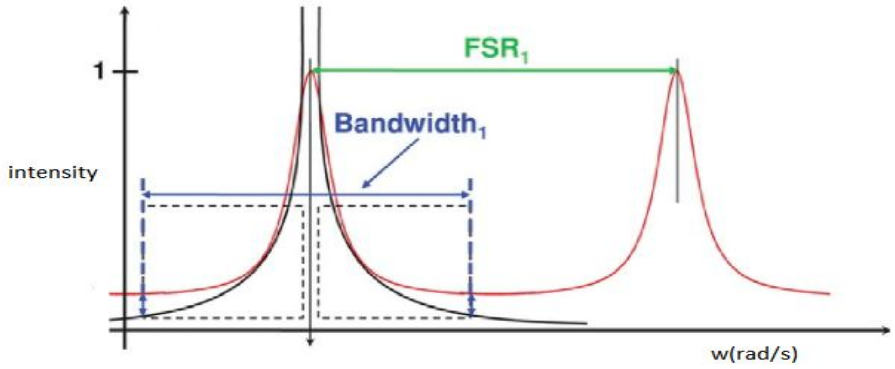

Fig. (3.9) *Comparison of spectral intensity transfer functions of a general resonator and that of an ideal integrator (black curve).[16,17]*

If the signal is band limited to F< FSR/20, we could approximate a single-pole RC filter with the following transfer function and impulse response of FP-FBG integrator

$$h(t) = c \times e^{-ct} \; for \; t > 0 \qquad (12)$$

The figure (3.10) shown below is the magnitude of {H(f)} of the FP-FBG filter and its comparison with RC filter (R=1kΩ and C=1μF) approximation. The simulation is done for reflectivity (R) = 0.99, Finesse (F) = 312.6, and the FSR = 3800 GHz. When If I > FSR/20, the magnitude of H(f) is very small, and therefore, the effect of adjacent channel interference beyond this frequency range is negligible.

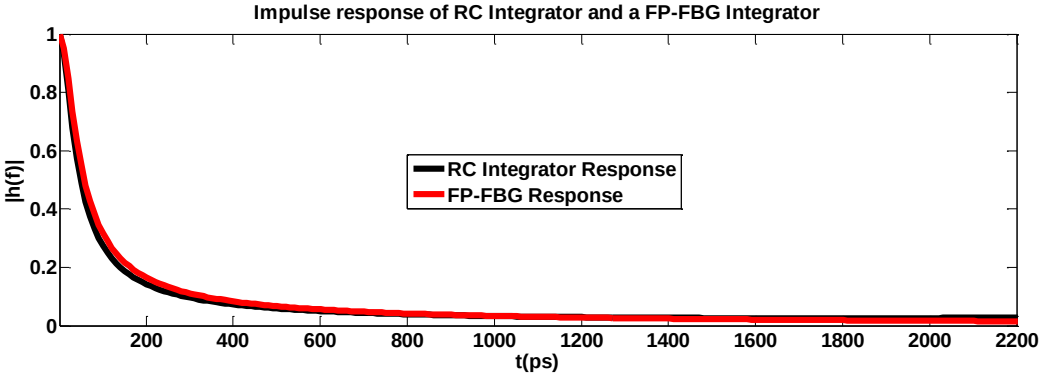

Fig. (3.10) *Impulse response of electrical RC integrator and FP-FBG integrator*

3.6 The FP-FBG Integrator Simulation Results

For testing the integration properties, individual pulses (Gaussian, Double Gaussian and π-Phase shifted Gaussian) with a FWHM time width of 70 ps was simulated. The output waveform approximates the temporal impulse response of the device. This happens when the bandwidth of the input pulse and the integrator are close to each other. The measured temporal impulse response closely follows the theoretical curve defined by equation (6). The estimation of integration time window (defined as the decay time required to reach 80% of the maximum intensity) of ~800 ps.

In all simulations of the FP-FBG integration the FBG length (L) is 3mm, and separation between FBGs (cavity length δL) is 1mm, the power reflectivitites of FBGs 95% and the n_{eff} =1.45. Figure (3.11) shows the FP-FBG integrator response to a Gaussian pulse.

In the next simulation we used a double-pulse waveform composed of two replicas of the same Gaussian pulse (in phase Gaussian pulses). For inter-pulse relative phases fixed to zero, in-phase pulses, we would expect the time cumulative integral to look like two steps with each corresponding to the integral of one pulse, separated by the pulses' relative time delay. Figure (3.12) also shows for the double-pulse simulation, the integrator simply sums up the area under the two field amplitude waveforms.

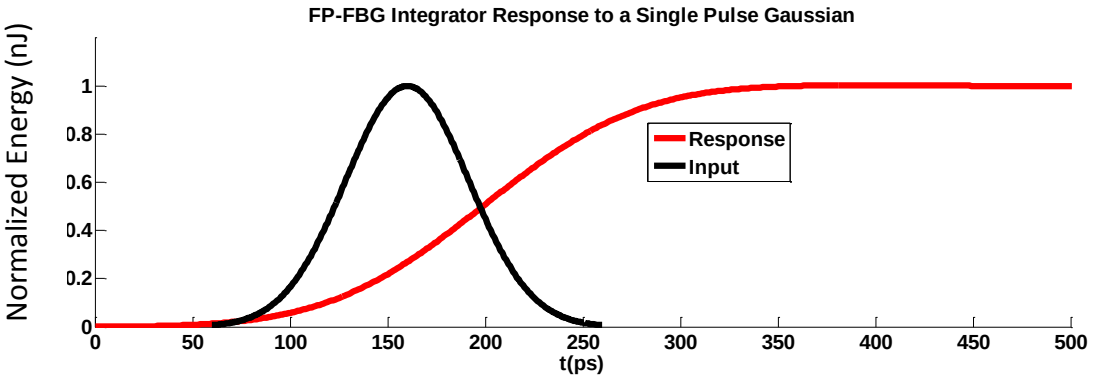

Fig. (3.11) *FP-FBG integrator response to Gaussian pulse*

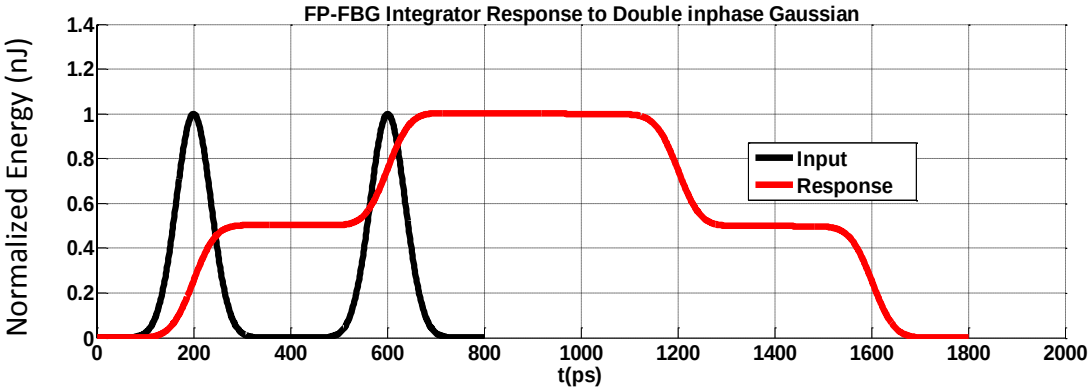

Fig. (3.12) *FP-FBG integrator response to double in-phase Gaussian pulses*

For inter-pulse relative phases fixed to π (out-of-phase pulses) the second step should have the opposite direction, forming thus a square-like temporal waveform. This phenomenon is schematically shown in figure (3.13). When the pulses are out of phase, the time integral of the second optical pulse will compensate that of the first pulse (assuming the two pulses are nearly identical). This leads to a square-like time profile with a duration given by the input inter-pulse delay [23].

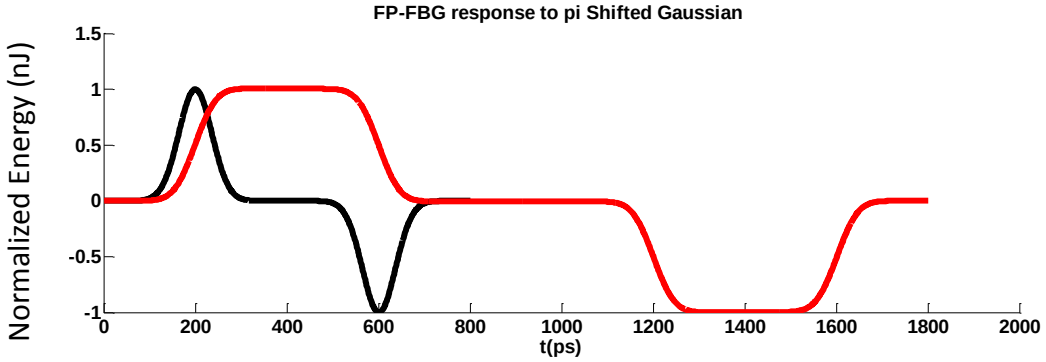

Fig. (3.13) *FP-FBG integrator response to pi-Shifted Gaussian pulses*

The above results suggest an important application. It can act as a 1-bit optical memory unit. When it is switched to the state '1' by launching an input 'set' pulse and subsequently to reset state '0' by a π-phase shifted pulse with respect to the 'set' pulse. In this scheme, the memory switching time is fixed by the integrator processing speed [25].

3.7 Conclusion

As mentioned, the optical integrator is the basic building block of the all optical signal processing circuits and devices. This chapter describes the operation of optical integrator using FBGs and FP-FBGs. FBG and FP-FBG are giving the same response to the standard input signals. But the FP-FBGs can operate at much higher operation widow and high energetic efficiency than the FBG based integrators, as spectral width (FWHM) of FBG fabricated is around 1nm and that of a FP-FBG is in the order of 0.01nm (figure 2.10 and 2.17).The processing error (deviation between the integrated signal outputs from FP-FBGs the ideal integral of the input signal along the integrator operation window) is slightly less as compared to FBGs for longer input time (narrow bandwidth) waveforms.

3.8 *References*

1. J. Azaña, *"Ultrafast analog all-optical signal processors based on fiber-grating devices,"* IEEE Photon Journal, Vol2, pp 359–386, (2010).

2. M. A. Preceiadio, M Muriel, "*Ultra-fast all-optical integrator based on a fiber Bragg grating"*. Optics Letters. Vol33, pp 1348–1350, (2008).

3. H.Mohammad Asghari, C.Wang, J.Yao, Jose Azana "*Demonstration of FBG-based first and second-order photonic temporal integrators with optimized energetic efficiencies" IEEE* LEOS Annual Meeting Conference Proceedings, (2009).

4. R.María. Fernández-Ruiz, Alejandro Carballar, José Azaña "*Design of Ultrafast All-Optical Signal Processing Devices Based on Fiber Bragg Gratings in Transmission"* Journal of Lightwave Technology, Vol. 31, pp1593-1600, (2013).

5. S.C. Dutta Roy (IIT Delhi) "Circuit Theory" NPTEL.

6. Sanjeev John *"Localization of light"* Physics Today,Vol 44, pp32-40 (1991).

7. Othonos and KyriacosKalli, *"Fiber Bragg Gratings, fundamentals and applications in telecommunications and sensing"*Artech House, Boston, London.

8. L.Nikolay, Kazanskiy and Pavel G. Serafimovich "*Coupled-resonator optical waveguides for temporal integration of optical signals*" Optics Express Vol. 22,pp. 14004-14013, (2014).

9. V.T Gopakumar, K.V Madhav, B.Srinivasan, S.Asokan "*Fabry-Perot Cavities Based on fiber Bragg gratings",* Paper OP-FIO-6. In: International Conference on Optoelectroncis and Lasers, Dehradun, (2005).

10. José Azaña "Ultrafast Analog All-Optical Signal Processors Based on Fiber-Grating Devices" IEEE Photonics Journal Vol: 2, pp 359 – 386,(2010).

11. J.Azaña "*Ultra-fast analog all optical signal processers based on fiber Bragg grating*". IEEE Photonics J. 2(3), pp359–386,(2010).

12. H. Mohammad Asghari and José Azaña "*Proposal for arbitrary-order temporal integration of ultrafast optical signals using a single uniform-period fiber Bragg grating" Optics* LettersVol. 33, pp 1548-1550, (2008).

13. A.V. Oppenheim, Alan V. Willsky, S. Hamid Nawab "*Signals and Systems*" Prentice-Hall India, (1992).

14. A.Papoulis, "The Fourier integral and its applications" (McGraw-Hill).

15. R.Feced, M N Zervas, MA Muriel "*An efficient inverse scattering algorithm for the design of nonuniform fiber Bragg gratings"* IEEE Journal of Quantum Electronics (Volume: 35, pp 1105-1115, (1999).

16. Joze Azana *"Proposal of a uniform fibre Bragg grating as an ultrafast all-optical integrator"* Optics letters Vol33, No 1, pp 4-7, (2008).

17. Y. Park, T.J Ahn, Y. Dai, "*All-optical temporal integration of ultrafast pulse waveforms*". Opt. Expr. 16(22), pp17817–17825, (2008).

18. J. Azana, L. K. Oxenløwe, E. Palushani, R. Slavık, M. Galili, H. C. H. Mulvad, H. Hu, Y. Park,A. T. Clausen and P. Jeppesen "*In-Fiber Sub picosecond Pulse Shaping for Nonlinear Optical Telecommunication Data Processing at 640 Gbit/s*". International Journal of Optics Volume 2012 , Review Article ID 895281, pp 1-16 (2012).

19. M. Ferrera, Y. Park,, L. Razzari, B. E. Little, S. T. Chu, R.Morandotti, D. J.Moss & J. Azaña*"On-chip CMOS-compatible all optical integrator" Nature Communications"* Vol1, pp 1-5, (2010).

20. C.K Madsen, J.H Zhao, "*Filter Design and Analysis: a Signal Processing Approach" Wiley, New York (1999).*

21. A.V Oppenheim, R.WSchafer, J.R Buck, "*Discrete-time signal proce ssing*" 2nd Edition, New Jercy,(1999).

22. R. Slavík, Y Park, N Ayotte, S Doucet, J Tae, L R Sophie,A José, "*Photonic temporal integrator for all-optical computing*". Opt. Expr. 16 (22), pp 18202-18214 (2008).

23. B.Jalali, J.Chan, M.H. Asghari "Time bandwidth Engineering" Inaugural Issue of OSA's High impact Journal, Optica, Vol 1,pp 23-31 (2014).

24. Marcello Ferrera, Yongwoo Park, Luca Razzari, Brent E. Little, Sai T. Chu, Roberto Morandotti, David J. Moss, and José Azaña*"All-optical 1st and 2nd order integration on a chip"* Optics Express vol 19,23,pp 23153-6,(2011).

25. H. Mohammad Asghari, Y Park, José Azaña*"New design for photonic temporal integration with combined high processing speed and long operation time window"* Optics Express 425, vol 19, pp425-435(2011).

.....ꕥ❋ꕥ.....

Chapter 4

FP-FBG DIFFRENTIATORS

4.1 Introduction

As explained in Chapter 1, all optical signal processing devices have operation speed in the order of hundreds of GHz or more, which is inaccessible to the current electronic technologies. Photonics devices are about three times faster than the current electronics-based devices and systems. This high speed all optical devices are required for a wide variety of applications including ultrafast computing, ultrahigh bit-rate telecommunications, ultrafast pulse shaping, and analysis of ultra-short optical pulses [1]. All optical signal processing also has some added advantages like small footprint and lower power consumption [2]. Performing signal processing in all optical domains will also reduce the opto-electronic conversion inefficiencies [3]. Numerous researches and techniques to design all-optical temporal signal processing devices have been reported,

especially with the fiber Bragg gratings (FBGs). The FBG based pulse shapers [4], differentiators [5], integrators [6] and Hilbert transformers [7] have already been demonstrated. The main advantages of FBGs are their low cost, low insertion loss and full compatibility with fiber-optic communication and sensing systems [8]. However, the FBGs usually work in reflection, which results a number of critical limitations like limited processing bandwidth, introducing phase noise and requirement of additional components like circulators and couplers. The addition of circulators and couplers to FBG based systems introduce additional cost and losses [9, 10]. Here we propose and design all optical differentiators based on Fabry-Perot filters using FBGs. This filter can overcome the limitations of FBG based devices, especially the processing bandwidth and requirement of additional optical devices, as the FP-FBGs are very narrow band filters (FWHM in the order of a few tenths of pico-meters compared to a few hundred nanometres for FBGs) working in transmission mode.

4.2 Theory and design of optical differentiator by FP-FBGs

A first-order optical temporal differentiator is a device that provides the first-order derivative of the complex envelope of an arbitrary input optical signal. This evaluates the real time derivative of the input optical signal intensity. There are many design techniques discussed in various literatures [11-13]. All of these are based on FBG and Long period grating (LPG). Here we propose a novel method of design of optical differentiator based on FP-FBGs. To the best of our knowledge, no scientific reports on optical differentiator based, till date on FP-FBGs. The optical differentiator together with the Optical integrator forms the basic building block for all optical signal processing.

Optical differentiators were first proposed by N. Q. Ngo et al [12] and this constitutes a basic device to analog all optical signal processing. Now a days the optical differentiators are widely used as pulse shapers in ultra-wideband (UWB)

communication systems [13]. Here the information encoded is transmitted by these shapes of pulses without a carrier. Hence the transmitters need precise pulse shapes.

An all-optical temporal differentiator is a fundamental function for ultrafast signal processing, which provides the derivative of the time-domain complex envelope of an arbitrary input optical signal.

As per the theory, a first-order temporal differentiator can be expressed as

$$f_{out}(t) = \frac{df_{in}(t)}{dt} \quad (1)$$

Where $f_{in}(t)$ and $f_{out}(t)$ are the complex envelopes of the input and output respectively, and it is essentially a linear filtering device providing a spectral transfer function of the form[10]

$$\frac{E_{diff}(\omega)}{E(\omega)} = H(\omega - \omega_0) = j(\omega - \omega_0) \quad (2)$$

Where ω is the optical carrier frequency and $(\omega - \omega_0)$ is the base-band frequency. Thus the two key features of the filter's transmission are that, it should depend linearly on the base band frequency and should be zero at the signal central frequency ω_0. These two features imply an exact π phase shift across the central frequency ω_0. This functionality can be implemented using a linear optical filter providing a linear amplitude (V-shaped) spectral response over its operation bandwidth with a complex zero at the carrier frequency of the signal under test [14].

The spectral response magnitude $H(\omega)$ and phase $argH(\omega)$ of an FBG are related by Hilbert transform[12]. An FBG in transmission can simultaneously obtain the amplitude and phase spectral response of a differentiator, since they are logarithm Hilbert transform (LHT) pairs [10]. That is;

$$\arg\left(\left|H_{diff}(\omega)\right|\right) = H\left(ln\left|H_{diff}(\omega)\right|\right) \quad (3)$$

Where the 'H[.]' stands for the Hilbert Transform,

The required energy depletion at the signal central frequency can be produced by resonance-induced complete energy transfer elsewhere. This can be achieved by resonant transfer of light between two spatially close waveguides, or between two modes of the same waveguide. Resonant light coupling is induced when the light propagates through both waveguides (modes) with identical speeds. Which is practically attainable e.g. by an increase or decrease of the light speed in one of the waveguides (modes) using a suitable diffraction grating.

Many works and implementations have been seen in different literatures for optical differentiators using long period gratings (LPGs) and FBGs [3, 15]. A FBG-based differentiator, however, has a comparatively higher tolerance to the environmental changes [16] although the LPG approach has been proved to have a good performance in a regime of huge bandwidths (up to 19 nm) [17]. But the transmission spectrum of an LPG is more difficult to be tailored as compared to that of an FBG [16, 5]. However the FBG based optical differentiator needs very complex fabrication techniques as it need very high reflectivity of 99.9999%, corresponding transmission dip of 60dB with very high coupling coefficient ~6600/m for an FBG length of 10cm [18]. Another technique seen in literature is phase shifted FBG differentiators [19] but of complex fabrication procedure.

We are proposing Fabry Perot filters based on FBGs (FP-FBGs) for all optical differentiators. As mentioned in section 3.3, there are some unique advantages of the FP-FBG based optical components and devices over the FBG-based optical devices.

FP-FBGs working in transmission can overcome two of the constraints facing with FBG based differentiators. They are, avoiding the need of additional devices like circulators and being more robust against phase noise. Secondly, the spectral transfer function of FP-FBG is minimum-phase [20]. This is imposing a

very tight relationship (Hilbert transform) between the filter's amplitude and phase spectral responses. High energetic efficiency and high processing speed of a differentiator depends on the band width (FWHM) of the filter response. A broad set of optical pulse processors (e.g., time differentiators, integrators) and shapers (e.g., for Flat-top, triangular, parabolic pulse generation, amongst others) can be realized using minimum-phase optical filters [19]. As the strong reflections of FBGs only appear in a narrow bandwidth near the Bragg wavelength, with FWHM in the order of a few hundreds of pico-meters, the processing speed is limited. The FBG based FP structures can produce the resonant peaks with FWHM in the order of a few tenths of pico-meters. Therefore, when it is used as filters a single resonant transmission peak can be at the Bragg wavelength (See figure 4.2). For this reason, the FBGs used to form FP structures are selected to have the same central wavelength (λ_B). That is; FP-FBGs formed by when two FBGs are separated by a finite distance, called cavity length δL, (See figure 2.14). All parameters of the both FBGs in FP-FBGs are identical, like FBG length (L), FBG period (Λ), and effective refractive index (n_{eff}) and maximum changes in the index of refraction (Δn) [21].

There are two conditions required for ideal differentiators. The spectral response should be zero transmission (100% reflectivity) at the central wavelength. A good approximation can be obtained by defining a limited operational bandwidth and a maximum transmission dip in the central wavelength. The phase shift in the uniform FBG structure causes a resonance-induced transmission peak (i.e. reflection dip) in the grating's spectral transmission band gap. For an FP-FBG filter, the two FBGs must be identical (i.e.; $L1 = L2 = L$ and $\kappa 1 = \kappa 2 = \kappa$), i.e. $R1 = R2 = R$, where L is the cavity length and κ is the coupling coefficient, and R is the power reflectivity maximum. Secondly the phase shift in the middle of the structure must be exactly $\phi = \pi$ [10].

If these conditions are satisfied, then the grating's reflection dip exhibits the precise spectral characteristics that are required for an optical differentiation.

The possibility of strong reflection near the central wavelength of FBGs can be utilized in the formation of all fiber Fabry-Perot cavities, replacing the conventional mirrors [22]. In order to realize a π phase shift between the two uniform gratings, the cavity length can be adjusted. A FP-FBG is formed by two identical FBGs separated by finite distance, called cavity length δL. Here we need the cavity length which will give a phase shift of π, the two uniform FBGs act as mirrors of the Fabry-Perot cavity. Light intensity inside the cavity takes a maximum value only during the resonance condition given by [23].

$$n \times \kappa \times L = m\pi \tag{4}$$

Where m, n are nonzero integers, 'κ'is the coupling coefficient and 'L' is the cavity length.

For a phase shift equal to π, the length of the cavity is given by

$$L = \frac{m\lambda}{2n_{eff}} \tag{5}$$

The schematic of Fabry-Perot filters based on FBG was given earlier (figure 2.14). It has to be noted that the cavity length (L) is the physical separation between the two FBGs and the effective cavity length (δL) is, generally the center to center separation between the FBGs, which signifies how far the light penetrate in to the FBGs before they coming out.

4.3 FP-FBG differentiator- Fabrication and simulation results

While designing the FP-FBG differentiators, the center wavelength of FP-FBGs is 1550nm with free spectral range of 9.36GHz. The phase mask used at IIT Madras will give out a FBG length of 3mm. The FP-FBG design for high speed differentiators uses FBG length of 1mm each and cavity length of 1mm. A 1mm length of FBG for FP-FBGs can be fabricated by putting an opaque slit of 1mm thickness in the UV beam path to the Phase mask [24] as shown in figure (4.1).

Each FBGs of length of 1mm and cavity length (L) of 1mm with n_{eff}=1.46 with maximum coupling coefficient ($\kappa(z)$)=5256.1 m^{-1}. The length of each uniform grating was fixed to be an exact integer multiple of the grating period $\Lambda = \lambda_B / (2 \times n_{eff})$, i.e. L = N.$\Lambda$, with N = 1884. Here N is the number of periods (interfaces) of the gratings.

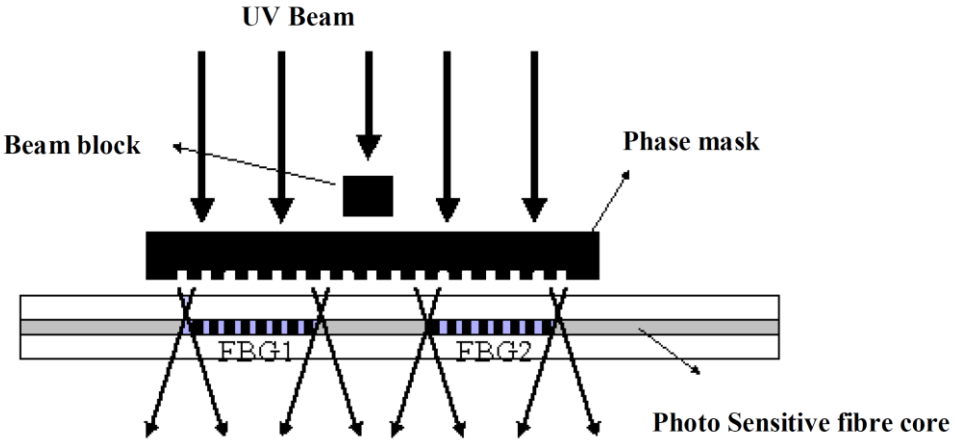

Fig. (4.1) *Fabrication set up for FP-FBG differentiator*

As per equation 2, the optical differentiator can be implemented [14] using an optical filter providing a linear amplitude (V-shaped) spectral response over its operation bandwidth with a complex zero at the carrier frequency of the signal under test as shown in figure 4.2. These two features imply an exact π phase shift across the central frequency ω_0 as shown in the phase profile in figure (4.3). Here we can see that the FWHM is around 50pm, which is much less than that of a FWHM of FBGs. This results higher speed differential operation is possible with FP-FBGs than that of FBG differentiator.

The amplitude and phase responses of a fabricated first-order optical differentiator are shown in figure 4.2 and 4.3 respectively.

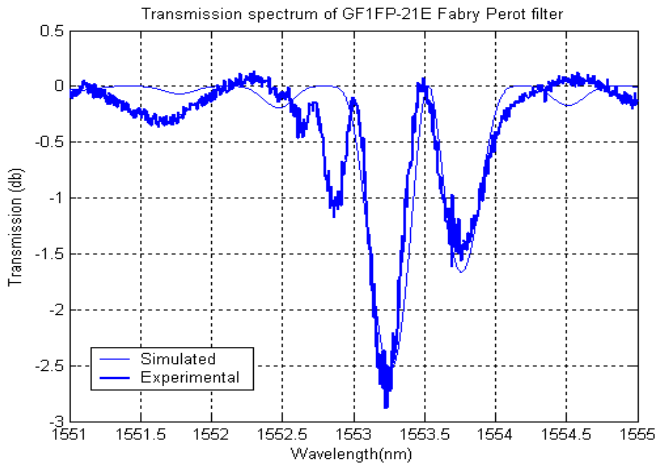

Fig. (4.2) *The transmission Spectrum of FP-FBG fabricated for differentiator*

The transmission dip (figure 4.2) exhibits the precise spectral characteristics ('V'-shape) that are required for optical differentiation. We recall that these characteristics involve an amplitude response that depends linearly on the frequency variable with a complex zero at the central frequency. From the phase response it can be seen that there is phase shift of 'π' at the central frequency (ω/2π). While doing the simulation, it is assumed that the FBG is an apodized one, so no side lobes in the figure. More transmission peaks at the central frequency and lesser side lobe's amplitude are required for a differentiator with less processing error.

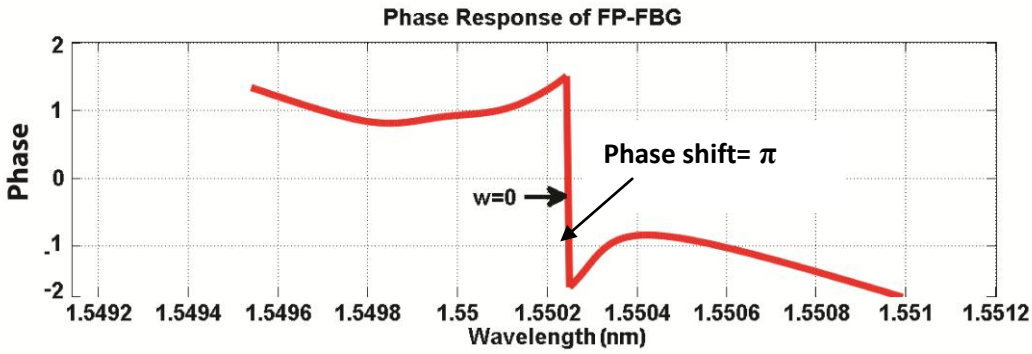

Fig. (4.3) *The phase response of a FP-FBG* differentiator

The simulated FP-FBG differentiator is tested with various pulse shapes like Gaussian, double Gaussian and Pi-Shifted Gaussian. A basic Gaussian pulse can be represented analytically by

$$x(t) = \frac{A}{\sigma\sqrt{2\pi}} e^{-\frac{t^2}{2\sigma^2}} \quad (6)$$

Where 'σ' is the standard deviation and σ^2 is the variance of the function and its first derivative is given by

$$x^{(1)}(t) = \frac{At}{\sigma^3\sqrt{2\pi}} e^{-\frac{t^2}{2\sigma^2}} \quad (7)$$

Here the simulation is done by the convolution of Gaussian pulse with a FP-FBG of transmission dip 15dB single peak as shown in figure (4.2).

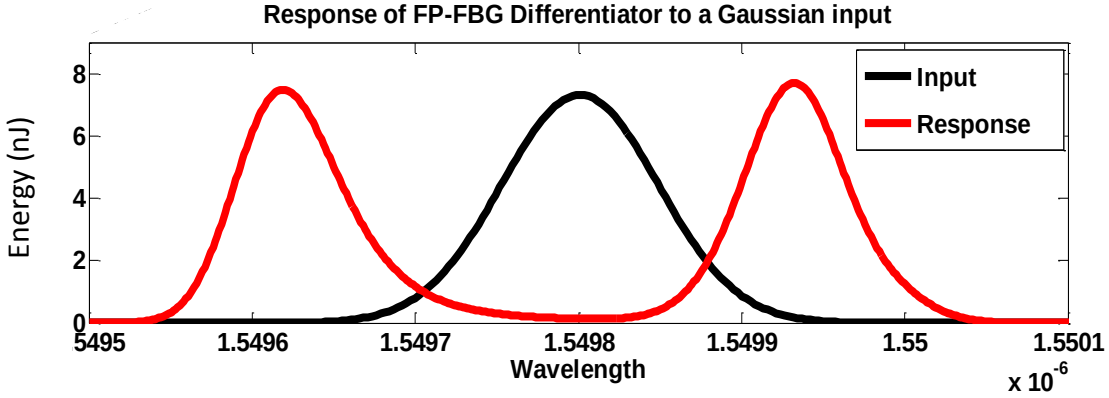

Fig. (4.4) *Response of FP-FBG differentiator to a Gaussian pulse*

In the above figure (4.4) the standard deviation of the Gaussian pulse is taken as 20ps. For the FP-FBG the center wavelength of 1550nm and the period of the grating (Λ) is 535.605nm and effective refractive index is 1.46. For a Gaussian input pulse the optical differentiator gives out an odd-symmetry Hermite–Gaussian (OSHG) waveform, consisting of two consecutive pulses. Each peak has around 15ps standard deviation, which is slightly narrower than the original Gaussian (20 ps). This Gaussian differentiated specific waveform is of interest for high speed dispersion managed optical communications. The OS-HG waveform is a good approximation of the second-order dispersion-managed (DM)

temporal soliton, also called a soliton molecule [25]. The result is fully agreeing with the latest simulation as well as fabrication results [26, 27].

And finally to study the response of FP-FBG based differentiator, the simulation is carried out with in phase bi-modal Gaussian and pi- shifted Gaussian pulses with same standard deviation and its response is shown in figures (4.5 and 4.6 respectively) below. In both the cases that is; differentiation of bi-modal Gaussian pulses and π- phase shifted Gaussian pulses, the differentiation is same as the response of single Gaussian pulse. For a Gaussian input pulse the optical differentiator gives out an odd-symmetry Hermite–Gaussian (OSHG) waveform, consisting of two consecutive pulses. There are challenges of generating such odd-symmetry pulse waveforms in a relatively simple and efficient manner, since accurate local changes in phase along the waveform duration are required.

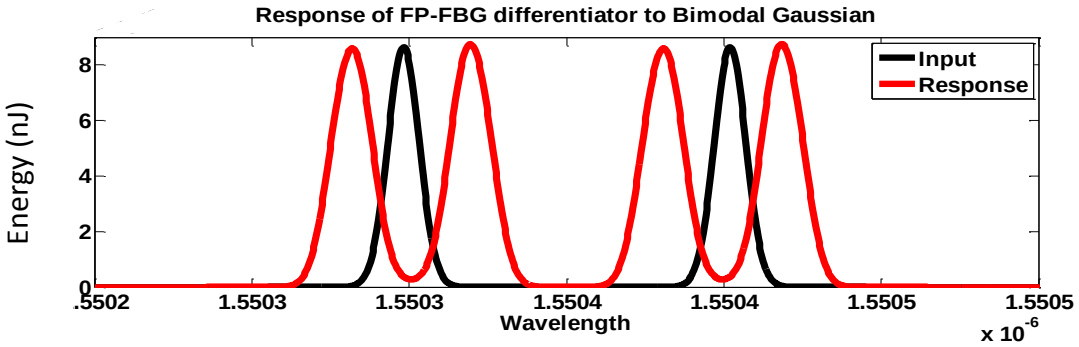

Fig. (4.5) *Response of FP-FBG differentiator to a bi-modal Gaussian pulses*

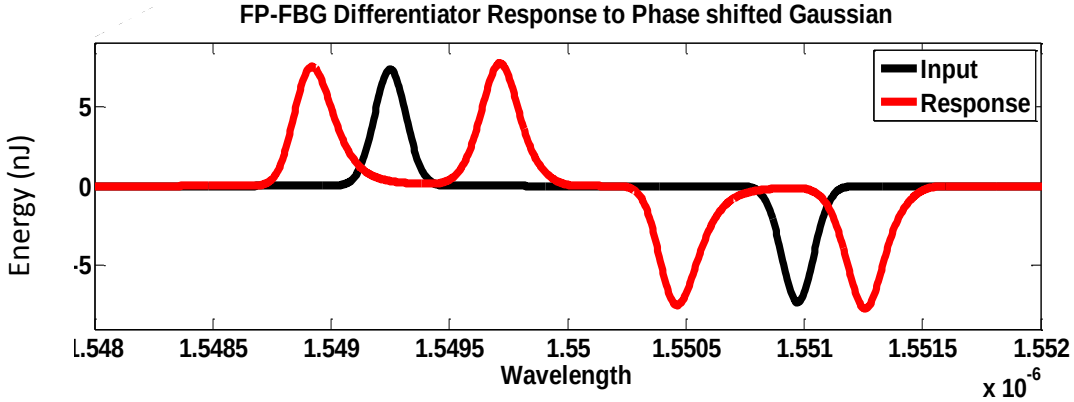

Fig (4.6) *Response of FP-FBG differentiator to pi-shifted Gaussian pulses*

Sub-picosecond HG waveforms were generated using propagation of the original Gaussian-like optical pulses through FP-FBG based photonic differentiators. Here the first-order OS-HG, pulse waveforms were generated by the first-order differentiation of sub picosecond Gaussian optical pulses.

Photonic temporal differentiators have also been proved useful for full (amplitude and phase) characterization of optical waveforms. The temporal intensity waveform at the differentiator output depends on both the intensity and the phase profiles of the input pulse [25]. Therefore the phase profile of a given optical signal can be recovered from the temporal intensity profiles of the signal under test before and after propagation through a first-order photonic differentiator [25]. This simple technique has proved particularly useful for accurate characterization of the group delay and phase spectral responses of dispersive devices [25-27].

4.4 Conclusion

This chapter, we discussed about the all optical differentiator using FP-FBGs. We have fabricated the FP-FBG, which will be working as a first order differentiator. An optical differentiator is a device that gives the first-order derivative of the complex envelope of an arbitrary input optical signal. The optical integrator and differentiator form the basic building blocks of all optical signal processing. Optical differentiators are widely used for the generation of optical monocycle pulses from an input Gaussian pulses for ultra-wideband systems. The optical differentiators are also used for the generation of a Hermite–Gaussian temporal wave form from an input Gaussian pulse and amplitude and phase characterization of different optical waveforms.

4.5 ***References***

1. Andrew M. Weiner *"Ultrafast optical pulse shaping: A tutorial review"* Optics Communications, Elsevier, Vol 284, pp 3669–3692, (2011).

2. D.J. Blumenthal, J. E. Bowers, L. Rau, H. F. Chou, S. Rangarajan, W. Wang and H. N. Poulsen, *"Optical signal processing for optical packet switching networks"*, IEEE Communication. Mag. pp. S16-S23, (2003).

3. J.Azaña, C.K. Madsen,K. Takiguchi, G. Cincontti, *"Optical signal processing,"*Journal of. Lightwave Technology, Vol. 24, no. 7, pp 2484–2486, (2006).

4. P. Petropoulos, M. Ibsen, A. D. Ellis, and D. J. Richardson, *"Rectangular pulse generation based on pulse reshaping using super structured fiber Bragg grating,"*Journal of Lightwave technology, vol. 19, no. 5, pp746–752, (2001).

5. R. Slavík, Y. Park, M. Kulishov, R. Morandotti, and J. Azaña, *"Ultrafast all-optical differentiators,"Optical Express.*, vol. 14, no. 22, pp10699–10707, (2006).

6. N. Q. Ngo, *"Design of an optical temporal integrator based on a phase shifted fiber Bragg grating in transmission,"*Optics Letters., vol. 32, no. 20, pp 3020–3022, (2007).

7. J. Ge, C.Wang, and X. Zhu, *"Fractional optical Hilbert transform using phase shifted fiber Bragg gratings," Optical Communications.*, vol. 284, no. 13, pp 3251–3257, (2011).

8. Andreas Othonos and KyriacosKalli, "*Fiber Bragg Gratings, fundamentals and applications in telecommunications and sensing"*Artech House, Boston, London, (1999).

9. R.María, Fernández-Ruiz, Alejandro Carballar *"Design of Ultrafast All-Optical Signal Processing Devices Based on FiberBragg Gratings in Transmission"* Journal of Lightwave Technology, VOL. 31, NO. 10, pp1593-1600, (2013).

10. J.Skaar,*"Synthesis of fiber Bragg grating for use in transmission".* Journal of Optical Society of America vol. 18, no. 3, pp 557–564, (2001).

11. N.Q Ngo, Yu, S.F., Tjin, S.C,C.H.Kam, *"A new theoretical basis of higher-derivative optical differentiators"* Optical Communication. 230, pp115–129,(2004).

12. Ming Li, DavideJanner, JianpingYao,ValerioPruneri**"***Arbitrary-order all-fiber temporal differentiator based on a fiber Bragg grating: design and experimental demonstration"* Optics Express, Vol. 17, No. 22 , pp19798-19807, (2009)

13. M.A Preceiadio, M.A Muriel, *"Design of an ultrafast all-optical differentiator based on a fiber Bragg grating in transmission"* Optics Letters.Vol33, pp2458–2460, (2008).

14. WenWentzlo and A. Chandrakasan, "Gaussian pulse genera-tors for subbanded ultra-wideband transmitters", *IEEE Transactions on Microwave Theory and Techniques*, Vol.54, No.4, pp 1645-1655, (2006)

15. M Kulishov, J.Azaña, *"Long-period fiber gratings as ultrafast optical differentiators"*. Opt. Lett. 30,pp 2700–2702, (2005)

16. N.K Berger, L. Boris, F. Baruch, K. Mykola, V.P David, J,Azaña *"Temporal differentiation of optical signals using a phase shifted fiber Bragg grating"*. Opt. Expr. 15(2), pp 617-620, (2007).

17. C.K Madsen, J.H.Zhao, *"Filter Design and Analysis: a Signal Processing Approach"* Wiley, New York (1999).

18. M.A Preceiadio, M.A.Muriel, *"Design of an ultrafast all-optical differentiator based on a fiber Bragg grating in transmission"* Optics Letters. 33(21), pp 2458–2460, (2008).

19. M.Kulishov, J.Azaña, *"Long-period fiber gratings as ultrafast optical differentiators"*. Opt. Lett. 30, PP 2700–2702, (2005).

20. Alejandro Carballar, Carlos L. Janer "*Complete Fiber Bragg Grating Characterization Using an Alternative Method Based on Spectral Interferometry and Minimum- Phase Reconstruction Algorithms"*Journal of Lightwave Technology ,Vol: 30, Issue: 16, pp 2574-2582, (2012).

21. V.S Hari, K.V Madhav, V.TGopakumar, B.Srinivasan, S. Asokan,"*Novel Technique for Fabricating Fabry-Perot Filters Based on Fiber Bragg gratings"* Paper OFD23.In: International Conference on Fiber Optics and Photonics, Hyderabad (2006).

22. C.K Madsen, J.H Zhao, *"Filter Design and Analysis: a Signal Processing Approach"* Wiley, New York, (1999).

23. Naum K. Berger, Boris Levit and Baruch Fischer ,MykolaKulishov, David V. Plant, José Azaña "*Temporal differentiation of optical signals using a phase-shifted fiber Bragg grating"* Optics Express, Vol. 15, No. 2 pp 371-381, (2007).

24. V.T Gopakumar, K.V Madhav, B. Srinivasan, S.Asokan, *"Fabry-Perot Cavities Based on fiber Bragg gratings"*, Paper OP-FIO-6. In: International Conference on Optoelectroncis and Lasers, Dehradun (2005).

25. José Azaña, "*Ultrafast Analog All-Optical Signal Processors Based on Fiber-Grating Devices"*, IEEE Photonics Journal,Vol 2, No 2 pp 359-386,(2010).

26. Siqi Yan, Yong Zhang, Jianji Dong, AolingZheng, Shasha Liao, Hailong Zhou, Zhao Wu, Jinsong Xia, Xinliang Zhang *"Operation bandwidth optimization of photonic differentiators"* Optics Express Vol. 23, No. 15 pp 18925-18936, (2015).

27. Ting Yang, Jianji Dong, Li Liu, Shasha Liao, Sisi Tan, Lei Shi, Dingshan Gao & Xinliang Zhang *"Experimental observation of optical differentiation and optical Hilbert transformation using a single SOI microdisk chip"* Microwave Photonics Vol 2, pp 1-6, (2014).

.....ꕥ.....

Chapter 5

THE ALL OPTICAL CLOCK RECOVERY

5.1 Introduction

Data clock recovery is an essential technique for a receiver to synchronize to a transmitted data signal in all communication system [1]. In an optical communication multiplexing system, (optical time-division multiplexing (OTDM)) the clock should be recovered at the base-rate for the requirement of optical de-multiplexing and add-drop multiplexing [2]. Normally the data clock recovery is by the comparison of injection locked optical phase of the received signal and the locally generated clock signal [3]. Non-linear phenomena such as four-wave mixing [4], cross-phase modulation in semiconductor optical amplifiers (SOAs) [4], three wave-mixing in periodically-poled lithium niobate (PPLN) waveguides [5] and electro-absorption modulation (EAM) [6], have been

exploited to provide the phase comparator functionality. When ultra-high speed operation (≥160 Gb/s) is involved, the major difficulty for the phase comparator lies in the very high time-resolution required because of the short duration of the bit time-slot [7]. There are 3 levels of synchronization in digital communications. They are (1) Bit synchronization (2) Frame or word synchronization (3) carrier synchronization [8]. The bit synchronization is also called the data clock synchronization. In synchronous transmission, data is not transferred byte-wise so there are no start bits or stop bits indicating the beginning or end of a word. But, there is a continuous stream of bits which have to be split up into bytes. Therefore the receiver has to sample the received data in the middle of bit period (T_b) and the sender's and receiver's clocks have to be kept in a synchronized state. The sampling clock frequency at the receiver is exactly the same as that of the transmitted signal sampling frequency. The retrieval of the transmitted clock at the receiver, which is transmitted along with the data stream, is called data clock recovery. In carrier synchronization the transmitter local oscillators are used for up-conversion and modulation. The receiver local oscillators are used for down-conversion and demodulation.

In modern computer network communications data is transferred as frames or packets, not as simple stream of bits or bytes. These types of networks are using the packet based routing, error correction and the sharing of one physical medium between multiple clients. Most often the physical medium is an optical fiber. The physical medium or channel is usually a serial link and does not have a concept of frames or separated data units. The transmitter and receiver have to recognize the frame borders in the data stream on the medium. The above process is called frame synchronization [9].

5.2 Need for Clock recovery

All-optical clock recovery is a key ingredient of all-optical signal processing such as 3R generation and network synchronization in the next generation high speed optical networks. The recovered clock signal is used for much functionality that requires synchronous operations, such as reshaping and retiming, OTDM de-multiplexing, modulation format conversion, and signal processing. The high-speed synchronization is a serious challenge for the current and development of future Optical Networks, whether it is addressed to point-to-point optical links or Optical Packet Switching (OPS) environment. These optical burst/packet switching is expected to improve the utilization of the network resources through statistical multiplexing and reduce latency in future optical networks. Development of a reliable clock recovery unit, efficient to extract the clock signal from short asynchronous bursts at high data rates, is essential for processing and routing the packets. All-optical clock recovery (CR) circuits are supposed to play a critical role in current and future high-speed all-optical networks as a stable and low-jitter synchronization signals will be required in several network sub-systems like receivers, regenerators etc.

In digital data communications we must take care of two types of synchronization problems. They are the carrier synchronization and bit synchronization. The carrier synchronization which concerns with the generation of a reference carrier with a phase at the receiver is closely matching that of the data signal being transmitted. This reference carrier is used at the receiver side to perform a coherent demodulation producing the output baseband data signal [10]. In the bit synchronization the receiver clock should synchronise with the baseband data-symbol sequence. Here we are discussing about the data clock recovery technique for the bit synchronization at the regenerative repeater or at the final receiver. Several optical timing extraction techniques suitable for high speed operation have been demonstrated [11]. Electrical data clock timing extraction

circuits usually use a phase-lock loop (PLL) configuration, where a microwave mixer acts as a phase detector. The speed of operation of such PLL circuits is limited by the phase detector to about 40 GHz (very high timing resolution is required as the bit-time slot is very short) [12]. Another problem faced with PLL based clock recovery is that the locking time works inversely with the timing jitter [7]. The advantage of using a PLL is low relative phase error as the phase of the incoming signal is constantly compared with the phase of the local oscillator. There is report of a self-clocking method that allows for fast synchronization, low timing jitter and highly stable clock performance for time-de-multiplexing functions. The method consists of inserting a 10 GHz clock pilot signal at the transmitter, and extracting this pilot signal at the receiver [13]. The above method is simple and scalable but has the disadvantages of manufacturing complexity and cost. The complexity and cost are coming from the high power consumption, pilot carrier generation, cross talk while combining with data signal and need for coupler and FBGs. The injection locking utilizes multi-electrode laser diodes (LDs) or optical inverters which switch between TE and TM modes. Here the output repetition frequency is locked to that of an injected optical pulse train. Using this technique, 5-GHz and 10-GHz clocks were generated all-optically [14]. The optical clock recovery by PLL and injection locking are intriguing since the clock is generated all-optically. But the disadvantages faced with these are rms jitter and relative phase error, which limits the operation speed up to 50Gbps [12]. Other methods are reported are all-optical clock recovery scheme based on a mode-locked Erbium fiber laser [15] and a nonlinear optical fiber loop mirror (NOLM) regenerator [16]. But it has insufficient performances for 3R operations though it finds applications for very long1R repeated transmission systems.

Broadly, the optical clock recovery methods may be divided into two main categories, active pulsating and passive filtering techniques. Active pulsating techniques employ an opto-electronic oscillator or a self-pulsating laser,

whose pulse repetition rate (B_S; Hz) is locked to the symbol rate (B_S; baud/s) of the incoming flow of information (at data rate B_B bit/s where $B_B = nB_S$ with n being the number of bits per symbol)[17]. The active techniques typically produce a high-quality clock signal, but usually at the price of higher device complexity and manufacturing costs [17, 18]. The passive filtering techniques simply remove a part or all of the information from the received signal and preserve only the base-frequency B_S associated with the symbol rate of the data signal. These techniques typically have simple construction and low manufacturing cost, with the quality of the recovered clock signal being the key challenge.

Among the passive methods, the optical clock recovery through direct filtering out of the frequency components of the clock signal with Fabry-Perot (FP) filter is very simple and very fast. The clock can be recovered within few bits, and the wavelength is transparent with respect to the data signal [19]. Moreover, the environmental sensitivity is relatively low since the FP filter is an optical passive tank circuit. Clock recovery does not necessarily require a self-pulsating arrangement. While the scheme is fully passive and uses no nonlinear components (such as an SOA), the operation speed of the method is virtually unlimited (depending on resonator length). Fabry-Perot filters based on fiber Bragg gratings are strong candidates for optical clock recovery, even in WDM passive optical networks [20]. Here we report all optical clock recovery at 10Gbps, using a Fabry-Perot filter consisting of two Bragg grating reflectors. Unlike bulk optical filters, the FBG-based FP filters possess high mechanical stability and ease of tuning.

5.2.1 The principle of Clock recovery by FP-FBGs

The principle of all optical clock recovery using a Fabry-Perot filter (FPF) is shown in figure (5.1). An optical signal created by return-to-zero (RZ) intensity modulation consists of continuous spectral components from data modulation and

line spectral components from clock, i.e. the optical carrier frequency f_c and the AM side bands $f_c \pm f_s$, $f_c \pm 2f_s$..., where f_s denotes the data clock frequency. All optical clock recovery can be achieved through extracting these line spectral components with narrow band filtering. A Fabry- Perot filter with a free spectral range (FSR) matched to the data rate and a relatively large finesse works effectively for this application. If 1) $f_c = q*FSR$ (where q is an integer), 2) $FSR = f_s$, and 3) the source line width is narrower than the resonator bandwidth, only the line spectral components which contain the carrier frequency f_c and the timing components $f_c \pm f_s$ are transmitted, resulting in the optical clock extraction[20,21].

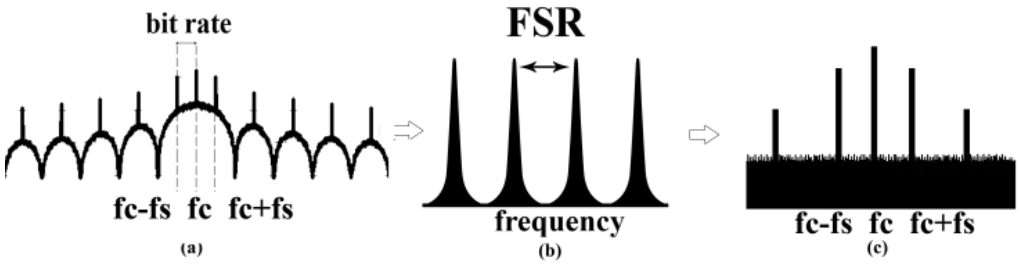

Fig. (5.1) *Principle of optical clock recovery based on FP filters. (a) Optical spectrum of an incoming RZ optical data, (b) Filtering characteristics of the FP filter, (c) Optical spectrum of the extracted optical clock.*

5.3 Simulation result of Clock Recovery

As explained in earlier chapters, the Fiber Bragg Gratings (FBGs) are widely using as narrow band filters as well as optical sensors. As explained, the all fibre Fabry-Perot (FP) structure can be realized using fibre Bragg gratings by replacing the conventional optical mirrors. When two identical FBGs are separated by a finite distance, δL, they form a frequency selective Fabry-Perot filters. Such a filter allows only certain frequencies falling within the bandwidth of FBGs to be transmitted, forming ultra-narrow band periodic transmission peaks as shown in figure (5.3).

The above devices show several advantages when compared with traditional Fabry-Perot filters. It is possible to choose the free spectral range (FSR) and the resonant wavelength of the cavity simultaneously, without changing the dispersive material between gratings [22]. Furthermore, the devices are very compact and suitable for high density integrated optics due to higher refractive index of the cavity material. Appropriate amplitude and phase transfer function of cavity is accessed by choosing grating parameters.

The proposed model to obtain the spectral response of the FP-FBG considers that interference occurs between reflected light and the one transmitted by the two Bragg gratings, generating multiple interference peaks in the reflection spectrum.

For uniform gratings, the complex reflectivity amplitude is given by [17, 23]

The reflection coefficient $(\rho^2) = \frac{Sinh^2}{Cosh^2}\frac{(\sqrt{\kappa^2-\sigma^2}}{(\sqrt{\kappa^2-\sigma^2}}\frac{L)}{L)-\frac{\sigma^2}{\kappa^2}}$ (1)

Where 'κ' is the ac coupling coefficient 'σ' is dc coupling coefficient (period averaged), 'L' is the length of the grating.

The cavity spectra are simulated introducing the power reflection coefficient $R_i = |r_i|^2$ in the Fabry- Perot field transfer function [23]

$$r_{BGFP}(\lambda) = \left[1-\sqrt{\frac{R_1 \times R_2}{2}}\right]\frac{exp\left(-i\pi\frac{\lambda}{FSR}\right)}{1\sqrt{\frac{R_1 \times R_2}{2}}exp\left(-i2\pi\frac{\lambda}{FSR}\right)} \quad (2)$$

used was 10Gbit/s RZ optical signal with 2^{31}-1 Pseudo Random Binary Sequence (PRBS) pattern were used, and figure (5.2) shows the optical spectrum of RZ signal.

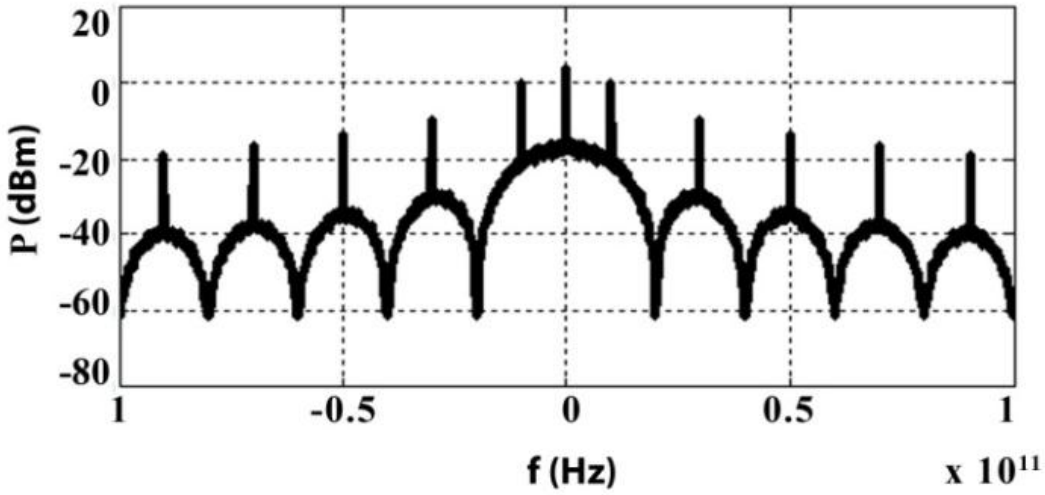

Fig. (5.2) *Optical spectrum of RZ signals @10 Gbps.*

To obtain a 10 GHz FSR, the desired FP filter consisted of two identical and uniform fiber Bragg gratings of 3mm separated by 11.5mm. The transmission spectrum of the FP filter fabricated with FSR = 10 GHz is shown in figure (5.3). The laser wavelength of the transmitter is adjusted to the central peak of the FP-FBG response.

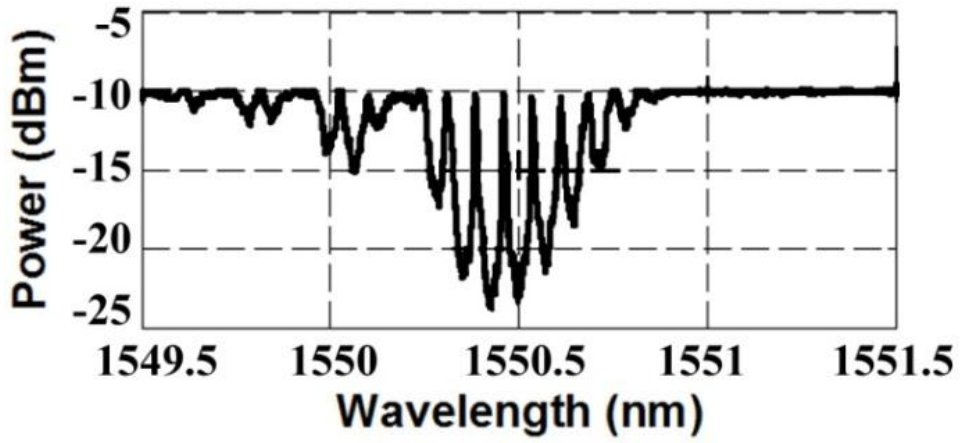

Fig. (5.3) *Transmission spectrum of the fabricated FP-FBG filter with transmission peaks are 10 GHz apart.*

The figure (5.4) shows the optically modulated PRBS data (a) The spectrum of modulated data (b) and the waveform of recovered clock at 10 GHz (c). We have also simulated the optical clock recovery at 40 Gbps and 100 Gbps using FP-FBG filters with appropriate FSR and tuned to the signal central wavelength.

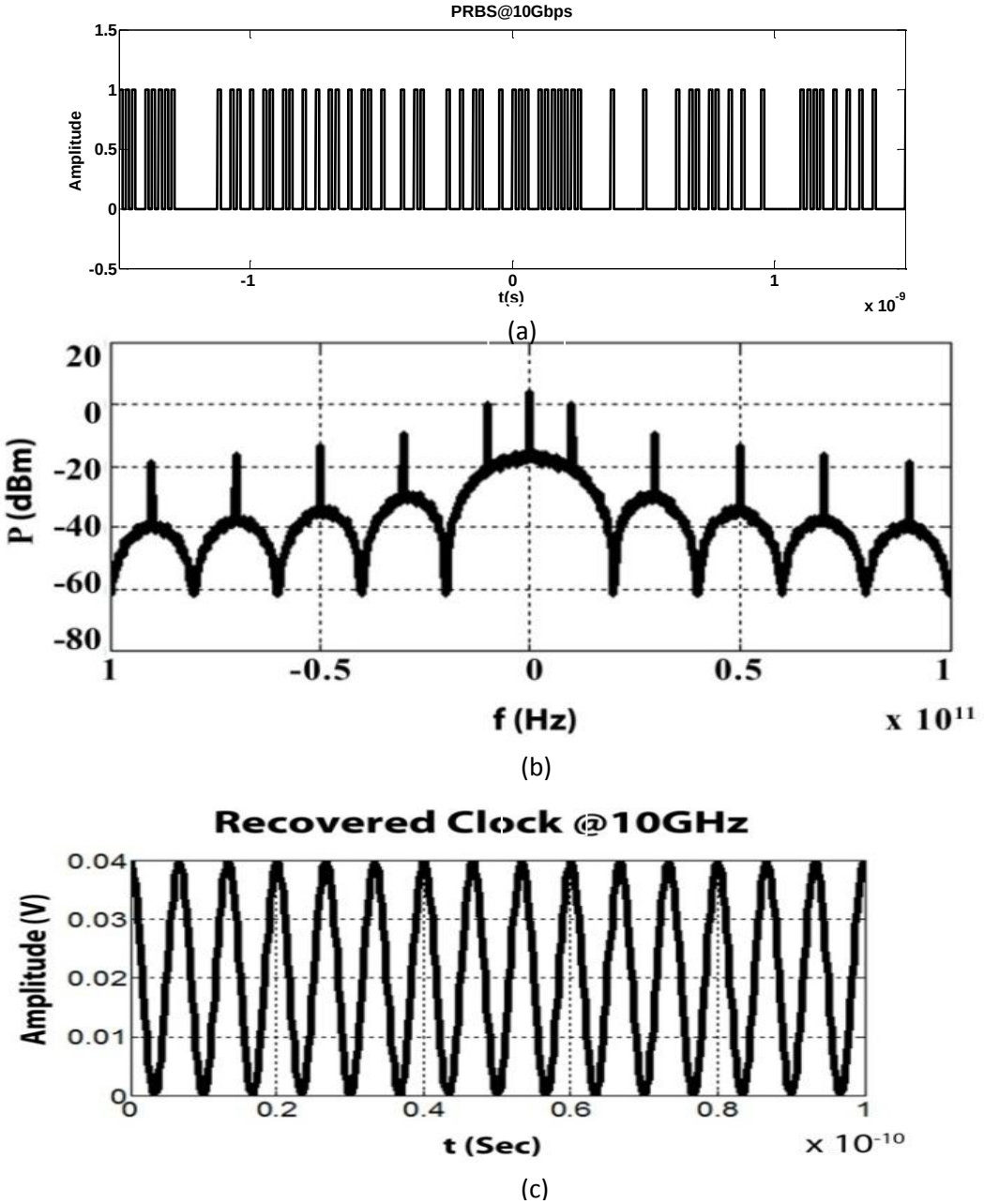

Fig. (5.4). *(a) The PRBS @ 10Gbps (b) The Optical spectrum (c) the recoverd clock using FP-FBG with FSR 10GHz*

5.4 Experimental results

Using the fabrication facility at IIT-Madras Chennai, we have fabricated the FP-FBGs, with length of 3mm, using Ibsen phase-mask with period 1071.21 nm, UV exposure time of 40 seconds on a Nufern GF1 photo sensitive fibre. The centre wavelengths of both the FP-FBGs are 1550.5 nm cavity length of 11.5 mm and the free spectral range (FSR) of 9.36 GHz.

The experimental set up for the optical clock recovery is shown in figure (5.5). It consists of an Agilent tuneable laser source, whose amplitude is modulated using an electro-optic modulator from Photline Technologies, whose modulation characterises we have measured at IIT Madras is shown in figure (5.6).

The modulator is driven using an Optellent OPGX110 PRBS generator (10 Gbps). Finally, the filtered optical signal is detected using a Discovery Semiconductor 10 GHz PIN-based optical receiver. The RF spectrum is observed using a Rhode & Schwarz Spectrum Analyzer (30 GHz).

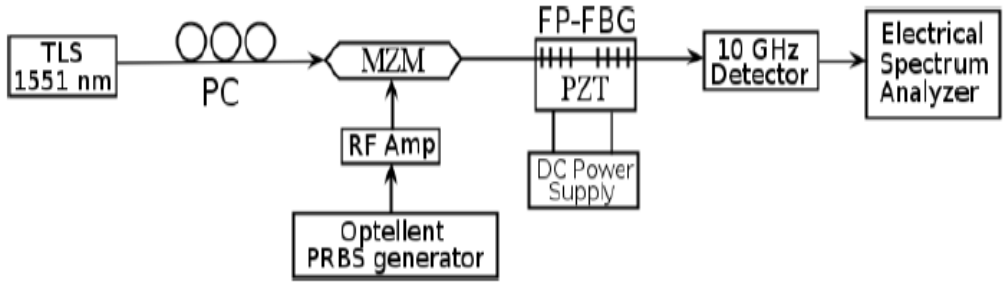

Fig. (5.5) *The experimental set up for 10GHz clock recovery using FP-FBG filter*

Modulator Bias Characteristics (Photline-MXLN-10)				
Bias Voltage (V)	Power reading 1	Power reading 2	Power reading 3	Average reading
5	-7.2	-7.45	-7.45	-7.37
3	-7.55	-7.8	-7.8	-7.72
2	-8.9	-8.7	-8.7	-8.77
1	-9.9	-9.5	-9.5	-9.63
0	-11.7	-11.15	-11.4	-11.42
-1	-14.1	-12.95	-13.35	-13.47
-2	-21.5	-17.9	-18.55	-19.32
-3	-41.3	-29.05	-33.65	-34.67
-4	-26.25	-33.75	-28.95	-29.65
-5	-15.15	-16.25	-15.95	-15.78

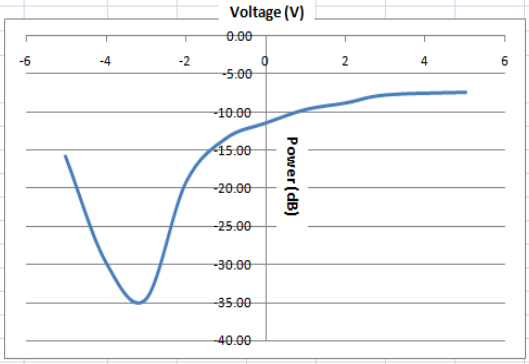

Fig. (5.6) *The Photline electro-optic modulator characteristics*

All-optical clock recovery using an FBG based phase-only optical filter has been demonstrated recently [24]. However, the extinction ratio of the filter is limited. In contrast, an all-fiber Fabry-Perot filter is capable of providing >20 dB extinction in a compact all-fibre device. A proposal and design based on FP-FBGs for all optical clock recovery is also put forward by us [25]. Below is the demonstration the use of a Fabry-Perot fiber Bragg grating (FP-FBG) for the filtering of the clock tone [26]. Two identical reflectors with a small separation together constitute a Fabry-Perot cavity. Hence an FP-FBG combines the functionalities of a narrowband filter and and FP filter. The use of an FP-FBG provides a compact and integrable solution for passive all-optical clock recovery [27].

The setup used for this experiment is shown in figure (5.7). The wavelength of the tunable laser source (TLS) was chosen such that it was coincident with one of the peaks of FP-FBG transmission in the region of operation. The laser was modulated by a 2^7-1 length PRBS signal at data rate of 10.3125 Gbps using a Mach-Zehnder modulator (MZM). The bias point was optimized in order to obtain the maximum extinction, thus generating an NRZ-OOK signal.

In order to reconstruct the clock, it is necessary to filter at least 2 spectral components of the signal which are separated by the clock frequency (10.3125 GHz in this case). This can be achieved if the carrier wavelength (frequency) and sidebands of the signal are aligned to the peaks of the transmission characteristics of the FP-FBG. The working principle of this implementation has two major conditions. As mentioned in section 5.2.1 the carrier wavelength should be matched to one of the peaks of FP-FBG transmission spectrum and secondly, the separation of various spectral components of signal (baud rate) should be matched to the separation between the peaks in the FP-FBG spectrum adjacent to the peak selected as carrier wavelength (figure 5.8).

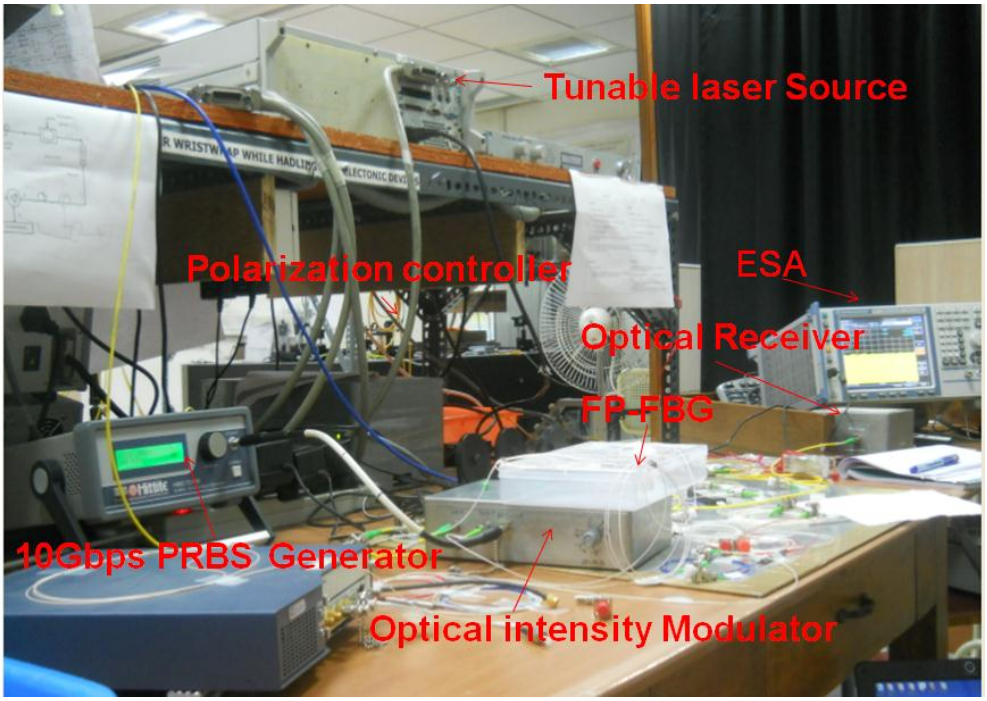

Fig. (5.7) *The experimental set up for the data clock recovery at IIT Madras.*

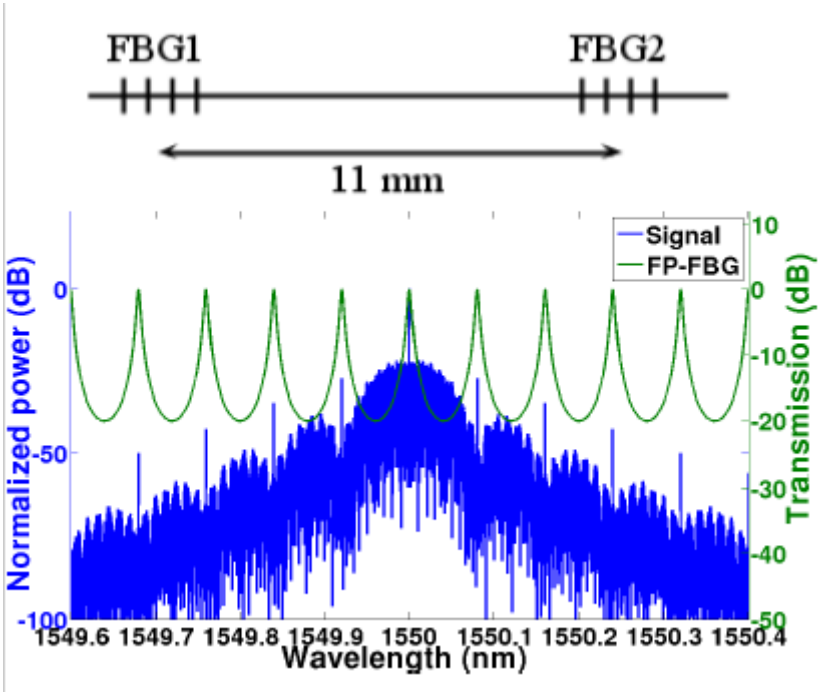

Fig. (5.8) *Transmission peaks of FP- Filter and RF data spectrum*

The precise alignment of the FP-FBG resonance to the carrier may be undertaken by tuning the FP-FBG using a piezo-electric transducer made of PZT (Lead Zirconate Titanate) crystal [27]. The FP-FBG used in this implementation has been fabricated. The FBGs constituting the FP cavity have peak reflectivity at wavelength of ~1551 nm and the separation between the FBGs is 11 mm. Figure (5.9) shows the transmission characteristics of the FP-FBG used for the experiment. It can be seen that the predominant characteristics span over 1 nm from 1550.5 nm to 1551.5 nm with a maximum extinction ratio of ~10 dB, limited only by the fabrication conditions. The preferred region of operation is zoomed and shown in the inset of figure (5.9).

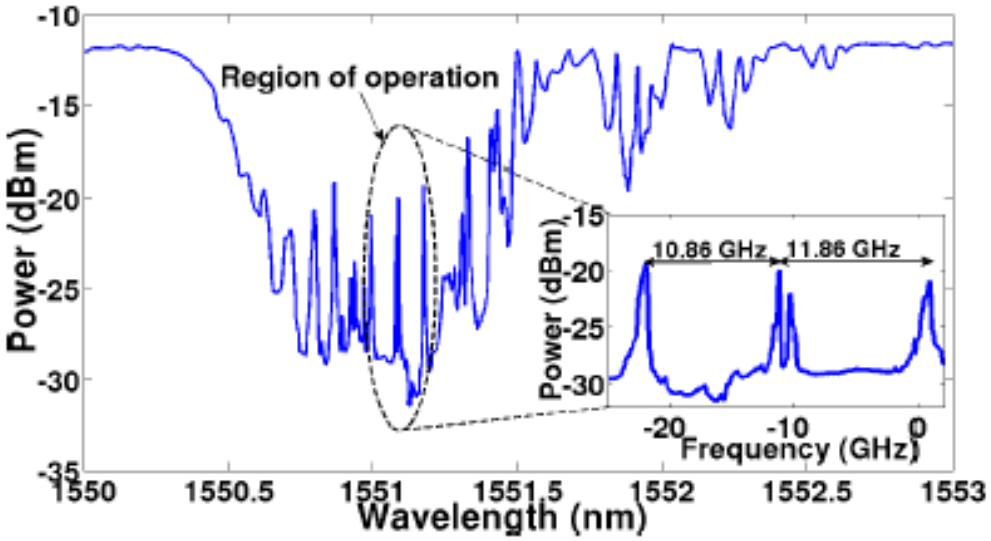

Fig. (5.9) *The FP-FBG (Spectrum) used for Clock recovery, (insect, the preferred peaks considered for clock recovery)*

The frequency separation between the peaks is not the same for adjacent pairs of peaks due to imperfections in the fabrication process of FP-FBG. In order to validate the working principle of the scheme, filtering was performed using a sinusoidally modulated optical signal. The carrier wavelength was chosen to be 1550.975 nm (corresponding to one of the peaks of FP-FBG transmission spectrum) and the modulation frequency was varied such that the position of sidebands with respect to carrier would vary. In this manner, the sideband was swept across the transmission peak of FP-FBG adjacent to the peak corresponding to carrier wavelength. The filtered signal was observed in time domain using a high-speed photo-detector of bandwidth 10 GHz. The peak-to-peak amplitude of the filtered signal was found to be the maximum for the modulation frequency corresponding to the separation transmission peaks of FP-FBG, which was 9 GHz in this case.

Electrical spectrum of the unfiltered data signal is shown in figure (5.10a). The prominent peak occurred at 10.3125 GHz which corresponds to the data rate. In addition, a number of other peaks were seen, which spanned over the entire spectrum (as far as the modulator bandwidth/detector bandwidth permitted). These peaks were regularly spaced with a frequency separation of ~81 MHz and could be attributed to the length of PRBS sequence which is 2^7-1 = 127 in this case ($10.3125*10^9/127$=81.2MHz). Electrical spectrum of signal after filtering from FP-FBG was observed on Electronic Spectrum Analyser (ESA) and the PZT voltage was varied in order to get the maximum power in the clock component. The corresponding results are shown in figure (5.10a).

The significant feature of the RF beat spectrum shown in figure (5.10b) is the suppression of pattern-related components (81.2MHz separated) and exclusive selection of clock component at 10.3125 GHz. Power in the clock component was found to increase as the PZT voltage was tuned to such a value that the FSR matched the data rate. Variation of power in the clock tone with respect to PZT bias voltage is shown in figure (5.10c). By proper tuning of FSR of FP-FBG, strength of the clock tone could be enhanced by ~13 dB with significant suppression of pattern-related peaks of the signal. The driving signal for PZT in order to achieve the maximum power in clock tone was ~70-80 V. The power of the filtered clock tone was ~20 dB less than the clock tone of unfiltered signal because of the non-optimal tuning of the FP resonance with respect to the signal wavelength. As the PZT voltage was increased, in addition to the change in FSR, the entire spectrum shifted towards the shorter wavelengths. Hence even if the FP peaks adjacent to the carrier wavelength were matched with the sidebands, the carrier wavelength got detuned from its original transmission peak, thus resulting in a reduction in the power of the clock tone.

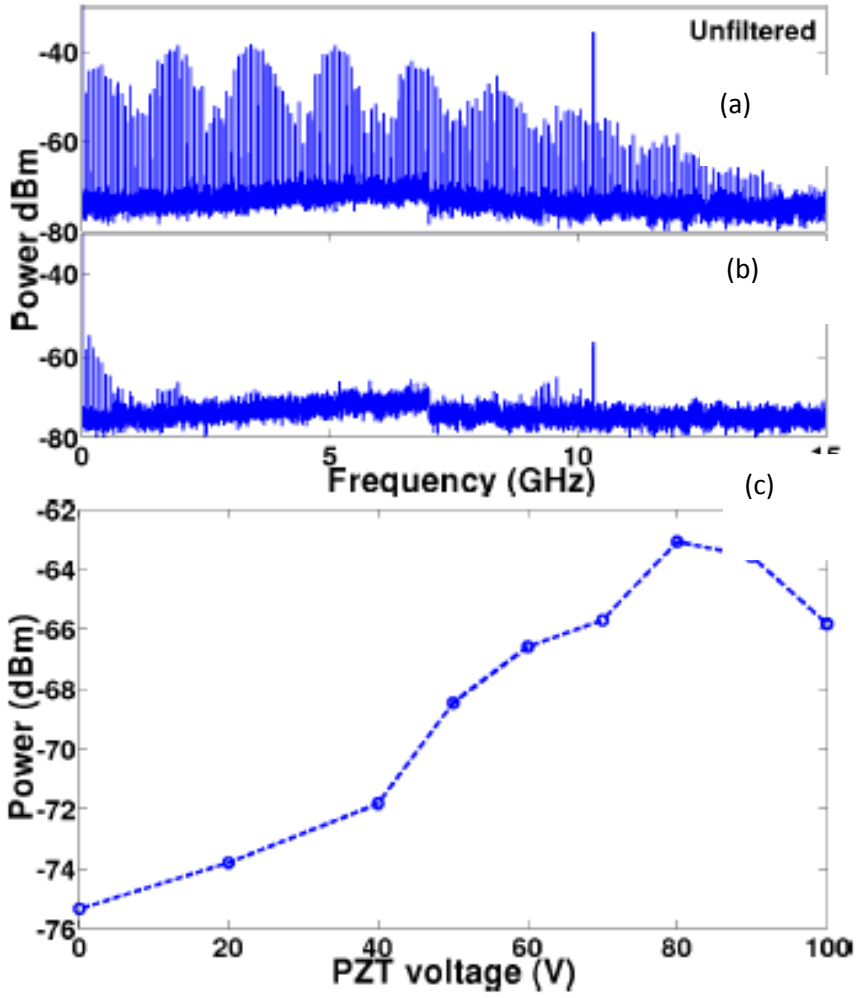

Fig. (5.10) (*a) The electrical of unfiltered data. (b) Filtered spectrum. (c) PZT characteristics used for the experiment*

The major challenge encountered in this implementation was the drift in the transmission spectrum of FP-FBG with time (figure (5.11). From the transmission spectrum measured every 3 minutes, it is seen that the spectrum is not stable. The position of peaks changes by ~0.01 nm, FSR drifts within a range of ~1 GHz which is substantial compared to the targeted data rates and can be detrimental for the quality of recovered clock.

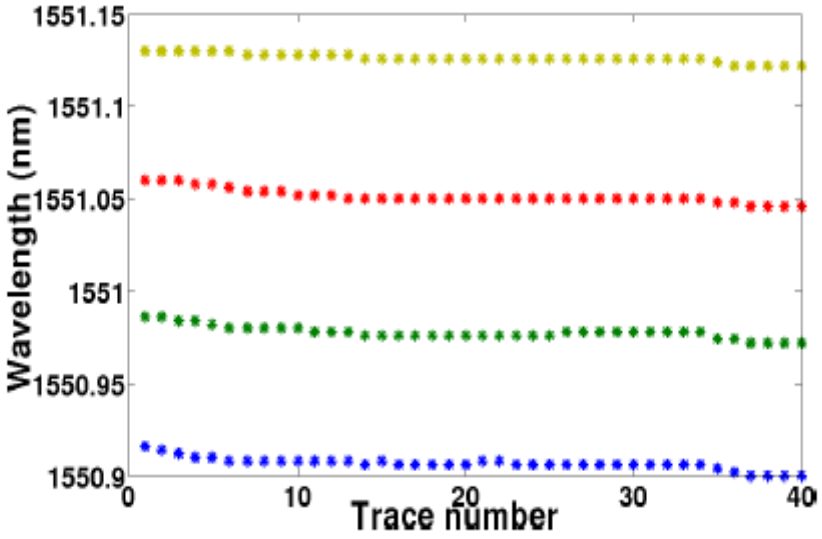

Fig. (5.11) *Changes in the peak wavelength with time,*

The use of PZT mitigates this effect to some extent. With the change in PZT voltage, the entire transmission spectrum shifted towards lower wavelengths. Hence, the carrier wavelength was also required to be adjusted simultaneously. For a practical implementation of this scheme, the FP-FBG has to be fabricated in such a precise manner that the peak wavelengths are coincident with the ITU-T grid wavelengths and the separation of FP peaks correspond to the targeted symbol rates (~10 GHz in this case) [28]. For such an FP-FBG, it can be safely assured that the carrier wavelength of the incoming signal is always coincident with one of the peaks of FP-FBG spectrum. If the baud rate of the signal is slightly different from separation of peaks, the FSR can be tuned by changing the PZT bias voltage, but that would also shift the entire spectrum. This would result in a detuning between carrier wavelength and peak wavelength, hence compromising the quality of the filtered clock. A dynamic control of PZT bias voltage using a feedback loop may be helpful in operating at an optimum PZT voltage to recover the best possible clock signal.

In addition to that low extinction ratio (<30dB) of FP-FBG peaks also deteriorates the quality of the clock. Proper clock signal obtained for high extinction ratios (> 50 dB); figure (5.12)

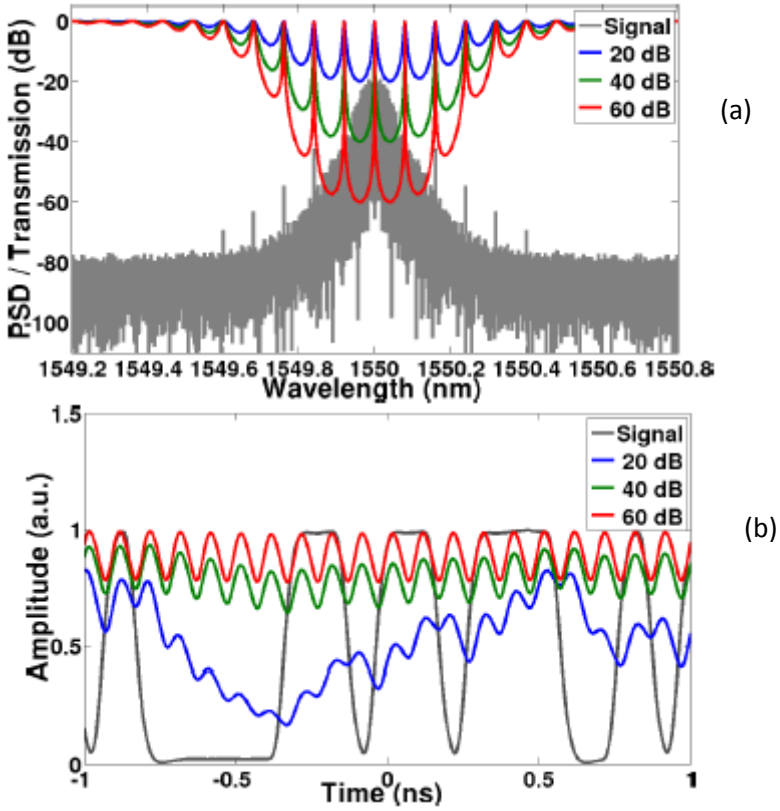

Fig. (5.12) *(a) The FP-FBG spectrum with different power extinctions (b) The more the power extinction of the FP-FBGs gives out high quality clock out.*

In addition to the extinction issue, precise fabrication techniques need to be used to get the transmission peaks matched to ITU-T grid wavelengths. This will help the FSR matched to targeted symbol rates. The dynamic feedback controlled PZT based implementation is required to mitigate the drift in spectrum, so as to get error free data clock signal.

5.5 Conclusion

We have simulated and experimentally validated the all optical data clock recovery by Fabry-Perot filters using fibre Bragg grating. Here the recovered data clock speed is 10Gbps. This approach can be extended to recover the clock speed at higher rates. The all optical data clock recovery using FP-FBGs are simple and cost effective. The challenges that we faced are, the FP-FBG pass bands must have higher extinctions (>50dB), which requires highly stable FP-FBG fabrication set up and, secondly the FP-FBG free spectral range (FSR) must be stable at ITU-T wavelengths. All such details are clearly explained in this chapter.

5.6 ***References***

1. H. Meyr, M. Moeneclaey, S.A. Fechtel, "*Digital Communications Receivers - Synchronization, Channel Estimation, and Signal Processing"*. Wiley, (1998).

2. U. Mengali, A.N. D'Adrea, "*Synchronization Techniques for Digital Receivers"*. Plenum Press, (1997).

3. O. Kamatani and S. Kawanishi, "*Ultrahigh-speed clock recovery with phase lock loop based on four-wave mixing in a traveling-wave laser diode amplifier"*, Journal of Lightwave Technology. Vol 14, pp 1757-1767, (1996).

4. H. C. Hansen Mulvad, E. Tangdiongga, H. de Waardt, and H. J. S. Dorren, "*40 GHz clock recovery from 640-Gbit/s OTDM signal using SOA-based phase comparator"*, Electron Letters., Vol 44, pp 146-148, (2008).

5. L.K. Oxenlowe, F.Gomez, C.Waren, SKurimura, H.C.HMulvad, MGalili, K.Kitamura, H.Nakajima, J.Inchikava, D.Erasme. "*640 Gbit/s clock recovery using periodically poled lithium niobate"*, Electron Letters., vol 44, pp 370-371, (2008).

6. C. Boerner, V. Marembert, S. Ferber, C. Schubert, C. Schmidt-Langhorst, R. Ludwig, and H.G. Weber, *"320 Gbit/s clock recovery with electro-optical PLL using a bi-directionally operated electro absorption modulator as phase comparator,"* in Optical Fiber Communication Conference, OSA Technical Digest Series (Optical Society of America), Vol 2 pp 349–351,(2005).

7. L.K. Oxenløwe, F. Gomez-Agis, C. Ware, S. Kurimura, H.C.H. Mulvad, M. Galili, H. Nakajima, J. Ichikawa, D. Erasme, A.T. Clausen, and P. Jeppesen, *"640-Gbit/s Data Transmission and Clock Recovery Using an Ultrafast Periodically Poled Lithium Niobate Device,"* Journal of Lightwave Technology. vol. 27, pp 205-213, (2009).

8. Yong Liu, Shangjian Zhang, and Yongzhi Liu, F. Gomez-Agis, E. Tangdiongga, and H. J. S. Dorren "*High-Speed Optical Signal Processing for Telecom Applications"* Wireless and Optical Communications Conference (WOCC) IEEE, pp 1-5,(2010).

9. Andrews S Tanenbaum, David J "*Computer Networks"*, Pearson Education LTD, (2013).

10. Leon W Couch*"Digital & Analog Communication Systems"*,Pearson Education India, (2009).

11. Tuomo von Lerber, SeijaHonkanen, A. Tervonen, Franko Kueppers *"Optical clock recovery methods: review,* Elsevier, optical fiber technology*"*, vol. 15, pp 363–372, (2009).

12. Masatoshi Saruwatari, Senior Member, *IEEE"All-Optical Signal Processing for Terabit/Second Optical Transmission"* IEEE Journal on selected topics in Quantum Electronics, vol. 6, pp 1363-1374, (2000).

13. Yong Liu, Shangjian Zhang, and Yongzhi Liu, F. Gomez-Agis, E. Tangdiongga, and H. J. S. Dorren *"High-Speed Optical Signal Processing for Telecom Applications"* Wireless and Optical Communications Conference (WOCC), 19th Annual, (2010)

14. M.Jinno and T.Matsumoto *"All optical timing extraction using a 1.5um self-pulsating multi-electrode DFB LD"* Electron letters Vol 24, pp 1426-27,(1988).

15. K.Smith and J.K Lucek *"All optical clock recovery using a mode locked Laser"* Electron letters Vol 28, pp 1814-16, (1992).

16. M.Jinno and M,Abe "*All optical regenerator based on nonlinear fibre Sagnac interferometer"* Electron letters, vol 28, pp 1350-1352,(1992).

17. Yu,Lzhao, DanLu, J.Zang, D.kong, J.Q.Pan, J.Oui, S.Wei. "All-optical clock recovery for 40 Gb/s NRZQPSK signals using an amplified feedback DFB laser" CLEO: 2013 Technical Digest © OSA (2013)

18. Jeon Min-Yong , Leem Young-Ahn , Kim Dong-Churl , SimEun-Deok , Kim Sung-Bock , Ko Hyun-Sung , Yee Dae-Su , Park Kyung-Hyun, *"40 Gbps all-optical 3R regeneration and format conversion with related InPBased Semiconductor Devices"*. ETRI Electron. Telecommun. Res. Inst. J. 29, pp 633–639, (2007).

19. M. Jinno, T.Matsumoto *"Optical tank circuits used for all optical timing recovery"*. J. Quantum Electron. 28, pp 895–900, (1992).

20. C. Johnson et al. *"Multiwavelength all-optical clock recovery photon"*. Tech. Lett. 11, pp 895–897, (1999).

21. W. Mao, YuhuaLi, Mohammed Al-Mumin, Guifang Li *"All-optical clock recovery for both RZ and NRZ data"* Photon. Tech. Lett. 14, pp 873–875, (2002).

22. A. Meloni, M. Floridi, F. Morichetti, M. Martinelli, *"Equivalent circuit of Bragg gratings and its application to Fabry-Perot cavities".* Journal of Optical. Society of America 20, pp 273–281, (2003).

23. R.Kashyap *"Fiber Bragg Gratings"*, San Diego, Academic Press, (1999).

24. R. Maram, Fernandez-Ruiz, M. R., & Azana, J. (2014). *"Design of an FBG-based phase-only (all-pass) filter for energy-efficient all-optical clock recovery, in Advanced Photonics"*, (Optical Society of America, paper BM4D.7, (2014).

25. V.S Nandu, VT Gopakumar, V P MahadevanPillai, Madhusoodhanan, Balaji Srinivasan "*Optical Clock Recovery with Fabry-Perot Filter Based on Fiber Bragg Gratings"*WPo.45, International Conference on Fiber Optics and Photonics © OSA, (2012).

26. Manas Srivastava, V.T. Gopakumar, Balaji Srinivasan, and Deepa Venkitesh *"Performance Analysis of All-optical Clock Recovery Using Fabry-Perot Fiber Bragg Gratings"* paper Tu2A.4 13th International Conference on Fiber Optics and Photonics OSA Technical Digest (online) (Optical Society of America) (2016).

27. VT Gopakumar, KN Madhusoodanan and Balaji Srinivasan *"Simulation and Experimental Validation of Optical Clock Recovery Using Fiber Fabry-Perot Filters"* Journal of Optics (Springer) Volume2, No 44, pp 178-181, (2015).

28. G. Gustav, "*Piezoelectric Sensorics"* Chapter 3, Springer Heidelberg, (2002).

29. ITU-T Recommendation G.692 *"Transmission systems and media, Digital systems and networks"* (1998).

.....ꕥ.....

Chapter 6

CONCLUSION AND FUTURE WORKS

6.1 Conclusion and Future works

In the thesis we try to address the solutions for current and future high speed signal processing devices for all optical communication technologies. The main focuses of the thesis are the design of optical integrator; optical differentiator and all optical clock recovery by Fabry-Perot cavities based on FBGs. Above signal processing devices are already designed and implemented with FBGs in the high speed optical networks. Here we have taken the unique advantages of FP-FBGs, as mentioned in section 3.4 of chapter 3, to design the above three signal processing components. The thesis can be summarised as follows.

- While considering the processing speed of the designed optical integrator, the impulse response of an ideal integrator is proportional to the unit step function u(t). A finite-time integrator can be implemented using a linear optical filter providing a constant temporal impulse response over a certain limited duration (operation time window of the integrator). A FBG/FP-FBG-based integrator provides a constant impulse response over a time fixed by total round-trip propagation time.The FP integrator's processing bandwidth is limited to ≈1/5 of the integrator free spectral range. In our design we have fabricated a FP-FBG with cavity separation of 1mm and each FBG length of 1mm. So it can process signals of time duration <10ps (from equation 6 of chapter 3) which gives the processing bandwidth of 100GHzor more. We could go up to a few hundreds of GHz processing bandwidth by adjusting the FP-FBG physical

parameters, like grating length of FBGs and FP-FBG centre to centre separation (δL). For example a 10μm cavity, the round-trip time as fast as 0.3ps, corresponding to processing speed up to ≈ 650 GHz. While testing the simulation performance, we have used the input Gaussian, bi-modal Gaussian and phase-shifted Gaussian pulses with variance of 20ps and 70ps, corresponding bandwidth of 50GHz and 20GHz, respectively. Even though we have designed and fabricated the FP-FBG for high speed integrator we couldn't experimentally validate the results. This is mainly because of the fabrication instability associated with Braggstar Excimer laser issues, which is shown in the table 2.1 of chapter 2. In addition to that non availability high speed signal generators to generate different input pulse waveforms are also affected the experimental validation. The input test waveforms are to be used for experimental validation are, a transform-limited Gaussian optical pulse, an odd-symmetry Hermite-Gaussian (OS-HG) pulse which is the first-order derivative of the Gaussian, a symmetric double-pulse and temporally separated out-of phase (π- phase shift) replicas of the same Gaussian pulse. But the simulation using above waveforms are plotted for FBGs and FP-FBGs in chapter3. The simulation results are agreeing with the results of latest optical integrators in various scientifically proven results.

- Another design we have proposed in this thesis is the high speed optical differentiator based on FP-FBGs. To date, to the best of our knowledge and belief there is no scientific reports on all optical differentiators based on FP-FBGs. We have fabricated a FP-FBG (as explained in the section 4.3 of chapter 4) which can work as a high speed optical differentiator. The amplitude spectrum of the fabricated FP-FBG is well matched the spectrum seen in the latest literatures. The method we proposed for the same is very simple, passive and cost effective and can be used for high speed processing sub picoseconds pulses used in optical communication. Unlike the simulation

results FBG integrator, here we have avoided the simulation of FBG based differentiators as the proposed one has far better performance than FBG differentiators seen in various scientific reports in various journals. The real time testing of the designed and fabricated FP-FBG differentiator is could not be carried out because of various reasons mentioned already.

- We have studied and experimentally demonstrated all optical data clock recovery at 10Gbps. The clock recovery at any date can be possible by adjusting the FSR by varying the cavity length (δL) of the FP-FBGs. The unique advantages of clock recovery by FP-FBGs are circuit completely in-fiber and low jitter high speed passive circuit. The problem we faced during the demonstration of FP-FBG based clock recovery at 10Gbps is the instability and shift in wavelengths of the narrowband peaks of FP-FBGs. The FSR values of the purchased FP-FBGs mentioned in the section 2.5 of chapter 2 are also not unique, even though we had requested for same FSR values (10GHz) throughout the transmission peaks. In order to overcome this problem we have used a PZT tuner. This addition of PZT tuner to data clock recovery circuit adds cost, more power requirement and operation complexity. The future clock recovery circuits with FP-FBGs must have very stable FSR values. By using highly accurate FBG writing set up to avoid the use of the PZT tuner and make the circuit cost effective and simple.

The proposed optical integrator, differentiator and clock recovery circuits open the doors for further research works in future. While we consider the performance of optical integrator, the energetic efficiency has to be tested in comparison with the FBG integrators.The energetic efficiency depends on the spectral bandwidth of the optical signal to be processed; a lower energetic efficiency is obtained when processing a waveform with a broader bandwidth since in this case, a larger portion of the input signal spectrum is filtered out by the FBG. The maximum input pulse duration Δt, which can be processed by an

integrator depends on the total round trip time. In an integrator the input pulse duration must be less than the total round trip time T ($\Delta t < T$). So in our proposed FP-FBG integrator, the round trip time can be easily adjusted and energy efficiency can be increased by varying the cavity length δL. In addition to that temporal duration of the input pulse can be made narrower as the round trip time is getting reduced by using the FP-FBG. The FP-FBG integrator that we designed to be tested and verified for high speed optical signal processing applications such as a dark-soliton detector and pulse shaper. In addition to that a photonic temporal integrator with its optical counterpart, the differentiators are, the key elements to build up ultrafast all-optical circuits for real-time computing of complex engineering and scientific problems described by differential equations. We also planned to fabricate and test the proposed integrator and differentiators with different types of doped fibers of varying photosensitivity.

The testing and verification of the proposed integrator and differentiator will need high speed pulse waveform generators and high resolution optical spectrum analyzers. For example.a passively mode-locked tunable fiber laser is required as pulse source, which generate nearly transform-limited Gaussian-like optical pulses, each with a Full-FWHM time duration of ≈ 6 ps, at a repetition rate of 16.7 MHz. The Gaussian-like pulse directly generated from the fiber laser was re-shaped into various different waveforms using an optical pulse shaper based on a single two-arm (Michelson) bulk-optics interferometer. In addition to that the input and the output beams have to be collimated and focused, respectively, by collimating lenses. A non-polarizing cube beam splitter is required to split and combine the beams. A fiber-optic polarization controller is required in front of the interferometer to properly select the polarization axis of the beam splitter as it was slightly polarization dependent. The proof-of-concept experiments are needed to establish various interesting specific applications of the realized photonic integrator, namely reconfigurable flat-top pulse generation and phase-encoded

pulse pattern recognition. The generation of ultra - short flat-top temporal intensity profiles is highly desired for a range of non-linear optical switching and frequency conversion applications. In these applications, the flat-top pulse time width needs to be optimized according to the data rate of the communication link.

The photonics differentiators are also very useful for a wide range of applications in ultrafast optical pulse processing and coding, shaping and metrology. These devices also find important applications as basic building blocks in ultra-high-speed all optical analog–digital signal-processing circuits. Moreover, optical differentiators are of immediate interest for the generation of optical monocycle pulses from input-optical Gaussian pulses for ultra wideband systems. These optical components, as mentioned in the introductory chapter, are emerging as a solution for future wideband personal access networks and generation of a Hermite–Gaussian temporal waveform from an input Gaussian pulse to synthesize any temporal shape by superposition. As mentioned the testing and characterization of the FP-FBG differentiator is to be done with ultra-narrow line width standard temporal test signals.

While we considering the all optical clock recovery of RZ-OOK signal at 10Gbps, as mentioned, we could not make it consistently because of FSR changes with time. We need to have highly stable FBG writing set up so that clocks of higher rates can also be extracted by changing the FSR values. In addition to that we need to demonstrate the feasibility of complete clock recovery operation by using FP-FBGs with a high finesse value and an SOA acting as an amplitude equalizer in a single pass configuration.

.....ॐ❋ॐ.....